

1 **Synthetic metabolic pathways for photobiological conversion of CO₂ into hydrocarbon fuel**

2

3 Ian Sofian Yunus^a, Julian Wichmann^b, Robin Wördenweber^b, Kyle J. Lauersen^b, Olaf Kruse^b and

4 Patrik R. Jones^{a*}

5

6 ^aDepartment of Life Sciences, Imperial College London, SW7 2AZ London, UK

7 ^bBielefeld University, Faculty of Biology, Center for Biotechnology (CeBiTec),

8 Universitätsstrasse 27, 33615, Bielefeld, Germany.

9 *Corresponding author: p.jones@imperial.ac.uk

10 ABSTRACT

11 Liquid fuels sourced from fossil sources are the dominant energy form for mobile transport
12 today. The consumption of fossil fuels is still increasing, resulting in a continued search for
13 more sustainable methods to renew our supply of liquid fuel. Photosynthetic microorganisms
14 naturally accumulate hydrocarbons that could serve as a replacement for fossil fuel, however
15 productivities remain low. We report successful introduction of five synthetic metabolic
16 pathways in two green cell factories, prokaryotic cyanobacteria and eukaryotic algae.

17 Heterologous thioesterase expression enabled high-yield conversion of native fatty acyl-acyl
18 carrier protein (ACP)ACP into free fatty acids (FFA) in *Synechocystis sp.* PCC 6803 but not in
19 *Chlamydomonas reinhardtii* where the polar lipid fraction instead was enhanced. Despite no
20 increase in measurable FFA in *Chlamydomonas*, genetic recoding and over-production of the
21 native fatty acid photodecarboxylase (FAP) resulted in increased accumulation of 7-
22 heptadecene. Implementation of a carboxylic acid reductase (CAR) and aldehyde
23 deformylating oxygenase (ADO) dependent synthetic pathway in *Synechocystis* resulted in
24 the accumulation of fatty alcohols and a decrease in the native saturated alkanes. In contrast,
25 the replacement of CAR and ADO with *Pseudomonas mendocina* UndB (so named as it is
26 responsible for 1-undecene biosynthesis in *Pseudomonas*) or *Chlorella variabilis* FAP resulted
27 in high-yield conversion of thioesterase-liberated FFAs into corresponding alkenes and
28 alkanes, respectively. At best, the engineering resulted in an increase in hydrocarbon
29 accumulation of 8- (from 1 to 8.5 mg/g cell dry weight) and 19-fold (from 4 to 77 mg/g cell
30 dry weight) for *Chlamydomonas* and *Synechocystis*, respectively. In conclusion, reconstitution
31 of the eukaryotic algae pathway in the prokaryotic cyanobacteria host generated the most
32 effective system, highlighting opportunities for mix-and-match synthetic metabolism. These
33 studies describe functioning synthetic metabolic pathways for hydrocarbon fuel synthesis in
34 photosynthetic microorganisms for the first time, moving us closer to the commercial
35 implementation of photobiocatalytic systems that directly convert CO₂ into infrastructure-
36 compatible fuels.

38 Keywords

39 Hydrocarbon fuel; Algae; Cyanobacteria; Alkanes; Alkenes; Fatty acids

41 Highlights

- 42 • Synthetic metabolic pathways for hydrocarbon fuels were engineered in algae
- 43 • Free fatty acids were effectively converted into alkenes and alkanes

- 44 • Transfer of algal pathway into cyanobacteria was the most effective
- 45 • Alkane yield was enhanced 19-fold in *Synechocystis spp.* PCC 6803
- 46 • Alkene yield was enhanced 8-fold in *Chlamydomonas reinhardtii*
- 47

48 INTRODUCTION

49 Cyanobacteria (prokaryotes) and algae (eukaryotes) are photosynthetic microorganisms that
50 have evolved to naturally accumulate C15-C19 alkanes or alkenes at very low concentrations
51 (0.02-1.12% alkane g/g cell dry weight (CDW_{edw})) (Lea-Smith et al., 2015; Schirmer et al.,
52 2010; Sorigué et al., 2017) with the exception of naturally oleagineous species (Ajjawi et al.,
53 2017; Metzger and Largeau, 2005; Peramuna et al., 2015). These hydrocarbons are postulated
54 to influence the fluidity of cell membranes and are therefore essential for achieving optimal
55 growth, indeed, the abolition of their biosynthetic capacities results in morphological defects
56 (Lea-Smith et al., 2016). Only two enzymes, acyl-ACP reductase (AAR) and aldehyde
57 deformylating oxygenase (ADO) are required to catalyze the bacterial conversion of acyl-ACP
58 into alkanes (Schirmer et al., 2010). Similarly, eukaryotic microalgae also biosynthesize small
59 quantities of alkanes and alkenes directly from fatty acids, employing the distinctly different
60 and recently discovered fatty acid photodecarboxylase (FAP; (Sorigué et al., 2017)).

61 In order to engineer sustainable biotechnological systems for production of
62 hydrocarbons for the fuel market, whether heterotrophic or light-driven, far greater yields are
63 needed alongside other complementary non-biochemical improvements such as improved
64 bio-process designs. Several studies have attempted to enhance alkane productivity in
65 cyanobacteria by over-expression of the native or non-native AAR and ADO enzyme couple
66 (Hu et al., 2013; Kageyama et al., 2015; Peramuna et al., 2015; Wang et al., 2013) which relies
67 on acyl-ACP as the precursor. Although naturally accumulating alkane amounts have been
68 enhanced through engineering and reported in high titres from the lipid-accumulating
69 cyanobacteria, *Nostoc punctiforme* (up to 12.9% (g/g) CDW_{edw}, (Peramuna et al., 2015)),
70 similar efforts in the non-lipid accumulating model cyanobacterium *Synechocystis sp.* PCC
71 6803 (hereafter *Synechocystis* 6803) have at best yielded only 1.1% (g/g) CDW_{edw} (Hu et al.,
72 2013; Wang et al., 2013). In eukaryotic algae, the native alkene/alkane pathway was only
73 recently discovered and there has been no work so far to engineer the specific pathways that
74 synthesize such hydrocarbons. Some species of algae are also known to naturally accumulate
75 hydrocarbons that could serve as a fuel following chemical conversion. For example, certain
76 races of the green alga *Botrococcus braunii* naturally secrete long-chain terpene
77 hydrocarbons as a significant portion of their biomass (Eroglu and Melis, 2010; Metzger and
78 Largeau, 2005). However, their use as a fuel source is made impossible by the incredibly slow
79 growth rates of this alga (Cook et al., 2017). Other oleaginous algal species can accumulate a
80 significant portion of their biomass as triacylglycerol compounds, generally under nitrogen
81 stress. Indeed, this phenomenon drove the push for the use of algae as third generation

82 biofuel feedstock in the first place. However, process design and downstream processing cost
83 considerations of large-scale algal cultivation have hindered the common adoption of algal
84 oils for transportation fuels (Quinn and Davis, 2015). Triacylglycerol stored by eukaryotic
85 algae can also be turned into transportation fuels via transesterification to liberate the
86 alkanes and alkenes from the glycerol backbone. An attractive alternative to the above
87 concepts is instead to directly secrete ready-to-use hydrocarbon products from algal cells as
88 this would overcome issues with biomass harvesting and chemical processing and thereby
89 greatly reduce process costs (Delrue et al., 2013).

90 In order to achieve such a one-step conversion of CO₂ into ready infrastructure-
91 compatible hydrocarbons with photosynthetic hosts, however, genetic reprogramming
92 becomes essential for introduction of synthetic metabolic pathways and optimization of the
93 entire system. Several enzymes have recently been reported to enable biosynthesis of fatty
94 aldehyde precursors (Akhtar et al., 2013), fatty alkanes (Bernard et al., 2012; Qiu et al., 2012),
95 and fatty alkenes (Rude et al., 2011; Rui et al., 2015; Rui et al., 2014). Combinatorial assembly
96 of such key enzymes into synthetic metabolic pathways consequently enabled a number of
97 novel opportunities for hydrocarbon biosynthesis, as described by many including (Akhtar et
98 al., 2013; Kallio et al., 2014; Sheppard et al., 2016; Zhu et al., 2017). Although such studies
99 have so far only been reported using heterotrophic microorganisms (*Escherichia coli* and
100 *Saccharomyces cerevisiae*) there are no reports of similar work in any phototrophic
101 microorganism.

102 In this study, we describe a first and systematic study to implement synthetic
103 metabolic pathways for the biosynthesis of hydrocarbon fuel in both prokaryotic and
104 eukaryotic photosynthetic microorganisms using the model strains *Synechocystis* 6803 and
105 *Chlamydomonas reinhardtii*. Several synthetic pathways towards saturated and unsaturated
106 hydrocarbons were functionally demonstrated in *Synechocystis* 6803, increasing the
107 hydrocarbon content up to 19-fold, and engineered *Chlamydomonas* accumulated 8-fold more
108 alkenes than the wild-type. Interestingly, the "best" system was achieved by transferring a
109 reconstructed pathway from eukaryotic algae into the prokaryotic cyanobacterium.

110 MATERIALS AND METHODS

111

112 *2.1 Growth conditions, genetic constructs, transformation and screening of Escherichia coli* 113 *and Synechocystis sp. PCC 6803*

114

115 *Escherichia coli* DH5 α was used to propagate all the plasmids used in this study. Strains were
116 cultivated in lysogeny broth (LB) medium (LB Broth, Sigma Aldrich), 37 °C, 180 rpm, and
117 supplemented with appropriate antibiotics (final concentration: carbenicillin 100 $\mu\text{g/ml}$,
118 chloramphenicol 37 $\mu\text{g/ml}$, kanamycin 50 $\mu\text{g/ml}$, gentamicin 10 $\mu\text{g/ml}$, and erythromycin 200
119 $\mu\text{g/ml}$).

120 *Synechocystis sp. PCC 6803*, obtained from Prof. Klaas Hellingwerf (University of
121 Amsterdam, Netherlands), was cultivated in BG11 medium without cobalt ((hereafter BG11-
122 Co), as the metal was used as an inducer in most cultures. All media contained appropriate
123 antibiotic(s) (final concentration: kanamycin 50 $\mu\text{g/ml}$, gentamicin 50 $\mu\text{g/ml}$, and
124 erythromycin 20 $\mu\text{g/ml}$). Gentamicin was only used for selection on agar plates. Precultures
125 inoculated from colonies on agar plates were grown in 6-well plates (5 ml). When the OD₇₃₀
126 reached 3-4, the culture was transferred to a 100-ml Erlenmeyer flask and the OD₇₃₀ was
127 adjusted to 0.2 by adding BG11-Co medium to a final volume of 25 ml containing appropriate
128 antibiotic(s). The cultivation was carried out for 10 days at 30 °C with continuous illumination
129 at 60 $\mu\text{mol photons m}^{-2} \text{s}^{-1}$ and 1% (v/v) CO₂. Each main treatment culture was induced on
130 day 2 and samples were taken for measurement of OD₇₃₀ and metabolites day 6 and 10. All
131 cultivations were carried out in an AlgaeTron230 (Photon Systems Instruments) (PSI) at
132 30 °C with continuous illumination at 60 $\mu\text{mol photons m}^{-2} \text{s}^{-1}$ and 1% (v/v) CO₂, except
133 where noted (100-300 $\mu\text{mol photons m}^{-2} \text{s}^{-1}$). A representative growth curve and all final
134 OD₇₃₀ values are shown in Supplementary Figure 1.

135 All plasmids (Supplementary Table 1A) used for transformation of cyanobacteria were
136 assembled using the BASIC Assembly method (Storch et al., 2015). Linkers were designed
137 using the R20DNA software: <http://www.r2odna.com/> and obtained from Integrated DNA
138 Technologies Incorporated. The details of all linkers, primers and DNA parts used to construct
139 each plasmid are given in Supplementary Tables 1B, 1C and 1D.

140 For transformation by natural assimilation, each *Synechocystis sp. PCC 6803* strain
141 was inoculated from freshly prepared colonies on agar plates into 25 ml BG11-Co with a
142 starting OD 0.02. The cells were harvested when the OD₇₃₀ reached 0.4-0.7, washed in 10 ml
143 BG11-Co twice, and resuspended in 500 μL BG11-Co. One hundred microliters of concentrated

144 liquid culture were mixed with four to seven micrograms of plasmid and incubated at 30°C
145 with continuous illumination at 60 $\mu\text{mol photons m}^{-2} \text{s}^{-1}$ and 1% (v/v) CO₂ for 12-16 h prior
146 to plating on BG11-Co agar containing 10% strength of antibiotic. To promote segregation,
147 individual colonies were restreaked on BG11-Co agar with higher antibiotic concentration. To
148 check the segregation, the biomass was resuspended in nuclease free water and exposed to
149 two freeze-thaw cycles (95°C, -80°C). Following centrifugation, 3 μL was used as a template
150 for a diagnostic polymerase chain reaction (PCR). Primers used for each PCR are listed in
151 Supplementary Table 1C. Only fully segregated mutants were used in further experiments. All
152 cyanobacteria strains used in the study are listed in Supplementary Table 2.

153 For transformation by triparental conjugation, one hundred microliters of the cargo
154 strain (*E. coli* HB101 (already carrying the pRL623 plasmid)), conjugate strain (ED8654
155 (Elhai and Wolk, 1988)), and *Synechocystis* sp. PCC 6803 (OD₇₃₀ ~1) were mixed and
156 incubated for 2 h (30 °C, 60 $\mu\text{mol photons m}^{-2} \text{s}^{-1}$). Prior to mixing, all the *E. coli* and
157 cyanobacteria strains were washed with fresh LB and BG11-Co medium, respectively, to
158 remove the antibiotics. After 2 h of incubation, the culture mix was transferred onto BG11
159 agar plates without antibiotic and incubated for 2 d (30 °C, 60 $\mu\text{mol photons m}^{-2} \text{s}^{-1}$). After 2 d
160 of incubation, cells were scraped from the agar plate, resuspended in 500 μL of BG11-Co
161 medium, and transferred onto a new agar plate containing 20 $\mu\text{g/ml}$ erythromycin. Cells were
162 allowed to grow for one week until colonies appeared. Individual colonies were restreaked
163 onto a new plate containing 20 $\mu\text{g/ml}$ erythromycin and used for subsequent experiments.

164

165 ***2.2 Growth conditions, genetic constructs, transformation and screening of Chlamydomonas*** 166 ***reinhardtii***

167 *C. reinhardtii* strain UVM4 was used in this work (Neupert et al., 2009) graciously provided by
168 Prof. Dr. Ralph Bock)). The strain was routinely maintained on Tris acetate phosphate (TAP)
169 medium (Gorman and Levine, 1965) either with 1.5% agar plates or in liquid with 250 μmol
170 $\text{photons m}^{-2} \text{s}^{-2}$. Transformation was conducted with glass bead agitation as previously
171 described (Kindle, 1990). The amino acid sequences of *C. reinhardtii* native fatty acid
172 photodecarboxylase (FAP) (Uniprot: A8JHB7; (Sorigué et al., 2017)), *E. coli* thioesterase A
173 (TesA: P0ADA1), *Jeotgalicoccus* sp. ATCC 8456 terminal olefin-forming fatty acid
174 decarboxylase (OleT_{JE}) (E9NSU2), and *Rhodococcus* sp. NCIMB 9784 P450 reductase RhFRED
175 (Q8KU27) were codon optimized and copies of the intron 1 of ribulose biphosphate
176 carboxylase small subunit 2 (RBCS2) were added throughout the coding sequences as
177 previously described (Baier et al., 2018). The nucleotide sequences of optimized intron

178 containing genes have been submitted to NCBI, accession numbers can be found in
179 Supplementary Table 3. All synthetic genes were chemically synthesized (GeneArt) and
180 cloned between *Bam*HI-*Bgl*II in the pOpt2_PsaD_mVenus_Paro or pOpt2_PsaD_mRuby2_Ble
181 vectors (Wichmann et al., 2018). PsaD represents the 36 amino acid photosystem I reaction
182 center subunit II (PsaD) chloroplast targeting peptide (CTP) (Lauersen et al., 2015) between
183 *Nde*I-*Bam*HI restriction sites of the pOpt2 vectors (Wichmann et al., 2018). The native FAP
184 enzyme was designed to contain an additional glycine codon at aa position 33 to allow the
185 insertion of a *Bam*HI site at the border of the predicted CTP. The whole synthetic enzyme
186 including native targeting peptide was cloned *Nde*I-*Bgl*II and a version was created with the
187 PsaD CTP built by cloning *Bam*HI-*Bgl*II into the vectors described above. Fusions of different
188 sequences were made by digestion and complementary overhang annealing of the *Bam*HI-
189 *Bgl*II mediated restriction sites for each respective construct as needed to obtain the fusions
190 used in the present work (Supplementary Figure 2). After transformation, expression was
191 confirmed by fluorescence microscopy screening for mVenus (YFP) or mRuby2 (RFP)
192 reporters as previously described (Lauersen et al., 2016; Wichmann et al., 2018). Individual
193 mutants were subjected to Western blotting and immuno detection to determine whether
194 full-length protein products were formed (anti-GFP polyclonal HRP linked antibody, Thermo
195 Fisher Scientific). Wide-field fluorescence microscopy was used to confirm chloroplast
196 localization of YFP-linked constructs as previously described (Lauersen et al., 2016).

197

198 ***2.3 Product analysis***

199 Three different extraction and analysis protocols were used for the analysis of (1) acids, (2)
200 alcohols and (3) alkanes as well as alkenes from cyanobacteria cultures. For each analyte
201 group, liquid cultures in flasks were mixed well by shaking prior to transferring 2 mL of liquid
202 culture into a PYREX round bottom threaded culture tube (Corning, Manufacturer Part
203 Number: 99449-13).

204 For fatty acid analysis, free fatty acid extraction was performed as described
205 previously (Liu et al., 2011; Yunus and Jones, 2018). In brief, two hundred microliters of 1 M
206 H₃PO₄ were added to acidify each 2 mL culture and spiked with 100 µg pentadecanoic acid
207 (Sigma Aldrich) as an internal standard. Four millilitres of n-hexane (VWR Chemicals) was
208 added and the mixture vortexed vigorously prior to centrifugation at 3500 x g for 3 min. The
209 upper hexane layer was then transferred to a fresh PYREX round bottom threaded culture
210 tube and evaporated completely under a stream of nitrogen gas. Five hundred microliters of
211 1.25 M HCl in methanolic solution were added to methyl esterify the free fatty acid at 85 °C for

212 2 h. Samples were cooled to room temperature and 500 μL of hexane was added for
213 extraction of the fatty acid methyl esters (FAMES).

214 For fatty alcohol, alkane and alkene analysis, extraction was done as described
215 previously (Zhou et al., 2016) with modification. Briefly, 2 mL of liquid culture were spiked
216 with 50 μg 1-nonanol, 100 μg octadecane, and 100 μg 1-pentadecanol and mixed with 4 mL of
217 chloroform:methanol (2:1 v/v) solution. The mixture was vortexed vigorously and
218 centrifuged at 3500 x g for 3 min. The lower organic phase was then transferred into a new
219 glass tube and extraction was repeated one more time. The lower organic phase was
220 combined and dried under a stream of nitrogen gas. For fatty alcohol derivatization, the
221 dried extract was resuspended in 100 μL chloroform, mixed with 100 μL of N, O-
222 bistrifluoroacetamide (BSTFA) (TCI Chemicals) and transferred to an insert in a GC vial that
223 was incubated at 60 $^{\circ}\text{C}$ for 1 h prior to GC analysis. Note that no derivatization was needed
224 for the analysis of hydrocarbons.

225 Samples (1 μL) were analyzed using an Agilent Technologies (Santa Clara, CA, USA)
226 7890B Series Gas Chromatograph (GC) equipped with an HP-5MS column (pulsed split ratio
227 10:1 and split flow 10 ml/min), a 5988B Mass Spectrophotometer (MS) and a 7693
228 Autosampler. For the acids the GC oven program followed an initial hold at 40 $^{\circ}\text{C}$ for 3 min, a
229 ramp at 10 $^{\circ}\text{C}\cdot\text{min}^{-1}$ to 150 $^{\circ}\text{C}$, a second ramp at 3 $^{\circ}\text{C}\cdot\text{min}^{-1}$ to 270 $^{\circ}\text{C}$, a third ramp at 30 $^{\circ}\text{C}\cdot\text{min}^{-1}$
230 to 300 $^{\circ}\text{C}$, and a final hold for 5 min. For alcohols and alkenes, there was an initial hold at 40
231 $^{\circ}\text{C}$ for 0.5 min, a ramp at 10 $^{\circ}\text{C}\cdot\text{min}^{-1}$ to 300 $^{\circ}\text{C}$, and a final hold for 4 min. For alkanes, the oven
232 was initially held at 70 $^{\circ}\text{C}$ for 0.5 min, a ramp at 30 $^{\circ}\text{C}\cdot\text{min}^{-1}$ to 250 $^{\circ}\text{C}$, a second ramp at 40
233 $^{\circ}\text{C}\cdot\text{min}^{-1}$ to 300 $^{\circ}\text{C}$, and a final hold for 2 min. The acids, alkanes and alcohols were quantified
234 by comparing the peak areas with that of the internal standards: pentadecanoate (for all
235 acids), octadecane (for all alkanes), 1-nonanol (for C8 to C12 alcohols) and 1-pentadecanol
236 (for C14 alcohols and above). The quantity of the main products (C15 and C17 alkanes, C15
237 alkene, and C12, C14, C16, and C18 alcohols and acids) were also corrected with their
238 respective mass spectrometer response factors obtained using dilution series of commercial
239 standards.

240 Gas chromatography mass spectroscopy (GC-MS) aimed at identification of
241 hydrocarbon products from *C. reinhardtii* was conducted with solvent extracted samples
242 following previously described protocols and internal standards (Lauersen et al., 2016).
243 Quantification of 7-heptadecene was performed with serial dilutions (1 to 900 μM) of
244 commercial 1-heptadecene standard (Acros Organics) in dodecane using extracted ion
245 chromatograms with masses 55.00, 69.00, 91.00, 93.00, 83.00, 97.00, and 111.00.

246 RESULTS AND DISCUSSION

247

248 Several synthetic pathway designs were considered, all commencing with the liberation of
249 "free" fatty acids from the native fatty acid biosynthesis pathway (Fig. 1), the presumed native
250 precursor for many of the decarboxylating enzymes evaluated in this study.

251

252 ***3.1 Over-production of free fatty acids as precursor for hydrocarbon biosynthesis -*** 253 ***Expression of Escherichia thioesterase deregulates lipid membrane biosynthesis in*** 254 ***Chlamydomonas***

255

256 In order to liberate FFAs in cyanobacteria we over-expressed the *E. coli* C16-C18 specific
257 thioesterase TesA (Cho and Cronan, 1995) lacking its native signal sequence peptide ("TesA")
258 and deleted the gene encoding the native fatty acyl ACP synthase (*aas*) (Kaczmarzyk et al.,
259 2010; Liu et al., 2011)(Fig. 1). The native signal sequence peptide directs TesA to the
260 periplasm in *E. coli* (Cho et al 1993) and its removal is assumed to maximize the liberation of
261 "free" fatty acids also in cyanobacteria by retaining the enzyme in the cytosol. Such
262 "TesA/ Δ *aas* engineering has previously been reported several times before in cyanobacteria
263 (Liu et al., 2011, Ruffing et al., 2014; Work et al., 2015; Kato et al., 2017), with 13% (g/g cell
264 dry weight (CDW)) as the highest reported fatty acid yield in *Synechocystis* 6803 (Liu et al.,
265 2011). Further potentially stackable modifications to the strain or process have also been
266 reported. For example, by employing a solvent overlay, Kato et al., 2017 reported up to 36%
267 (g/g ~~cdw~~-CDW) of fatty acids excreted into the media using "TesA/ Δ *aas* *Synechococcus*
268 *elongatus* sp. PCC 7942. In the present study, the chromosomal integration of '*tesA* into the
269 *psbA2* site (slr1311) of *Synechocystis* 6803 Δ *aas* (Δ *aas*-"TesA), under the control of the light-
270 inducible promoter PpsbA2S, resulted in the excretion of ~~of~~ C14:0 (3.5 mg/g CDW), C16:0
271 (23.2 mg/g CDW) and C18:0 (5.7 mg/g CDW) fatty acids with a chain-length distribution that
272 is in agreement with previously reported findings (Liu et al., 2011) (Fig. 2A; Supplementary
273 Fig. 3).

274 Overproduction of the same thioesterase ("TesA) and targeting of the enzyme product
275 to the chloroplast was possible in *C. reinhardtii*. The synthetic algal optimized *E. coli*' *tesA*
276 gene was fused with an N-terminal PsaD-based chloroplast targeting peptide and a C-terminal
277 yellow fluorescent protein (YFP) encoding gene. Both the coding genes were interspersed by
278 synthetic introns (Fig. 2B) as previously described to enhance transgene expression from the
279 nuclear genome (Baier et al., 2018). Fluorescence microscopy indicated correct localization of

280 the 'TesA fluorescent protein fusion to the algal chloroplast (Fig. 2C). Although no FFA could
281 be detected in the culture medium, a difference was observed in the lipid profile of the green
282 algal cells, suggesting a de-regulation of fatty acid synthesis that specifically affected the polar
283 lipid fraction of the alga. This was indicated by an over-accumulation of C18:1n9c chain
284 lengths in the polar lipid membranes, with subtle changes observed in other acyl-ACP species
285 such as C14:0 (Fig. 2D; Supplementary Fig. 4). Thus, 'TesA_YFP clearly had an impact on lipid
286 metabolism in the eukaryotic algal host, but, the capture of liberated FFAs by acyl-ACP or -
287 CoA synthases [areis](#) likely too effective, thereby limiting the application of the same
288 engineering principles carried out for cyanobacteria. An annotated gene product in
289 *Chlamydomonas* Cre06.g299800 (Phytozome v5.5) has some sequence similarity to
290 *Synechocystis aas* and therefore represents an interesting target for future strategies to block
291 native re-uptake of FFA in the green algal cell.

292 Having achieved strains with enhanced accumulation of FFA in *Synechocystis*, or at
293 least a perturbation to the lipid biosynthetic system in *Chlamydomonas*, we proceeded to
294 investigate enzymes that further convert FFAs into hydrocarbon end-products.

295 296 **3.2 Effective conversion of free fatty acids into alkenes using UndB**

297 Three different enzymes that catalyze the conversion of fatty acids into alkenes have been
298 recently reported, OleT (Rude et al., 2011), UndA (Rui et al., 2014), and UndB (Rui et al., 2015)
299 (Fig. 1). So far, the best reported productivity in both *E. coli* (Rui et al., 2015) and *S. cerevisiae*
300 (Zhou et al., 2018) has been with UndB.

301 In *Synechocystis* 6803, we transformed the Δaas -'TesA strain with an RSF1010-based
302 plasmid harboring a codon-optimized *undB* under the control of the P_{clac143} promoter
303 (Markeley et al., 2014), thereby generating the strain Δaas -'TesA-1010-UndB (Fig. 3A). After
304 10 days of cultivation, both the free fatty acids and alkanes were extracted and analyzed as
305 described in the Materials and Methods section. The accumulation of free fatty acids was
306 markedly reduced in the Δaas -'TesA-1010-UndB strain (Fig. 3B, 3C). In its place, both 1-
307 pentadecene and 1-heptadecene accumulated with a molar yield suggesting approximately
308 55% conversion of 'TesA-liberated FFAs (compare Fig. 3C with Fig. 3D). More than >84% of
309 the FFAs disappeared relative to the Δaas -'TesA strain suggesting that UndB was catalytically
310 efficient *in vivo* and that the electrons required in the UndB reaction were fortunately
311 supplied by an unknown source. The Δaas -'TesA-1010-UndB strain displayed a lower biomass
312 accumulation than the controls (Δaas -empty and Δaas -'TesA strains) (Supplementary Fig. 1),
313 presumably due to product toxicity imparted by the alkenes. A direct comparison with the

314 conversion efficiency in *E. coli* is not possible since the FFA conversion efficiency was not
315 reported in the original work (Rui et al., 2015). Despite the disappearance of C14:0 fatty acids
316 in the Δaas -TesA-1010-UndB strain, no measurable 1-tridecene (the expected corresponding
317 alkene) was observed in the whole culture extracts (Fig. 3C). None of the observed alkene
318 products were secreted extracellularly (Fig. 3E).

319 In *Chlamydomonas*, we attempted to over-produce the *Jeotgalicoccus* sp. terminal
320 olefin-forming fatty acid decarboxylase (OleT_{JE}) and the *Rhodococcus* sp. P450 reductase
321 (RhFRED). OleT_{JE} was chosen as it could theoretically produce C17:1 and C15:0 hydrocarbons
322 from the major lipid species of the green algal cell, C18:1 and C16:0, respectively (Fig. 1).
323 Fusion to RhFRED has been reported to enable hydrogen peroxide-independent
324 decarboxylase activity (Liu et al., 2014). The protein products of this decarboxylase and its
325 fusion in either orientation to RhFRED could be detected by Western blotting and located to
326 the algal chloroplast in fluorescence microscopy (Supplementary Figure 5). However, no
327 differences in GC-MS profiles between the parental and expression strains could be found in
328 either dodecane solvent overlays or cell-pellet solvent extracts.

329

330 ***3.3 Transfer of the CAR/ADO based pathway from E. coli to Synechocystis 6803 resulted in*** 331 ***the accumulation of fatty alcohols and a reduction in alkane accumulation***

332 Carboxylic acid reductases (CAR) have been previously used to construct a number of
333 synthetic pathways for alkane biosynthesis in heterotrophic microorganisms (Akhtar et al.,
334 2013; Kallio et al., 2014; Sheppard et al., 2016; Zhu et al., 2016). Although CAR appears to
335 have a high capability for converting fatty acids into corresponding fatty aldehydes (Akhtar et
336 al., 2013) (Fig. 1), a bottleneck in previous heterotrophic pathways is the subsequent
337 conversion into alkanes by kinetically slow ADO enzymes and competition with native
338 aldehyde reductases that more effectively convert aldehydes into alcohols (Kallio et al., 2014;
339 Sheppard et al., 2016).

340 Since *Synechocystis* 6803 natively harbors an aldehyde deformylating oxygenase
341 (ADO) with the appropriate substrate specificity (Khara et al., 2013) (Fig. 1), we first
342 combined TesA with CAR and evaluated its ability to supply the native ADO. A synthetic
343 operon expressing all required parts (including the CAR maturation protein Sfp) was
344 introduced to the RSF1010 plasmid backbone (Fig. 4A) and used to transform *Synechocystis*
345 6803 Δaas , thus creating the strain Δaas -1010-TPC2. This strain accumulated both fatty acids
346 (Fig. 4B and 4D) and fatty alcohols (Fig. 4C and 4E). The quantity of heptadecane was reduced
347 in Δaas -1010-TPC2 relative to Δaas -1010-'TesA (Fig. 4F). This suggests that the introduced

348 CAR-based pathway had not managed to increase the supply of fatty aldehydes to the native
349 ADO. CAR and native aldehyde reductase(s) had instead very effectively converted >90% of
350 the FFA pool (Fig. 4D) into corresponding alcohols (Fig. 4E). The most likely reason for the
351 increase in FFA in latter experiments is due to increased expression of 'TesA using the
352 RSF1010 plasmid in Δaas -1010-'TesA (Fig. 4D), relative to the amount of 'TesA when
353 expressed from the chromosomal location in Δaas -'TesA (Fig. 3C). Similar observations have
354 also been previously reported by Angermayr et al. (Angermayr et al., 2014). The different
355 promoters used in the two strains are also likely to have influenced the outcome, however, we
356 are not aware of any studies that directly compare the two promoters head-to-head.

357 Substantial quantities of fatty alcohols did accumulate in the Δaas -1010-TPC2 strain,
358 suggesting that the supply of fatty aldehydes is not the limiting factor. One possibility is that
359 the native aldehyde reductases are simply much more active than the native ADO (Eser et al.,
360 2011; Lin et al., 2013). Another possibility is that native ADO and AAR form a close metabolon
361 *in vivo* (Warui et al., 2015) that locks out access to ADO from external supplies of fatty
362 aldehydes. In order to test this possibility, we attempted to create a variant of Δaas -1010-
363 TPC2 that also included chromosomal ADO over-expression cassette under the PpsbA2S
364 promoter. Despite numerous transformation and segregation attempts, however, we were
365 unable to isolate any stable segregants. Another complementary strategy that could be
366 considered in future work would be to eliminate native aldehyde reductases, as previously
367 carried out in earlier *E. coli* studies (Kallio et al., 2014; Sheppard et al., 2016), although the full
368 complement of fatty aldehyde reductase encoding genes in cyanobacteria remains unknown.
369 Given the lack of success in producing alkanes with the CAR/ADO route in cyanobacteria we
370 then considered alternative options for both cyanobacteria and algae.

371 372 ***3.4 Engineering of the native eukaryotic algae pathway and transfer to cyanobacteria results*** 373 ***in enhanced conversion of CO₂ into alkanes***

374 A fatty acid photodecarboxylase (FAP) that directly converts saturated and unsaturated FFAs
375 into alkanes and alkenes, respectively, was recently discovered in eukaryotic algae (Sorigué et
376 al., 2017). In *Chlamydomonas*, the source of free fatty acids for the native alkene pathway
377 remains unknown, although the degradation of membrane lipids may release some FFA
378 (illustrated in Fig. 1). However, we would expect increased accumulation of alkanes in algae if
379 we were able to increase the cellular quantity of the native FAP and/or introduce synthetic
380 routes to the FFA precursors.

381 Accordingly, we overproduced native FAP from *C. reinhardtii* (CrFAP) on its own or in
382 combination with co-production of *E. coli*'TesA. The over-expression of CrFAP was carried
383 out either with its native chloroplast targeting peptide (CTP) or the robust PsaD CTP which
384 has been previously used to mediate chloroplast localization of numerous reporters
385 (Lauersen et al., 2015; Lauersen et al., 2018; Rasala et al., 2013). In order to minimize any
386 native regulation of the genomic sequence, the gene was subjected to a strategy of gene design
387 which has recently been shown to enable robust transgene expression from the nuclear
388 genome of this alga (Baier et al., 2018). Briefly, the sequence was codon optimized based on
389 its amino acid sequence and multiple copies of the first intron of the *C. reinhardtii* ribulose-
390 1,5-bisphosphate carboxylase/oxygenase (RuBisCo) small subunit 2 (rbcS2i1,
391 NCBI: X04472.1) were spread throughout the coding sequence *in silico*. This nucleotide
392 sequence was chemically synthesized and used for expression from the algal nuclear genome.
393 This strategy has previously enabled heterologous overproduction of non-native
394 sesquiterpene synthases (Lauersen et al., 2016; Lauersen et al., 2018; Wichmann et al., 2018),
395 and in the present study also the 'TesA, OleT_{JE}, and RhFRED proteins. However, complete
396 codon optimization and synthetic intron spreading of a native gene has not yet been
397 demonstrated in eukaryotic algae. Both constructs mediated full-length target protein
398 production which was detectible in Western blots (Supplementary Fig. 5B). Replacing the
399 native CTP with the PsaD CTP enabled more reliable and robust accumulation, which was
400 detectible as YFP signal in the algal chloroplast (Supplementary Fig. 6) and strong bands in
401 transformants expressing this construct in Western blots (Supplementary Fig. 5B). The
402 parental UVM4 strain was found to contain ~0.5 mg/g 7-heptadecene as a natural product
403 (Supplementary Fig. 7). Transformants generated with the CrFAP construct (Cr8) were found
404 to contain up to 8x more of this alkene compared to the empty vector (Cr2) control strain (up
405 to 8.5 ± 1.5 mg/g, Fig. 5) which was found almost exclusively within the biomass
406 (Supplementary Fig. 7). The product was not detected in dodecane solvent overlays. CrFAP
407 accepts a very specific substrate (*cis*-vaccenic acid, C18:1 *cis*Δ11) *in vivo* (Sorigué et al., 2017),
408 which corresponds to the accumulation of only 7-heptadecene as the only detected increased
409 product. This substrate is an unusual FA, and is likely not naturally abundant in the algal cell.
410 Notably, any attempts to increase the availability of free fatty acids using *E. coli*'TesA did not
411 result in any increase in the quantity or diversity of accumulated alkanes. Future enzyme
412 engineering will likely be able to overcome this substrate specificity and increase overall
413 yields of liberated hydrocarbons. However, a strategy which would allow secretion of these
414 molecules, similar to the capture of heterologous terpenoids in dodecane solvent overlay

415 (Lauersen et al., 2016; Lauersen et al., 2018; Wichmann et al., 2018), would be an attractive
416 next target in order to enable photo-biocatalysis of hydrocarbons from the algal biomass.

417 Given the success with the FAP pathway in *Chlamydomonas* (present study) and
418 earlier work in *E. coli* (Sorigué et al., 2017), as well as finding that 'TesA expression can
419 substantially enhance the FFA pool in cyanobacteria, a synthetic FAP pathway was an obvious
420 choice to consider also for the prokaryotic host. We therefore proceeded to implement a
421 reconstituted variant of the eukaryotic algae pathway in cyanobacteria by combining TesA
422 with FAP. Given the genetic instability challenges with the CAR/ADO system (see Section 3.3)
423 we shifted our constructs to the more tightly repressed Pcoa promoter (Peca et al., 2008) for
424 controlling the expression of *E. coli* TesA and the *Chlorella variabilis* FAP from the RSF1010
425 plasmid (Fig. 6A). We noted that the yield of FFA was substantially increased when driving the
426 expression of TesA with the Pcoa promoter (Fig. 6C) compared to Pclac143 (Fig. 4D).

427 Despite the dominance of C16:0 fatty acids released by 'TesA in *Synechocystis* 6803,
428 alongside minor fractions of C14:0 and C18:0, the C17:0 alkanes dominated the hydrocarbon
429 fraction at the lower light intensity ($100 \mu\text{mol photons m}^{-2} \text{s}^{-1} \mu\text{E}$) (Fig. 6B and 6D). This
430 alkane profile in *Synechocystis* 6803 is very different to that observed in *E. coli* without over-
431 expression of 'TesA (see Fig. S4 in (Sorigué et al., 2017)). We also observed substantial peaks
432 of 8-heptadecene and 6,9-heptadecadiene, as suggested by comparison with a NIST mass
433 spectrometry library, although a lack of standards prohibited confirmation (Supplementary
434 Figure 8). Curiously, these alkenes were only detected at day 6 and were not present in
435 samples harvested on day 10. As the fatty chain-length profiles differ when the same
436 thioesterase is expressed in different *E. coli* strains (Akhtar et al., 2015; Jing et al., 2011), this
437 suggests that the *in vivo* product profile of any thioesterase-dependent pathway also is
438 dependent on what the fatty acid synthesis pathway provides, not just the substrate
439 specificity of the thioesterase used.

440 Removal of the predicted chloroplast targeting sequence of FAP ('FAP) resulted in a
441 doubling of the alkane yield, this time accompanied also by C15 pentadecane. As the FAP
442 reaction is light-dependent, we also did a simple evaluation of this environmental factor.
443 When the light intensity was tripled, the total alkane production with the Δaas -1010-'TesA-
444 'FAP strain increased to a yield of 77.1 mg/g CDW (19-fold enhancement relative to Δaas) and
445 a titer of 111.2 mg/L. The product profile also shifted (Fig. 6D) despite the lack of a similar
446 shift in the remaining FFA fraction (Fig. 6B), suggesting that the substrate specificity of FAP is
447 flexible and interestingly might change in response to a change in its cellular environment.

448 At 100 $\mu\text{mol photons m}^{-2} \text{s}^{-1}$ the introduction of 'FAP resulted in a drop in FFA
449 accumulation of up to 90% (for C18:0), whilst for C16:0 there was only a 60% reduction (Fig.
450 6C). Despite repeated trials, the recovery in the measurable fatty acid to alkane conversion
451 remained poor for C16:0 in comparison to C18:0 and the other pathways tested in
452 *Synechocystis* 6803. This may be explained by an impact on 'TesA accumulation in the
453 constructs also carrying the gene coding for 'FAP. Nevertheless, the reconstituted eukaryotic
454 algae alkane pathway was more responsive to introduced modifications in the prokaryotic
455 cyanobacterium than in its native host, though this most likely is explained by challenges
456 associated with the release of FFA in the latter.

457 Although a substantial amount of both alkanes and alkenes were produced by the
458 engineered strains, their performance likely needs to be improved before any application can
459 be considered. Given that no genetically engineered phototrophic microalgae is currently used
460 for commercial purposes (as far as we are aware), and LCA-studies with non-catalytic systems
461 indicate a low predicted energy return on investment (EROI) (Carneiro et al., 2017), also
462 other challenges with commercial algal biotechnology (e.g. contamination, bioreactor cost,
463 energy consumption, etc) will need to be addressed.

464

465 **CONCLUSIONS**

466 The different biosynthetic systems presented in this study varied in terms of cellular context,
467 compartmentation, promoters, operon structures and expression platforms, thus precluding a
468 any direct comparison within and between the two species studied. However, the relative
469 conversion efficiencies and absolute functionalities provide for a valid comparison. As such, it
470 could be seen that the conversion of free fatty acids into alkenes by UndB and alkanes by FAP
471 were effective (>50% conversion, for individual fatty acids up to >90% conversion), and that
472 the native FAP pathway in *Chlamydomonas* was amenable to manipulation but that the
473 inability to increase the FFA pool hindered further progress. Consequently, for alkanes, the
474 reconstruction of the eukaryotic algae pathway in the prokaryotic cyanobacteria host
475 provided a more productive system than the partially synthetic pathways in either of the
476 prokaryotic (CAR-ADO) or eukaryotic hosts (TesA-FAP).

477 This work describes several approaches to employ synthetic metabolism and
478 substantially exceed native capabilities for hydrocarbon biosynthesis in well-established
479 model cyanobacteria and algae. Although even greater yields have been reported in
480 oleaginous algae and cyanobacteria that are natively endowed to accumulate lipids, the ability
481 to introduce synthetic metabolic pathways in model strains opens up possibilities for tailored
482 choice of both products and hosts. Importantly, the present work is based on first generation
483 strains and further improvement is likely with systematic optimization of both strains and
484 cultivation conditions, including the use of superior engineered or natural enzyme variants.

485

486

487 **ACKNOWLEDGEMENTS**

488 This project has received funding from the European Union's Horizon 2020 research and
489 innovation programme project PHOTOFUEL under grant agreement No 640720. IY received a
490 PhD scholarship from Indonesia Endowment Fund for Education (LPDP). The authors would
491 also like to thank Dr. Daniel Jaeger for assistance with lipid extraction from *C. reinhardtii*.

492

493

494

495 **FIGURE LEGENDS**

496

497 **Figure 1. Native and synthetic metabolic pathways evaluated in the present study with**
498 **incomplete stoichiometry.** The graphic illustration shows the introduced TesA (thioesterase
499 (Cho and Cronan, 1995)), CAR (carboxylic acid reductase (Akhtar et al., 2013)), UndA
500 (responsible for 1-undecene biosynthesis in *Pseudomonas* (Rui et al., 2014)), UndB (also
501 responsible for 1-undecene biosynthesis in *Pseudomonas* (Rui et al., 2015)), OleT
502 (responsible for olefin biosynthesis in *Jeotgaliococcus* (Rude et al., 2011)) and FAP (fatty acid
503 photodecarboxylase (Sorigué et al., 2017)) enzymes alongside the native AAR/ADO (acyl-ACP
504 reductase and aldehyde deformylating oxygenase (Schirmer et al., 2010)), AHR (aldehyde
505 reductase, unknown) and FAP enzymes. Blue reactions are non-native and those in grey are
506 native. The red cross indicates deletion of the *aas* gene.

507

508 **Figure 2. Engineering for enhanced accumulation of free fatty acids.** (A) Representative total
509 ion count chromatograms for *Synechocystis* 6803 strains Δaas -TesA (black) vs. Δaas only
510 (orange) extracted on day 10 of cultivation (induced day 2). Peak identities: (3) Heptadecane,
511 (4) Tetradecanoic acid, (5) Hexadecanoic acid, (6) 9,12-octadecadienoic acid, (7) 9-
512 octadecenoic acid, (8) Octadecanoic acid. (B) Graphic representation of the constructs used to
513 transform *Chlamydomonas*. CTP = Chloroplast Transit Peptide. (C) Fluorescence microscopy
514 of representative strains indicating appropriate chloroplast localization of the CTP_'TesA_YFP
515 construct. (D) Total (TL), polar (PL), and neutral (NL) gravimetric lipid fractions of
516 *Chlamydomonas* parental strain and TesA overproducing strains under nutrient replete
517 conditions (N+) and after 96 hours of nitrogen depletion (N-). PL is significantly greater in +N
518 for TesA: ttest, p:0.047 (indicated by an asterisk).

519

520 **Figure 3. Over-expression of UndB results in effective (>50%) conversion of fatty acids into**
521 **corresponding alkenes.** (A) Graphic representation of the genetic modification of
522 *Synechocystis* sp. PCC 6803 and the plasmid used for UndB expression. (B) GC-MS
523 chromatograms with extracts from the two different strains (w/wo UndB); Δaas -1010-'TesA
524 (black) and Δaas -1010-'TesA-UndB (orange). (C) The free fatty acid yield (relative to biomass)
525 in the whole cultures of the two strains, subdivided into the three dominant chain-lengths. (D)
526 The yield of alkenes in the whole cultures of the two strains, subdivided into the three
527 dominant chain-lengths. (E) The localization of the alkene products in whole cultures of the
528 two strains. Peak identities: (1) 1-pentadecene, (2) 1-heptadecene, (3) heptadecane, (4)

529 tetradecanoic acid, (5) hexadecanoic acid, (6) 9,12-octadecadienoic acid, (7) 9-octadecenoic
530 acid, (8) octadecanoic acid. Data are mean \pm SD from three biological replicates. All samples
531 were extracted on day 10.

532

533 **Figure 4. The CAR-dependent pathway produces mainly fatty alcohols.** (A) Graphic overview
534 (not to scale) illustrating the main constructs studied in the figure. (B) Total ion
535 chromatogram from extracts of $\Delta aas-1010$ -*TesA* (black) and $\Delta aas-1010$ -TPC2 (orange). (C)
536 Fatty alcohol profile from extracts of Δaas -TPC2. The yield of fatty acids (D), alcohols (E) and
537 alkanes (F). Peak identities: (2) 1-dodecanol, (3) heptadecane, (4) 1-tetradecanol, (5) 1-
538 hexadecanol, (6) 9,12-octadecadien-1-ol, (7) 9-octadecen-1-ol, (8) 1-octadecanol, (9)
539 dodecanoic acid, (10) tetradecanoic acid, (11) hexadecanoic acid, (12) octadecanoic acid. Data
540 are mean \pm SD of three biological replicates. Cultures were induced on day 2 following
541 dilution and samples were extracted on day 10.

542

543 **Figure 5. CrFAP over-expression increases 7-heptadecene yield, but heterologous thioesterase**
544 **(*TesA*) expression, its co-expression, and C- or N-terminal fusion with CrFAP has no benefit.**
545 Mutants expressing indicated constructs (left panel) were cultivated for seven days in TAP
546 medium with 250 $\mu\text{mol photons s}^{-1} \text{m}^{-2}$ constant illumination and cell pellets were extracted
547 with cell rupture by glass beads and dodecane for yield quantification of 7-heptadecene via
548 GC-MS (bar graph, right). All constructs bear a PsaD chloroplast targeting peptide (CTP) to
549 allow protein transit to the chloroplast. Arrows and plus sign indicate co-expression in double
550 transformed mutants. Error bars represent 95% confidence intervals of single strains
551 cultivated in biological triplicates.

552

553 **Figure 6. Conversion of free fatty acids into alkanes in cyanobacteria using FAP.** (A) Graphic
554 representative of the plasmids used to transform *Synechocystis* sp. PCC 6803. (B) Total ion
555 chromatogram from Δaas -Pcoa-*TesA* (left) and $\Delta aas-1010$ -Pcoa-*TesA*-FAP (100 [μmol](#)
556 [photons s⁻¹ m⁻² \(μE\)](#)~~mE~~, middle; 300 [μmol photons s⁻¹ m⁻²mE](#), right). The free fatty acid (C)
557 and alkane (D) yield in all tested strains. Data are mean \pm SD of three biological replicates.
558 Samples were extracted on day 10. Peak: (1) heptadecane, (2) octadecane (internal standard),
559 (3) pentadecane, (4) undecane, (5) tridecane, (6) hexadecanoic acid.

560

561

562

563 **REFERENCES**

- 564 Ajjawi, I., Verruto, J., Aqui, M., Soriaga, L. B., Coppersmith, J., Kwok, K., Peach, L., Orchard, E.,
565 Kalb, R., Xu, W., Carlson, T. J., Francis, K., Konigsfeld, K., Bartalis, J., Schultz, A., Lambert,
566 W., Schwartz, A. S., Brown, R., Moellering, E. R., 2017. Lipid production in
567 *Nannochloropsis gaditana* is doubled by decreasing expression of a single
568 transcriptional regulator. *Nat Biotechnol.* 35, 647-652.
- 569 Akhtar, M. K., Dandapani, H., Thiel, K., Jones, P. R., 2015. Microbial production of 1-octanol - a
570 naturally excreted biofuel with diesel-like properties. *Metabolic Engineering*
571 *Communications.* 2, 1-5.
- 572 Akhtar, M. K., Turner, N. J., Jones, P. R., 2013. Carboxylic acid reductase is a versatile enzyme
573 for the conversion of fatty acids into fuels and chemical commodities. *Proc Natl Acad*
574 *Sci U S A.* 110, 87-92.
- 575 Angermayr, S. A., van der Woude, A. D., Correddu, D., Vreugdenhil, A., Verrone, V., Hellingwerf,
576 K. J., 2014. Exploring metabolic engineering design principles for the photosynthetic
577 production of lactic acid by *Synechocystis* sp. PCC6803. *Biotechnol Biofuels.* 7, 99.
- 578 Baier, T., Wichmann, J., Kruse, O., Lauersen, K. J., 2018. Intron-containing algal transgenes
579 mediate efficient recombinant gene expression in the green microalga *Chlamydomonas*
580 *reinhardtii*. *Nucleic Acids Research.* gky532-gky532.
- 581 Bernard, A., Domergue, F., Pascal, S., Jetter, R., Renne, C., Faure, J. D., Haslam, R. P., Napier, J. A.,
582 Lessire, R., Joubès, J., 2012. Reconstitution of Plant Alkane Biosynthesis in Yeast
583 Demonstrates That *Arabidopsis* ECERIFERUM1 and ECERIFERUM3 Are Core
584 Components of a Very-Long-Chain Alkane Synthesis Complex. *Plant Cell.* 24, 3106-18.
- 585 Carneiro, M. L. N. M., Pradelle, F., Braga, S. L., Gomes, M. S. P., Martins, A. R. F. A., Turkovics, F.,
586 Pradelle, R. N. C., 2017. Potential of biofuels from algae: Comparison with fossil fuels,
587 ethanol and biodiesel in Europe and Brazil through life cycle assessment (LCA).
588 *Renewable and Sustainable Energy Reviews.* 73, 632-653.
- 589 Cho, H., Cronan, J. E., 1995. Defective export of a periplasmic enzyme disrupts regulation of
590 fatty acid synthesis. *J Biol Chem.* 270, 4216-9.
- 591 Cook, C., Dayananda, C., Tennant Richard, K., Love, J., 2017. Third-Generation Biofuels from the
592 Microalga, *Botryococcus braunii*. *Biofuels and Bioenergy.*
- 593 Delrue, F., Li-Beisson, Y., Setier, P. A., Sahut, C., Roubaud, A., Froment, A. K., Peltier, G., 2013.
594 Comparison of various microalgae liquid biofuel production pathways based on
595 energetic, economic and environmental criteria. *Bioresour Technol.* 136C, 205-212.

596 Elhai, J., Wolk, C. P., 1988. Conjugal transfer of DNA to cyanobacteria. *Methods Enzymol.* 167,
597 747-54.

598 Eroglu, E., Melis, A., 2010. Extracellular terpenoid hydrocarbon extraction and quantitation
599 from the green microalgae *Botryococcus braunii* var. *Showa*. *Bioresource Technology.*
600 101, 2359-2366.

601 Eser, B. E., Das, D., Han, J., Jones, P. R., Marsh, E. N., 2011. Oxygen-independent alkane
602 formation by non-heme iron-dependent cyanobacterial aldehyde decarbonylase:
603 investigation of kinetics and requirement for an external electron donor. *Biochemistry.*
604 50, 10743-50.

605 Gorman, D. S., Levine, R. P., 1965. Cytochrome f and plastocyanin: their sequence in the
606 photosynthetic electron transport chain of *Chlamydomonas reinhardtii*. *Proc Natl Acad*
607 *Sci U S A.* 54, 1665-9.

608 Hu, P., Borglin, S., Kamennaya, N. A., Chen, L., Park, H., Mahoney, L., Kijac, A., Shan, G.,
609 Chavarría, K. L., Zhang, C., Quinn, N. W. T., Wemmer, D., Holman, H.-Y., Jansson, C., 2013.
610 Metabolic phenotyping of the cyanobacterium *Synechocystis* 6803 engineered for
611 production of alkanes and free fatty acids. *Applied Energy.* 102, 850-859.

612 Jing, F., Cantu, D. C., Tvaruzkova, J., Chipman, J. P., Nikolau, B. J., Yandeu-Nelson, M. D., Reilly,
613 P. J., 2011. Phylogenetic and experimental characterization of an acyl-ACP thioesterase
614 family reveals significant diversity in enzymatic specificity and activity. *BMC Biochem.*
615 12, 44.

616 Kaczmarzyk, D., Cengic, I., Yao, L., Hudson, E.P., 2018. Diversion of the long-chain acyl- ACP
617 pool in *Synechocystis* to fatty alcohols through CRISPRi repression of the es- sential
618 phosphate acyltransferase *PlsX*. *Metab. Eng.* 45, 59-66.

619 Kageyama, H., Waditee-Sirisattha, R., Sirisattha, S., Tanaka, Y., Mahakhant, A., Takabe, T., 2015.
620 Improved Alkane Production in Nitrogen-Fixing and Halotolerant Cyanobacteria via
621 Abiotic Stresses and Genetic Manipulation of Alkane Synthetic Genes. *Curr Microbiol.*
622 71, 115-20.

623 Kallio, P., Pasztor, A., Thiel, K., Akhtar, M. K., Jones, P. R., 2014. An engineered pathway for the
624 biosynthesis of renewable propane. *Nature Communications.* 5:4731.

625 Kato, A., Takatani, N., Ikeda, K., Maeda, S.I., Omata, T., 2017. Removal of the product from the
626 culture medium strongly enhances free fatty acid production by genetically
627 engineered. *Biotechnol. Biofuels* 10, 141.

628 Khara, B., et al., 2013. Production of propane and other short-chain alkanes by structure-
629 based engineering of ligand specificity in aldehyde-deformylating oxygenase.
630 ChemBioChem 14, 1204–1208.

631 Kindle, K. L., 1990. High-frequency nuclear transformation of *Chlamydomonas reinhardtii*.
632 Proc Natl Acad Sci U S A. 87, 1228-32.

633 Lauersen, K. J., Baier, T., Wichmann, J., Wördenweber, R., Mussgnug, J. H., Hübner, W., Huser,
634 T., Kruse, O., 2016. Efficient phototrophic production of a high-value sesquiterpenoid
635 from the eukaryotic microalga *Chlamydomonas reinhardtii*. Metab Eng. 38, 331-343.

636 Lauersen, K. J., Kruse, O., Mussgnug, J. H., 2015. Targeted expression of nuclear transgenes in
637 *Chlamydomonas reinhardtii* with a versatile, modular vector toolkit. Appl Microbiol
638 Biotechnol. 99, 3491-503.

639 Lauersen, K. J., Wichmann, J., Baier, T., Kampranis, S. C., Pateraki, I., Møller, B. L., Kruse, O.,
640 2018. Phototrophic production of heterologous diterpenoids and a hydroxy-
641 functionalized derivative from *Chlamydomonas reinhardtii*. Metabolic Engineering.

642 Lea-Smith, D. J., Biller, S. J., Davey, M. P., Cotton, C. A., Perez Sepulveda, B. M., Turchyn, A. V.,
643 Scanlan, D. J., Smith, A. G., Chisholm, S. W., Howe, C. J., 2015. Contribution of
644 cyanobacterial alkane production to the ocean hydrocarbon cycle. Proc Natl Acad Sci U
645 S A. 112, 13591-6.

646 Lea-Smith, D. J., Ortiz-Suarez, M. L., Lenn, T., Nürnberg, D. J., Baers, L. L., Davey, M. P., Parolini,
647 L., Huber, R. G., Cotton, C. A., Mastroianni, G., Bombelli, P., Ungerer, P., Stevens, T. J.,
648 Smith, A. G., Bond, P. J., Mullineaux, C. W., Howe, C. J., 2016. Hydrocarbons Are Essential
649 for Optimal Cell Size, Division, and Growth of Cyanobacteria. Plant Physiol. 172, 1928-
650 1940.

651 Lin, F., Das, D., Lin, X. N., Marsh, E. N., 2013. Aldehyde-forming fatty acyl-CoA reductase from
652 cyanobacteria: expression, purification and characterization of the recombinant
653 enzyme. FEBS J. 280, 4773-81.

654 Liu, X., Sheng, J., Curtiss, R., 2011. Fatty acid production in genetically modified cya-
655 nobacteria. Proc. Natl. Acad. Sci. USA 108, 6899–6904.

656 Liu, Y., Wang, C., Yan, J., Zhang, W., Guan, W., Lu, X., Li, S., 2014. Hydrogen peroxide-
657 independent production of α -alkenes by OleTJE P450 fatty acid decarboxylase.
658 Biotechnol Biofuels. 7, 28.

659 Markley, A.L., Begemann, M.B., Clarke, R.E., Gordon, G.C., Pfleger, B.F, 2015. . A syn- thetic
660 biology toolbox for controlling gene expression in the cyanobacterium *Synechococcus*
661 sp. PCC 7002. ACS Synth. Biol. 4, 595–603.

662 Metzger, P., Largeau, C., 2005. *Botryococcus braunii*: a rich source for hydrocarbons and
663 related ether lipids. *Appl Microbiol Biotechnol.* 66, 486-96.

664 Neupert, J., Karcher, D., Bock, R., 2009. Generation of *Chlamydomonas* strains that efficiently
665 express nuclear transgenes. *Plant J.* 57, 1140-50.

666 Peca, L., Kós, P. B., Máté, Z., Farsang, A., Vass, I., 2008. Construction of bioluminescent
667 cyanobacterial reporter strains for detection of nickel, cobalt and zinc. *FEMS Microbiol*
668 *Lett.* 289, 258-64.

669 Peramuna, A., Morton, R., Summers, M. L., 2015. Enhancing alkane production in
670 cyanobacterial lipid droplets: a model platform for industrially relevant compound
671 production. *Life (Basel).* 5, 1111-26.

672 Qiu, Y., Tittiger, C., Wicker-Thomas, C., Le Goff, G., Young, S., Wajnberg, E., Fricaux, T., Taquet,
673 N., Blomquist, G. J., Feyereisen, R., 2012. An insect-specific P450 oxidative
674 decarboxylase for cuticular hydrocarbon biosynthesis. *Proc Natl Acad Sci U S A.*

675 Quinn, J. C., Davis, R., 2015. The potentials and challenges of algae based biofuels: a review of
676 the techno-economic, life cycle, and resource assessment modeling. *Bioresour Technol.*
677 184, 444-452.

678 Rasala, B. A., Barrera, D. J., Ng, J., Plucinak, T. M., Rosenberg, J. N., Weeks, D. P., Oyler, G. A.,
679 Peterson, T. C., Haerizadeh, F., Mayfield, S. P., 2013. Expanding the spectral palette of
680 fluorescent proteins for the green microalga *Chlamydomonas reinhardtii*. *Plant J.* 74,
681 545-56.

682 Rude, M. A., Baron, T. S., Brubaker, S., Alibhai, M., Del Cardayre, S. B., Schirmer, A., 2011.
683 Terminal olefin (1-alkene) biosynthesis by a novel p450 fatty acid decarboxylase from
684 *Jeotgalicoccus* species. *Appl Environ Microbiol.* 77, 1718-27.

685 Ruffing, A.M., 2014. Improved free fatty acid production in cyanobacteria with *Synechococcus*
686 sp. PCC 7002 as host. *Front. Bioeng. Biotechnol.* 2, 17.

687 Rui, Z., Harris, N. C., Zhu, X., Huang, W., Zhang, W., 2015. Discovery of a Family of Desaturase-
688 Like Enzymes for 1-Alkene Biosynthesis. *ACS Catalysis.* 5, 7091-7094.

689 Rui, Z., Li, X., Zhu, X., Liu, J., Domigan, B., Barr, I., Cate, J. H., Zhang, W., 2014. Microbial
690 biosynthesis of medium-chain 1-alkenes by a nonheme iron oxidase. *Proc Natl Acad Sci*
691 *U S A.* 111, 18237-42.

692 Schirmer, A., Rude, M., Li, X., Popova, E., del Cardayre, S., 2010. Microbial biosynthesis of
693 alkanes. *Science.* 329, 559-62.

694 Sheppard, M. J., Kunjapur, A. M., Prather, K. L. J., 2016. Modular and selective biosynthesis of
695 gasoline-range alkanes. *Metab Eng.* 33, 28-40.

696 Sorigué, D., Légeret, B., Cuiné, S., Blangy, S., Moulin, S., Billon, E., Richaud, P., Brugière, S.,
697 Couté, Y., Nurizzo, D., Müller, P., Brettel, K., Pignol, D., Arnoux, P., Li-Beisson, Y., Peltier,
698 G., Beisson, F., 2017. An algal photoenzyme converts fatty acids to hydrocarbons.
699 Science. 357, 903-907.

700 Storch, M., Casini, A., Mackrow, B., Fleming, T., Trewitt, H., Ellis, T., Baldwin, G. S., 2015.
701 BASIC: A New Biopart Assembly Standard for Idempotent Cloning Provides Accurate,
702 Single-Tier DNA Assembly for Synthetic Biology. ACS Synth Biol. 4, 781-7.

703 Wang, W., Liu, X., Lu, X., 2013. Engineering cyanobacteria to improve photosynthetic
704 production of alka(e)nes. Biotechnol Biofuels. 6, 69.

705 Warui, D. M., Pandelia, M. E., Rajakovich, L. J., Krebs, C., Bollinger, J. M., Booker, S. J., 2015.
706 Efficient delivery of long-chain fatty aldehydes from the Nostoc punctiforme acyl-acyl
707 carrier protein reductase to its cognate aldehyde-deformylating oxygenase.
708 Biochemistry. 54, 1006-15.

709 Wichmann, J., Baier, T., Wentnagel, E., Lauersen, K. J., Kruse, O., 2018. Tailored carbon
710 partitioning for phototrophic production of (E)- α -bisabolene from the green microalga
711 Chlamydomonas reinhardtii. Metab Eng. 45, 211-222.

712 Work, V.H., Melnicki, M.R., Hill, E.A., Davies, F.K., Kucek, L.A., Beliaev, A.S., et al., 2015. Lauric
713 acid production in a glycogen-less strain of Synechococcus sp. PCC 7002. Front Bioeng.
714 Biotechnol. 3.

715 Yunus, I.Y., Jones, P.R., 2018. Photosynthesis-dependent biosynthesis of medium chain-length
716 fatty acids and alcohols. Metab Eng. 49, 59-68.

717 Zhou, Y. J., Hu, Y., Zhu, Z., Siewers, V., Nielsen, J., 2018. Engineering 1-Alkene Biosynthesis and
718 Secretion by Dynamic Regulation in Yeast. ACS Synth Biol. 7, 584-590.

719 Zhu, Z., Zhou, Y. J., Kang, M. K., Krivoruchko, A., Buijs, N. A., Nielsen, J., 2017. Enabling the
720 synthesis of medium chain alkanes and 1-alkenes in yeast. Metab Eng. 44, 81-88.

721

Highlights

- Synthetic metabolic pathways for hydrocarbon fuels were engineered in algae
- Free fatty acids were effectively converted into alkenes and alkanes
- Transfer of algal pathway into cyanobacteria was the most effective
- Alkane yield was enhanced 19-fold in *Synechocystis spp.* PCC 6803
- Alkene yield was enhanced 8-fold in *Chlamydomonas reinhardtii*

1 **Synthetic metabolic pathways for photobiological conversion of CO₂ into hydrocarbon fuel**

2

3 Ian Sofian Yunus^a, Julian Wichmann^b, Robin Wördenweber^b, Kyle J. Lauersen^b, Olaf Kruse^b and

4 Patrik R. Jones^{a*}

5

6 ^aDepartment of Life Sciences, Imperial College London, SW7 2AZ London, UK

7 ^bBielefeld University, Faculty of Biology, Center for Biotechnology (CeBiTec),

8 Universitätsstrasse 27, 33615, Bielefeld, Germany.

9 *Corresponding author: p.jones@imperial.ac.uk

10 ABSTRACT

11 Liquid fuels sourced from fossil sources are the dominant energy form for mobile transport
12 today. The consumption of fossil fuels is still increasing, resulting in a continued search for
13 more sustainable methods to renew our supply of liquid fuel. Photosynthetic microorganisms
14 naturally accumulate hydrocarbons that could serve as a replacement for fossil fuel, however
15 productivities remain low. We report successful introduction of five synthetic metabolic
16 pathways in two green cell factories, prokaryotic cyanobacteria and eukaryotic algae.
17 Heterologous thioesterase expression enabled high-yield conversion of native fatty acyl-acyl
18 carrier protein (ACP) into free fatty acids (FFA) in *Synechocystis sp.* PCC 6803 but not in
19 *Chlamydomonas reinhardtii* where the polar lipid fraction instead was enhanced. Despite no
20 increase in measurable FFA in *Chlamydomonas*, genetic recoding and over-production of the
21 native fatty acid photodecarboxylase (FAP) resulted in increased accumulation of 7-
22 heptadecene. Implementation of a carboxylic acid reductase (CAR) and aldehyde
23 deformylating oxygenase (ADO) dependent synthetic pathway in *Synechocystis* resulted in
24 the accumulation of fatty alcohols and a decrease in the native saturated alkanes. In contrast,
25 the replacement of CAR and ADO with *Pseudomonas mendocina* UndB (so named as it is
26 responsible for 1-undecene biosynthesis in *Pseudomonas*) or *Chlorella variabilis* FAP resulted
27 in high-yield conversion of thioesterase-liberated FFAs into corresponding alkenes and
28 alkanes, respectively. At best, the engineering resulted in an increase in hydrocarbon
29 accumulation of 8- (from 1 to 8.5 mg/g cell dry weight) and 19-fold (from 4 to 77 mg/g cell
30 dry weight) for *Chlamydomonas* and *Synechocystis*, respectively. In conclusion, reconstitution
31 of the eukaryotic algae pathway in the prokaryotic cyanobacteria host generated the most
32 effective system, highlighting opportunities for mix-and-match synthetic metabolism. These
33 studies describe functioning synthetic metabolic pathways for hydrocarbon fuel synthesis in
34 photosynthetic microorganisms for the first time, moving us closer to the commercial
35 implementation of photobiocatalytic systems that directly convert CO₂ into infrastructure-
36 compatible fuels.

37 38 Keywords

39 Hydrocarbon fuel; Algae; Cyanobacteria; Alkanes; Alkenes; Fatty acids

40 41 Highlights

- 42 • Synthetic metabolic pathways for hydrocarbon fuels were engineered in algae
- 43 • Free fatty acids were effectively converted into alkenes and alkanes

- 44 • Transfer of algal pathway into cyanobacteria was the most effective
- 45 • Alkane yield was enhanced 19-fold in *Synechocystis spp.* PCC 6803
- 46 • Alkene yield was enhanced 8-fold in *Chlamydomonas reinhardtii*
- 47

48 INTRODUCTION

49 Cyanobacteria (prokaryotes) and algae (eukaryotes) are photosynthetic microorganisms that
50 have evolved to naturally accumulate C15-C19 alkanes or alkenes at very low concentrations
51 (0.02-1.12% alkane g/g cell dry weight (CDW)) (Lea-Smith et al., 2015; Schirmer et al., 2010;
52 Sorigué et al., 2017) with the exception of naturally oleagineous species (Ajjawi et al., 2017;
53 Metzger and Largeau, 2005; Peramuna et al., 2015). These hydrocarbons are postulated to
54 influence the fluidity of cell membranes and are therefore essential for achieving optimal
55 growth, indeed, the abolition of their biosynthetic capacities results in morphological defects
56 (Lea-Smith et al., 2016). Only two enzymes, acyl-ACP reductase (AAR) and aldehyde
57 deformylating oxygenase (ADO) are required to catalyze the bacterial conversion of acyl-ACP
58 into alkanes (Schirmer et al., 2010). Similarly, eukaryotic microalgae also biosynthesize small
59 quantities of alkanes and alkenes directly from fatty acids, employing the distinctly different
60 and recently discovered fatty acid photodecarboxylase (FAP; (Sorigué et al., 2017)).

61 In order to engineer sustainable biotechnological systems for production of
62 hydrocarbons for the fuel market, whether heterotrophic or light-driven, far greater yields are
63 needed alongside other complementary non-biochemical improvements such as improved
64 bio-process designs. Several studies have attempted to enhance alkane productivity in
65 cyanobacteria by over-expression of the native or non-native AAR and ADO enzyme couple
66 (Hu et al., 2013; Kageyama et al., 2015; Peramuna et al., 2015; Wang et al., 2013) which relies
67 on acyl-ACP as the precursor. Although naturally accumulating alkane amounts have been
68 enhanced through engineering and reported in high titres from the lipid-accumulating
69 cyanobacteria, *Nostoc punctiforme* (up to 12.9% (g/g) CDW, (Peramuna et al., 2015)), similar
70 efforts in the non-lipid accumulating model cyanobacterium *Synechocystis sp.* PCC 6803
71 (hereafter *Synechocystis* 6803) have at best yielded only 1.1% (g/g) CDW (Hu et al., 2013;
72 Wang et al., 2013). In eukaryotic algae, the native alkene/alkane pathway was only recently
73 discovered and there has been no work so far to engineer the specific pathways that
74 synthesize such hydrocarbons. Some species of algae are also known to naturally accumulate
75 hydrocarbons that could serve as a fuel following chemical conversion. For example, certain
76 races of the green alga *Botrococcus braunii* naturally secrete long-chain terpene
77 hydrocarbons as a significant portion of their biomass (Eroglu and Melis, 2010; Metzger and
78 Largeau, 2005). However, their use as a fuel source is made impossible by the incredibly slow
79 growth rates of this alga (Cook et al., 2017). Other oleaginous algal species can accumulate a
80 significant portion of their biomass as triacylglycerol compounds, generally under nitrogen
81 stress. Indeed, this phenomenon drove the push for the use of algae as third generation

82 biofuel feedstock in the first place. However, process design and downstream processing cost
83 considerations of large-scale algal cultivation have hindered the common adoption of algal
84 oils for transportation fuels (Quinn and Davis, 2015). Triacylglycerol stored by eukaryotic
85 algae can also be turned into transportation fuels via transesterification to liberate the
86 alkanes and alkenes from the glycerol backbone. An attractive alternative to the above
87 concepts is instead to directly secrete ready-to-use hydrocarbon products from algal cells as
88 this would overcome issues with biomass harvesting and chemical processing and thereby
89 greatly reduce process costs (Delrue et al., 2013).

90 In order to achieve such a one-step conversion of CO₂ into ready infrastructure-
91 compatible hydrocarbons with photosynthetic hosts, however, genetic reprogramming
92 becomes essential for introduction of synthetic metabolic pathways and optimization of the
93 entire system. Several enzymes have recently been reported to enable biosynthesis of fatty
94 aldehyde precursors (Akhtar et al., 2013), fatty alkanes (Bernard et al., 2012; Qiu et al., 2012),
95 and fatty alkenes (Rude et al., 2011; Rui et al., 2015; Rui et al., 2014). Combinatorial assembly
96 of such key enzymes into synthetic metabolic pathways consequently enabled a number of
97 novel opportunities for hydrocarbon biosynthesis, as described by many including (Akhtar et
98 al., 2013; Kallio et al., 2014; Sheppard et al., 2016; Zhu et al., 2017). Although such studies
99 have so far only been reported using heterotrophic microorganisms (*Escherichia coli* and
100 *Saccharomyces cerevisiae*) there are no reports of similar work in any phototrophic
101 microorganism.

102 In this study, we describe a first and systematic study to implement synthetic
103 metabolic pathways for the biosynthesis of hydrocarbon fuel in both prokaryotic and
104 eukaryotic photosynthetic microorganisms using the model strains *Synechocystis* 6803 and
105 *Chlamydomonas reinhardtii*. Several synthetic pathways towards saturated and unsaturated
106 hydrocarbons were functionally demonstrated in *Synechocystis* 6803, increasing the
107 hydrocarbon content up to 19-fold, and engineered *Chlamydomonas* accumulated 8-fold more
108 alkenes than the wild-type. Interestingly, the "best" system was achieved by transferring a
109 reconstructed pathway from eukaryotic algae into the prokaryotic cyanobacterium.

110 MATERIALS AND METHODS

111

112 *2.1 Growth conditions, genetic constructs, transformation and screening of Escherichia coli* 113 *and Synechocystis sp. PCC 6803*

114

115 *Escherichia coli* DH5 α was used to propagate all the plasmids used in this study. Strains were
116 cultivated in lysogeny broth (LB) medium (LB Broth, Sigma Aldrich), 37 °C, 180 rpm, and
117 supplemented with appropriate antibiotics (final concentration: carbenicillin 100 $\mu\text{g/ml}$,
118 chloramphenicol 37 $\mu\text{g/ml}$, kanamycin 50 $\mu\text{g/ml}$, gentamicin 10 $\mu\text{g/ml}$, and erythromycin 200
119 $\mu\text{g/ml}$).

120 *Synechocystis sp. PCC 6803*, obtained from Prof. Klaas Hellingwerf (University of
121 Amsterdam, Netherlands), was cultivated in BG11 medium without cobalt ((hereafter BG11-
122 Co), as the metal was used as an inducer in most cultures. All media contained appropriate
123 antibiotic(s) (final concentration: kanamycin 50 $\mu\text{g/ml}$, gentamicin 50 $\mu\text{g/ml}$, and
124 erythromycin 20 $\mu\text{g/ml}$). Gentamicin was only used for selection on agar plates. Precultures
125 inoculated from colonies on agar plates were grown in 6-well plates (5 ml). When the OD₇₃₀
126 reached 3-4, the culture was transferred to a 100-ml Erlenmeyer flask and the OD₇₃₀ was
127 adjusted to 0.2 by adding BG11-Co medium to a final volume of 25 ml containing appropriate
128 antibiotic(s). The cultivation was carried out for 10 days at 30 °C with continuous illumination
129 at 60 $\mu\text{mol photons m}^{-2} \text{s}^{-1}$ and 1% (v/v) CO₂. Each main treatment culture was induced on
130 day 2 and samples were taken for measurement of OD₇₃₀ and metabolites day 6 and 10. All
131 cultivations were carried out in an AlgaeTron230 (Photon Systems Instruments) (PSI) at
132 30 °C with continuous illumination at 60 $\mu\text{mol photons m}^{-2} \text{s}^{-1}$ and 1% (v/v) CO₂, except
133 where noted (100-300 $\mu\text{mol photons m}^{-2} \text{s}^{-1}$). A representative growth curve and all final
134 OD₇₃₀ values are shown in Supplementary Figure 1.

135 All plasmids (Supplementary Table 1A) used for transformation of cyanobacteria were
136 assembled using the BASIC Assembly method (Storch et al., 2015). Linkers were designed
137 using the R20DNA software: <http://www.r2odna.com/> and obtained from Integrated DNA
138 Technologies Incorporated. The details of all linkers, primers and DNA parts used to construct
139 each plasmid are given in Supplementary Tables 1B, 1C and 1D.

140 For transformation by natural assimilation, each *Synechocystis sp. PCC 6803* strain
141 was inoculated from freshly prepared colonies on agar plates into 25 ml BG11-Co with a
142 starting OD 0.02. The cells were harvested when the OD₇₃₀ reached 0.4-0.7, washed in 10 ml
143 BG11-Co twice, and resuspended in 500 μL BG11-Co. One hundred microliters of concentrated

144 liquid culture were mixed with four to seven micrograms of plasmid and incubated at 30°C
145 with continuous illumination at 60 $\mu\text{mol photons m}^{-2} \text{s}^{-1}$ and 1% (v/v) CO₂ for 12-16 h prior
146 to plating on BG11-Co agar containing 10% strength of antibiotic. To promote segregation,
147 individual colonies were restreaked on BG11-Co agar with higher antibiotic concentration. To
148 check the segregation, the biomass was resuspended in nuclease free water and exposed to
149 two freeze-thaw cycles (95°C, -80°C). Following centrifugation, 3 μL was used as a template
150 for a diagnostic polymerase chain reaction (PCR). Primers used for each PCR are listed in
151 Supplementary Table 1C. Only fully segregated mutants were used in further experiments. All
152 cyanobacteria strains used in the study are listed in Supplementary Table 2.

153 For transformation by triparental conjugation, one hundred microliters of the cargo
154 strain (*E. coli* HB101 (already carrying the pRL623 plasmid)), conjugate strain (ED8654
155 (Elhai and Wolk, 1988)), and *Synechocystis* sp. PCC 6803 (OD₇₃₀ ~1) were mixed and
156 incubated for 2 h (30 °C, 60 $\mu\text{mol photons m}^{-2} \text{s}^{-1}$). Prior to mixing, all the *E. coli* and
157 cyanobacteria strains were washed with fresh LB and BG11-Co medium, respectively, to
158 remove the antibiotics. After 2 h of incubation, the culture mix was transferred onto BG11
159 agar plates without antibiotic and incubated for 2 d (30 °C, 60 $\mu\text{mol photons m}^{-2} \text{s}^{-1}$). After 2 d
160 of incubation, cells were scraped from the agar plate, resuspended in 500 μL of BG11-Co
161 medium, and transferred onto a new agar plate containing 20 $\mu\text{g/ml}$ erythromycin. Cells were
162 allowed to grow for one week until colonies appeared. Individual colonies were restreaked
163 onto a new plate containing 20 $\mu\text{g/ml}$ erythromycin and used for subsequent experiments.

164

165 ***2.2 Growth conditions, genetic constructs, transformation and screening of Chlamydomonas*** 166 ***reinhardtii***

167 *C. reinhardtii* strain UVM4 was used in this work (Neupert et al., 2009) graciously provided by
168 Prof. Dr. Ralph Bock)). The strain was routinely maintained on Tris acetate phosphate (TAP)
169 medium (Gorman and Levine, 1965) either with 1.5% agar plates or in liquid with 250 μmol
170 $\text{photons m}^{-2} \text{s}^{-2}$. Transformation was conducted with glass bead agitation as previously
171 described (Kindle, 1990). The amino acid sequences of *C. reinhardtii* native fatty acid
172 photodecarboxylase (FAP) (Uniprot: A8JHB7; (Sorigué et al., 2017)), *E. coli* thioesterase A
173 (TesA: P0ADA1), *Jeotgalicoccus* sp. ATCC 8456 terminal olefin-forming fatty acid
174 decarboxylase (OleT) (E9NSU2), and *Rhodococcus* sp. NCIMB 9784 P450 reductase RhFRED
175 (Q8KU27) were codon optimized and copies of the intron 1 of ribulose biphosphate
176 carboxylase small subunit 2 (RBCS2) were added throughout the coding sequences as
177 previously described (Baier et al., 2018). The nucleotide sequences of optimized intron

178 containing genes have been submitted to NCBI, accession numbers can be found in
179 Supplementary Table 3. All synthetic genes were chemically synthesized (GeneArt) and
180 cloned between *Bam*HI-*Bgl*II in the pOpt2_PsaD_mVenus_Paro or pOpt2_PsaD_mRuby2_Ble
181 vectors (Wichmann et al., 2018). PsaD represents the 36 amino acid photosystem I reaction
182 center subunit II (PsaD) chloroplast targeting peptide (CTP) (Lauersen et al., 2015) between
183 *Nde*I-*Bam*HI restriction sites of the pOpt2 vectors (Wichmann et al., 2018). The native FAP
184 enzyme was designed to contain an additional glycine codon at aa position 33 to allow the
185 insertion of a *Bam*HI site at the border of the predicted CTP. The whole synthetic enzyme
186 including native targeting peptide was cloned *Nde*I-*Bgl*II and a version was created with the
187 PsaD CTP built by cloning *Bam*HI-*Bgl*II into the vectors described above. Fusions of different
188 sequences were made by digestion and complementary overhang annealing of the *Bam*HI-
189 *Bgl*II mediated restriction sites for each respective construct as needed to obtain the fusions
190 used in the present work (Supplementary Figure 2). After transformation, expression was
191 confirmed by fluorescence microscopy screening for mVenus (YFP) or mRuby2 (RFP)
192 reporters as previously described (Lauersen et al., 2016; Wichmann et al., 2018). Individual
193 mutants were subjected to Western blotting and immuno detection to determine whether
194 full-length protein products were formed (anti-GFP polyclonal HRP linked antibody, Thermo
195 Fisher Scientific). Wide-field fluorescence microscopy was used to confirm chloroplast
196 localization of YFP-linked constructs as previously described (Lauersen et al., 2016).

197

198 ***2.3 Product analysis***

199 Three different extraction and analysis protocols were used for the analysis of (1) acids, (2)
200 alcohols and (3) alkanes as well as alkenes from cyanobacteria cultures. For each analyte
201 group, liquid cultures in flasks were mixed well by shaking prior to transferring 2 mL of liquid
202 culture into a PYREX round bottom threaded culture tube (Corning, Manufacturer Part
203 Number: 99449-13).

204 For fatty acid analysis, free fatty acid extraction was performed as described
205 previously (Liu et al., 2011; Yunus and Jones, 2018). In brief, two hundred microliters of 1 M
206 H₃PO₄ were added to acidify each 2 mL culture and spiked with 100 µg pentadecanoic acid
207 (Sigma Aldrich) as an internal standard. Four millilitres of n-hexane (VWR Chemicals) was
208 added and the mixture vortexed vigorously prior to centrifugation at 3500 x g for 3 min. The
209 upper hexane layer was then transferred to a fresh PYREX round bottom threaded culture
210 tube and evaporated completely under a stream of nitrogen gas. Five hundred microliters of
211 1.25 M HCl in methanolic solution were added to methyl esterify the free fatty acid at 85 °C for

212 2 h. Samples were cooled to room temperature and 500 μL of hexane was added for
213 extraction of the fatty acid methyl esters (FAMES).

214 For fatty alcohol, alkane and alkene analysis, extraction was done as described
215 previously (Zhou et al., 2016) with modification. Briefly, 2 mL of liquid culture were spiked
216 with 50 μg 1-nonanol, 100 μg octadecane, and 100 μg 1-pentadecanol and mixed with 4 mL of
217 chloroform:methanol (2:1 v/v) solution. The mixture was vortexed vigorously and
218 centrifuged at 3500 x g for 3 min. The lower organic phase was then transferred into a new
219 glass tube and extraction was repeated one more time. The lower organic phase was
220 combined and dried under a stream of nitrogen gas. For fatty alcohol derivatization, the dried
221 extract was resuspended in 100 μL chloroform, mixed with 100 μL of N, O-
222 bistrifluoroacetamide (BSTFA) (TCI Chemicals) and transferred to an insert in a GC vial that
223 was incubated at 60 $^{\circ}\text{C}$ for 1 h prior to GC analysis. Note that no derivatization was needed for
224 the analysis of hydrocarbons.

225 Samples (1 μL) were analyzed using an Agilent Technologies (Santa Clara, CA, USA)
226 7890B Series Gas Chromatograph (GC) equipped with an HP-5MS column (pulsed split ratio
227 10:1 and split flow 10 ml/min), a 5988B Mass Spectrophotometer (MS) and a 7693
228 Autosampler. For the acids the GC oven program followed an initial hold at 40 $^{\circ}\text{C}$ for 3 min, a
229 ramp at 10 $^{\circ}\text{C}\cdot\text{min}^{-1}$ to 150 $^{\circ}\text{C}$, a second ramp at 3 $^{\circ}\text{C}\cdot\text{min}^{-1}$ to 270 $^{\circ}\text{C}$, a third ramp at 30 $^{\circ}\text{C}\cdot\text{min}^{-1}$
230 to 300 $^{\circ}\text{C}$, and a final hold for 5 min. For alcohols and alkenes, there was an initial hold at 40
231 $^{\circ}\text{C}$ for 0.5 min, a ramp at 10 $^{\circ}\text{C}\cdot\text{min}^{-1}$ to 300 $^{\circ}\text{C}$, and a final hold for 4 min. For alkanes, the oven
232 was initially held at 70 $^{\circ}\text{C}$ for 0.5 min, a ramp at 30 $^{\circ}\text{C}\cdot\text{min}^{-1}$ to 250 $^{\circ}\text{C}$, a second ramp at 40
233 $^{\circ}\text{C}\cdot\text{min}^{-1}$ to 300 $^{\circ}\text{C}$, and a final hold for 2 min. The acids, alkanes and alcohols were quantified
234 by comparing the peak areas with that of the internal standards: pentadecanoate (for all
235 acids), octadecane (for all alkanes), 1-nonanol (for C8 to C12 alcohols) and 1-pentadecanol
236 (for C14 alcohols and above). The quantity of the main products (C15 and C17 alkanes, C15
237 alkene, and C12, C14, C16, and C18 alcohols and acids) were also corrected with their
238 respective mass spectrometer response factors obtained using dilution series of commercial
239 standards.

240 Gas chromatography mass spectroscopy (GC-MS) aimed at identification of
241 hydrocarbon products from *C. reinhardtii* was conducted with solvent extracted samples
242 following previously described protocols and internal standards (Lauersen et al., 2016).
243 Quantification of 7-heptadecene was performed with serial dilutions (1 to 900 μM) of
244 commercial 1-heptadecene standard (Acros Organics) in dodecane using extracted ion
245 chromatograms with masses 55.00, 69.00, 91.00, 93.00, 83.00, 97.00, and 111.00.

246 RESULTS AND DISCUSSION

247

248 Several synthetic pathway designs were considered, all commencing with the liberation of
249 "free" fatty acids from the native fatty acid biosynthesis pathway (Fig. 1), the presumed native
250 precursor for many of the decarboxylating enzymes evaluated in this study.

251

252 ***3.1 Over-production of free fatty acids as precursor for hydrocarbon biosynthesis -*** 253 ***Expression of Escherichia thioesterase deregulates lipid membrane biosynthesis in*** 254 ***Chlamydomonas***

255

256 In order to liberate FFAs in cyanobacteria we over-expressed the *E. coli* C16-C18 specific
257 thioesterase TesA (Cho and Cronan, 1995) lacking its native signal sequence peptide ("TesA)
258 and deleted the gene encoding the native fatty acyl ACP synthase (*aas*) (Kaczmarzyk et al.,
259 2010; Liu et al., 2011)(Fig. 1). The native signal sequence peptide directs TesA to the
260 periplasm in *E. coli* (Cho et al 1993) and its removal is assumed to maximize the liberation of
261 "free" fatty acids also in cyanobacteria by retaining the enzyme in the cytosol. Such
262 "TesA/ Δaas engineering has previously been reported several times before in cyanobacteria
263 (Liu et al., 2011, Ruffing et al., 2014; Work et al., 2015; Kato et al., 2017), with 13% (g/g cell
264 dry weight (CDW)) as the highest reported fatty acid yield in *Synechocystis* 6803 (Liu et al.,
265 2011). Further potentially stackable modifications to the strain or process have also been
266 reported. For example, by employing a solvent overlay, Kato et al., 2017 reported up to 36%
267 (g/g) CDW of fatty acids excreted into the media using "TesA/ Δaas *Synechococcus elongatus*
268 *sp.* PCC 7942. In the present study, the chromosomal integration of 'tesA into the *psbA2* site
269 (slr1311) of *Synechocystis* 6803 Δaas (Δaas -TesA), under the control of the light-inducible
270 promoter PpsbA2S, resulted in the excretion of C14:0 (3.5 mg/g CDW), C16:0 (23.2 mg/g
271 CDW) and C18:0 (5.7 mg/g CDW) fatty acids with a chain-length distribution that is in
272 agreement with previously reported findings (Liu et al., 2011) (Fig. 2A; Supplementary Fig. 3).

273 Overproduction of the same thioesterase ("TesA) and targeting of the enzyme product
274 to the chloroplast was possible in *C. reinhardtii*. The synthetic algal optimized *E. coli*' tesA
275 gene was fused with an N-terminal PsaD-based chloroplast targeting peptide and a C-terminal
276 yellow fluorescent protein (YFP) encoding gene. Both the coding genes were interspersed by
277 synthetic introns (Fig. 2B) as previously described to enhance transgene expression from the
278 nuclear genome (Baier et al., 2018). Fluorescence microscopy indicated correct localization of
279 the "TesA fluorescent protein fusion to the algal chloroplast (Fig. 2C). Although no FFA could

280 be detected in the culture medium, a difference was observed in the lipid profile of the green
281 algal cells, suggesting a de-regulation of fatty acid synthesis that specifically affected the polar
282 lipid fraction of the alga. This was indicated by an over-accumulation of C18:1n9c chain
283 lengths in the polar lipid membranes, with subtle changes observed in other acyl-ACP species
284 such as C14:0 (Fig. 2D; Supplementary Fig. 4). Thus, 'TesA_YFP clearly had an impact on lipid
285 metabolism in the eukaryotic algal host, but, the capture of liberated FFAs by acyl-ACP or -
286 CoA synthases are likely too effective, thereby limiting the application of the same engineering
287 principles carried out for cyanobacteria. An annotated gene product in *Chlamydomonas*
288 Cre06.g299800 (Phytozome v5.5) has some sequence similarity to *Synechocystis aas* and
289 therefore represents an interesting target for future strategies to block native re-uptake of
290 FFA in the green algal cell.

291 Having achieved strains with enhanced accumulation of FFA in *Synechocystis*, or at
292 least a perturbation to the lipid biosynthetic system in *Chlamydomonas*, we proceeded to
293 investigate enzymes that further convert FFAs into hydrocarbon end-products.

294 295 ***3.2 Effective conversion of free fatty acids into alkenes using UndB***

296 Three different enzymes that catalyze the conversion of fatty acids into alkenes have been
297 recently reported, OleT (Rude et al., 2011), UndA (Rui et al., 2014), and UndB (Rui et al., 2015)
298 (Fig. 1). So far, the best reported productivity in both *E. coli* (Rui et al., 2015) and *S. cerevisiae*
299 (Zhou et al., 2018) has been with UndB.

300 In *Synechocystis* 6803, we transformed the Δaas -'TesA strain with an RSF1010-based
301 plasmid harboring a codon-optimized *undB* under the control of the P_{lac143} promoter
302 (Markeley et al., 2014), thereby generating the strain Δaas -'TesA-1010-UndB (Fig. 3A). After
303 10 days of cultivation, both the free fatty acids and alkanes were extracted and analyzed as
304 described in the Materials and Methods section. The accumulation of free fatty acids was
305 markedly reduced in the Δaas -'TesA-1010-UndB strain (Fig. 3B, 3C). In its place, both 1-
306 pentadecene and 1-heptadecene accumulated with a molar yield suggesting approximately
307 55% conversion of 'TesA-liberated FFAs (compare Fig. 3C with Fig. 3D). More than >84% of
308 the FFAs disappeared relative to the Δaas -'TesA strain suggesting that UndB was catalytically
309 efficient *in vivo* and that the electrons required in the UndB reaction were fortunately
310 supplied by an unknown source. The Δaas -'TesA-1010-UndB strain displayed a lower biomass
311 accumulation than the controls (Δaas -empty and Δaas -'TesA strains) (Supplementary Fig. 1),
312 presumably due to product toxicity imparted by the alkenes. A direct comparison with the
313 conversion efficiency in *E. coli* is not possible since the FFA conversion efficiency was not

314 reported in the original work (Rui et al., 2015). Despite the disappearance of C14:0 fatty acids
315 in the Δaas -TesA-1010-UndB strain, no measurable 1-tridecene (the expected corresponding
316 alkene) was observed in the whole culture extracts (Fig. 3C). None of the observed alkene
317 products were secreted extracellularly (Fig. 3E).

318 In *Chlamydomonas*, we attempted to over-produce the *Jeotgalicoccus* sp. terminal
319 olefin-forming fatty acid decarboxylase (OleT) and the *Rhodococcus* sp. P450 reductase
320 (RhFRED). OleT was chosen as it could theoretically produce C17:1 and C15:0 hydrocarbons
321 from the major lipid species of the green algal cell, C18:1 and C16:0, respectively (Fig. 1).
322 Fusion to RhFRED has been reported to enable hydrogen peroxide-independent
323 decarboxylase activity (Liu et al., 2014). The protein products of this decarboxylase and its
324 fusion in either orientation to RhFRED could be detected by Western blotting and located to
325 the algal chloroplast in fluorescence microscopy (Supplementary Figure 5). However, no
326 differences in GC-MS profiles between the parental and expression strains could be found in
327 either dodecane solvent overlays or cell-pellet solvent extracts.

328

329 ***3.3 Transfer of the CAR/ADO based pathway from E. coli to Synechocystis 6803 resulted in*** 330 ***the accumulation of fatty alcohols and a reduction in alkane accumulation***

331 Carboxylic acid reductases (CAR) have been previously used to construct a number of
332 synthetic pathways for alkane biosynthesis in heterotrophic microorganisms (Akhtar et al.,
333 2013; Kallio et al., 2014; Sheppard et al., 2016; Zhu et al., 2016). Although CAR appears to
334 have a high capability for converting fatty acids into corresponding fatty aldehydes (Akhtar et
335 al., 2013) (Fig. 1), a bottleneck in previous heterotrophic pathways is the subsequent
336 conversion into alkanes by kinetically slow ADO enzymes and competition with native
337 aldehyde reductases that more effectively convert aldehydes into alcohols (Kallio et al., 2014;
338 Sheppard et al., 2016).

339 Since *Synechocystis* 6803 natively harbors an aldehyde deformylating oxygenase
340 (ADO) with the appropriate substrate specificity (Khara et al., 2013) (Fig. 1), we first
341 combined TesA with CAR and evaluated its ability to supply the native ADO. A synthetic
342 operon expressing all required parts (including the CAR maturation protein Sfp) was
343 introduced to the RSF1010 plasmid backbone (Fig. 4A) and used to transform *Synechocystis*
344 6803 Δaas , thus creating the strain Δaas -1010-TPC2. This strain accumulated both fatty acids
345 (Fig. 4B and 4D) and fatty alcohols (Fig. 4C and 4E). The quantity of heptadecane was reduced
346 in Δaas -1010-TPC2 relative to Δaas -1010-'TesA (Fig. 4F). This suggests that the introduced
347 CAR-based pathway had not managed to increase the supply of fatty aldehydes to the native

348 ADO. CAR and native aldehyde reductase(s) had instead very effectively converted >90% of
349 the FFA pool (Fig. 4D) into corresponding alcohols (Fig. 4E). The most likely reason for the
350 increase in FFA in latter experiments is due to increased expression of 'TesA using the
351 RSF1010 plasmid in Δaas -1010-'TesA (Fig. 4D), relative to the amount of 'TesA when
352 expressed from the chromosomal location in Δaas -'TesA (Fig. 3C). Similar observations have
353 also been previously reported by Angermayr et al. (Angermayr et al., 2014). The different
354 promoters used in the two strains are also likely to have influenced the outcome, however, we
355 are not aware of any studies that directly compare the two promoters head-to-head.

356 Substantial quantities of fatty alcohols did accumulate in the Δaas -1010-TPC2 strain,
357 suggesting that the supply of fatty aldehydes is not the limiting factor. One possibility is that
358 the native aldehyde reductases are simply much more active than the native ADO (Eser et al.,
359 2011; Lin et al., 2013). Another possibility is that native ADO and AAR form a close metabolon
360 *in vivo* (Warui et al., 2015) that locks out access to ADO from external supplies of fatty
361 aldehydes. In order to test this possibility, we attempted to create a variant of Δaas -1010-
362 TPC2 that also included chromosomal ADO over-expression cassette under the PpsbA2S
363 promoter. Despite numerous transformation and segregation attempts, however, we were
364 unable to isolate any stable segregants. Another complementary strategy that could be
365 considered in future work would be to eliminate native aldehyde reductases, as previously
366 carried out in earlier *E. coli* studies (Kallio et al., 2014; Sheppard et al., 2016), although the full
367 complement of fatty aldehyde reductase encoding genes in cyanobacteria remains unknown.
368 Given the lack of success in producing alkanes with the CAR/ADO route in cyanobacteria we
369 then considered alternative options for both cyanobacteria and algae.

370

371 ***3.4 Engineering of the native eukaryotic algae pathway and transfer to cyanobacteria results*** 372 ***in enhanced conversion of CO₂ into alkanes***

373 A fatty acid photodecarboxylase (FAP) that directly converts saturated and unsaturated FFAs
374 into alkanes and alkenes, respectively, was recently discovered in eukaryotic algae (Sorigué et
375 al., 2017). In *Chlamydomonas*, the source of free fatty acids for the native alkene pathway
376 remains unknown, although the degradation of membrane lipids may release some FFA
377 (illustrated in Fig. 1). However, we would expect increased accumulation of alkanes in algae if
378 we were able to increase the cellular quantity of the native FAP and/or introduce synthetic
379 routes to the FFA precursors.

380 Accordingly, we overproduced native FAP from *C. reinhardtii* (CrFAP) on its own or in
381 combination with co-production of *E. coli*'TesA. The over-expression of CrFAP was carried

382 out either with its native chloroplast targeting peptide (CTP) or the robust PsaD CTP which
383 has been previously used to mediate chloroplast localization of numerous reporters
384 (Lauersen et al., 2015; Lauersen et al., 2018; Rasala et al., 2013). In order to minimize any
385 native regulation of the genomic sequence, the gene was subjected to a strategy of gene design
386 which has recently been shown to enable robust transgene expression from the nuclear
387 genome of this alga (Baier et al., 2018). Briefly, the sequence was codon optimized based on
388 its amino acid sequence and multiple copies of the first intron of the *C. reinhardtii* ribulose-
389 1,5-bisphosphate carboxylase/oxygenase (RuBisCo) small subunit 2 (rbcS2i1,
390 NCBI: X04472.1) were spread throughout the coding sequence *in silico*. This nucleotide
391 sequence was chemically synthesized and used for expression from the algal nuclear genome.
392 This strategy has previously enabled heterologous overproduction of non-native
393 sesquiterpene synthases (Lauersen et al., 2016; Lauersen et al., 2018; Wichmann et al., 2018),
394 and in the present study also the 'Tesa, OleT, and RhFRED proteins. However, complete codon
395 optimization and synthetic intron spreading of a native gene has not yet been demonstrated
396 in eukaryotic algae. Both constructs mediated full-length target protein production which was
397 detectible in Western blots (Supplementary Fig. 5B). Replacing the native CTP with the PsaD
398 CTP enabled more reliable and robust accumulation, which was detectible as YFP signal in the
399 algal chloroplast (Supplementary Fig. 6) and strong bands in transformants expressing this
400 construct in Western blots (Supplementary Fig. 5B). The parental UVM4 strain was found to
401 contain ~0.5 mg/g 7-heptadecene as a natural product (Supplementary Fig. 7). Transformants
402 generated with the CrFAP construct (Cr8) were found to contain up to 8x more of this alkene
403 compared to the empty vector (Cr2) control strain (up to 8.5 ± 1.5 mg/g, Fig. 5) which was
404 found almost exclusively within the biomass (Supplementary Fig. 7). The product was not
405 detected in dodecane solvent overlays. CrFAP accepts a very specific substrate (*cis*-vaccenic
406 acid, C18:1 *cis* Δ 11) *in vivo* (Sorigué et al., 2017), which corresponds to the accumulation of
407 only 7-heptadecene as the only detected increased product. This substrate is an unusual FA
408 and is likely not naturally abundant in the algal cell. Notably, any attempts to increase the
409 availability of free fatty acids using *E. coli*'Tesa did not result in any increase in the quantity
410 or diversity of accumulated alkanes. Future enzyme engineering will likely be able to
411 overcome this substrate specificity and increase overall yields of liberated hydrocarbons.
412 However, a strategy which would allow secretion of these molecules, similar to the capture of
413 heterologous terpenoids in dodecane solvent overlay (Lauersen et al., 2016; Lauersen et al.,
414 2018; Wichmann et al., 2018), would be an attractive next target in order to enable photo-
415 biocatalysis of hydrocarbons from the algal biomass.

416 Given the success with the FAP pathway in *Chlamydomonas* (present study) and
417 earlier work in *E. coli* (Sorigué et al., 2017), as well as finding that 'TesA expression can
418 substantially enhance the FFA pool in cyanobacteria, a synthetic FAP pathway was an obvious
419 choice to consider also for the prokaryotic host. We therefore proceeded to implement a
420 reconstituted variant of the eukaryotic algae pathway in cyanobacteria by combining TesA
421 with FAP. Given the genetic instability challenges with the CAR/ADO system (see Section 3.3)
422 we shifted our constructs to the more tightly repressed Pcoa promoter (Peca et al., 2008) for
423 controlling the expression of *E. coli* TesA and the *Chlorella variabilis* FAP from the RSF1010
424 plasmid (Fig. 6A). We noted that the yield of FFA was substantially increased when driving the
425 expression of TesA with the Pcoa promoter (Fig. 6C) compared to P_{lac143} (Fig. 4D).

426 Despite the dominance of C16:0 fatty acids released by 'TesA in *Synechocystis* 6803,
427 alongside minor fractions of C14:0 and C18:0, the C17:0 alkanes dominated the hydrocarbon
428 fraction at the lower light intensity (100 $\mu\text{mol photons m}^{-2} \text{s}^{-1}$) (Fig. 6B and 6D). This alkane
429 profile in *Synechocystis* 6803 is very different to that observed in *E. coli* without over-
430 expression of 'TesA (see Fig. S4 in (Sorigué et al., 2017)). We also observed substantial peaks
431 of 8-heptadecene and 6,9-heptadecadiene, as suggested by comparison with a NIST mass
432 spectrometry library, although a lack of standards prohibited confirmation (Supplementary
433 Figure 8). Curiously, these alkenes were only detected at day 6 and were not present in
434 samples harvested on day 10. As the fatty chain-length profiles differ when the same
435 thioesterase is expressed in different *E. coli* strains (Akhtar et al., 2015; Jing et al., 2011), this
436 suggests that the *in vivo* product profile of any thioesterase-dependent pathway also is
437 dependent on what the fatty acid synthesis pathway provides, not just the substrate
438 specificity of the thioesterase used.

439 Removal of the predicted chloroplast targeting sequence of FAP ('FAP) resulted in a
440 doubling of the alkane yield, this time accompanied also by C15 pentadecane. As the FAP
441 reaction is light-dependent, we also did a simple evaluation of this environmental factor.
442 When the light intensity was tripled, the total alkane production with the $\Delta\text{aas-1010}$ -'TesA-
443 'FAP strain increased to a yield of 77.1 mg/g CDW (19-fold enhancement relative to Δaas) and
444 a titer of 111.2 mg/L. The product profile also shifted (Fig. 6D) despite the lack of a similar
445 shift in the remaining FFA fraction (Fig. 6B), suggesting that the substrate specificity of FAP is
446 flexible and interestingly might change in response to a change in its cellular environment.

447 At 100 $\mu\text{mol photons m}^{-2} \text{s}^{-1}$ the introduction of 'FAP resulted in a drop in FFA
448 accumulation of up to 90% (for C18:0), whilst for C16:0 there was only a 60% reduction (Fig.
449 6C). Despite repeated trials, the recovery in the measurable fatty acid to alkane conversion

450 remained poor for C16:0 in comparison to C18:0 and the other pathways tested in
451 *Synechocystis* 6803. This may be explained by an impact on 'Tesa accumulation in the
452 constructs also carrying the gene coding for 'FAP. Nevertheless, the reconstituted eukaryotic
453 algae alkane pathway was more responsive to introduced modifications in the prokaryotic
454 cyanobacterium than in its native host, though this most likely is explained by challenges
455 associated with the release of FFA in the latter.

456 Although a substantial amount of both alkanes and alkenes were produced by the
457 engineered strains, their performance likely needs to be improved before any application can
458 be considered. Given that no genetically engineered phototrophic microalgae is currently used
459 for commercial purposes (as far as we are aware), and LCA-studies with non-catalytic systems
460 indicate a low predicted energy return on investment (EROI) (Carneiro et al., 2017), also
461 other challenges with commercial algal biotechnology (e.g. contamination, bioreactor cost,
462 energy consumption, etc) will need to be addressed.

463

464 **CONCLUSIONS**

465 The different biosynthetic systems presented in this study varied in terms of cellular context,
466 compartmentation, promoters, operon structures and expression platforms, thus precluding a
467 any direct comparison within and between the two species studied. However, the relative
468 conversion efficiencies and absolute functionalities provide for a valid comparison. As such, it
469 could be seen that the conversion of free fatty acids into alkenes by UndB and alkanes by FAP
470 were effective (>50% conversion, for individual fatty acids up to >90% conversion), and that
471 the native FAP pathway in *Chlamydomonas* was amenable to manipulation but that the
472 inability to increase the FFA pool hindered further progress. Consequently, for alkanes, the
473 reconstruction of the eukaryotic algae pathway in the prokaryotic cyanobacteria host
474 provided a more productive system than the partially synthetic pathways in either of the
475 prokaryotic (CAR-ADO) or eukaryotic hosts (TesA-FAP).

476 This work describes several approaches to employ synthetic metabolism and
477 substantially exceed native capabilities for hydrocarbon biosynthesis in well-established
478 model cyanobacteria and algae. Although even greater yields have been reported in
479 oleaginous algae and cyanobacteria that are natively endowed to accumulate lipids, the ability
480 to introduce synthetic metabolic pathways in model strains opens up possibilities for tailored
481 choice of both products and hosts. Importantly, the present work is based on first generation
482 strains and further improvement is likely with systematic optimization of both strains and
483 cultivation conditions, including the use of superior engineered or natural enzyme variants.

484

485

486 **ACKNOWLEDGEMENTS**

487 This project has received funding from the European Union's Horizon 2020 research and
488 innovation programme project PHOTOFUEL under grant agreement No 640720. IY received a
489 PhD scholarship from Indonesia Endowment Fund for Education (LPDP). The authors would
490 also like to thank Dr. Daniel Jaeger for assistance with lipid extraction from *C. reinhardtii*.

491

492

493

494 **FIGURE LEGENDS**

495

496 **Figure 1. Native and synthetic metabolic pathways evaluated in the present study with**
497 **incomplete stoichiometry.** The graphic illustration shows the introduced TesA (thioesterase
498 (Cho and Cronan, 1995)), CAR (carboxylic acid reductase (Akhtar et al., 2013)), UndA
499 (responsible for 1-undecene biosynthesis in *Pseudomonas* (Rui et al., 2014)), UndB (also
500 responsible for 1-undecene biosynthesis in *Pseudomonas* (Rui et al., 2015)), OleT
501 (responsible for olefin biosynthesis in *Jeotgalicoccus* (Rude et al., 2011)) and FAP (fatty acid
502 photodecarboxylase (Sorigué et al., 2017)) enzymes alongside the native AAR/ADO (acyl-ACP
503 reductase and aldehyde deformylating oxygenase (Schirmer et al., 2010)), AHR (aldehyde
504 reductase, unknown) and FAP enzymes. Blue reactions are non-native and those in grey are
505 native. The red cross indicates deletion of the *aas* gene.

506

507 **Figure 2. Engineering for enhanced accumulation of free fatty acids.** (A) Representative total
508 ion count chromatograms for *Synechocystis* 6803 strains Δaas -TesA (black) vs. Δaas only
509 (orange) extracted on day 10 of cultivation (induced day 2). Peak identities: (3) Heptadecane,
510 (4) Tetradecanoic acid, (5) Hexadecanoic acid, (6) 9,12-octadecadienoic acid, (7) 9-
511 octadecenoic acid, (8) Octadecanoic acid. (B) Graphic representation of the constructs used to
512 transform *Chlamydomonas*. CTP = Chloroplast Transit Peptide. (C) Fluorescence microscopy
513 of representative strains indicating appropriate chloroplast localization of the CTP_'TesA_YFP
514 construct. (D) Total (TL), polar (PL), and neutral (NL) gravimetric lipid fractions of
515 *Chlamydomonas* parental strain and TesA overproducing strains under nutrient replete
516 conditions (N+) and after 96 hours of nitrogen depletion (N-). PL is significantly greater in +N
517 for TesA: ttest, p:0.047 (indicated by an asterisk).

518

519 **Figure 3. Over-expression of UndB results in effective (>50%) conversion of fatty acids into**
520 **corresponding alkenes.** (A) Graphic representation of the genetic modification of
521 *Synechocystis* sp. PCC 6803 and the plasmid used for UndB expression. (B) GC-MS
522 chromatograms with extracts from the two different strains (w/wo UndB); Δaas -1010-'TesA
523 (black) and Δaas -1010-'TesA-UndB (orange). (C) The free fatty acid yield (relative to biomass)
524 in the whole cultures of the two strains, subdivided into the three dominant chain-lengths. (D)
525 The yield of alkenes in the whole cultures of the two strains, subdivided into the three
526 dominant chain-lengths. (E) The localization of the alkene products in whole cultures of the
527 two strains. Peak identities: (1) 1-pentadecene, (2) 1-heptadecene, (3) heptadecane, (4)

528 tetradecanoic acid, (5) hexadecanoic acid, (6) 9,12-octadecadienoic acid, (7) 9-octadecenoic
529 acid, (8) octadecanoic acid. Data are mean \pm SD from three biological replicates. All samples
530 were extracted on day 10.

531

532 **Figure 4. The CAR-dependent pathway produces mainly fatty alcohols.** (A) Graphic overview
533 (not to scale) illustrating the main constructs studied in the figure. (B) Total ion
534 chromatogram from extracts of $\Delta aas-1010$ -*TesA* (black) and $\Delta aas-1010$ -TPC2 (orange). (C)
535 Fatty alcohol profile from extracts of Δaas -TPC2. The yield of fatty acids (D), alcohols (E) and
536 alkanes (F). Peak identities: (2) 1-dodecanol, (3) heptadecane, (4) 1-tetradecanol, (5) 1-
537 hexadecanol, (6) 9,12-octadecadien-1-ol, (7) 9-octadecen-1-ol, (8) 1-octadecanol, (9)
538 dodecanoic acid, (10) tetradecanoic acid, (11) hexadecanoic acid, (12) octadecanoic acid. Data
539 are mean \pm SD of three biological replicates. Cultures were induced on day 2 following
540 dilution and samples were extracted on day 10.

541

542 **Figure 5. CrFAP over-expression increases 7-heptadecene yield, but heterologous thioesterase**
543 **(*TesA*) expression, its co-expression, and C- or N-terminal fusion with CrFAP has no benefit.**
544 Mutants expressing indicated constructs (left panel) were cultivated for seven days in TAP
545 medium with 250 $\mu\text{mol photons s}^{-1} \text{m}^{-2}$ constant illumination and cell pellets were extracted
546 with cell rupture by glass beads and dodecane for yield quantification of 7-heptadecene via
547 GC-MS (bar graph, right). All constructs bear a PsaD chloroplast targeting peptide (CTP) to
548 allow protein transit to the chloroplast. Arrows and plus sign indicate co-expression in double
549 transformed mutants. Error bars represent 95% confidence intervals of single strains
550 cultivated in biological triplicates.

551

552 **Figure 6. Conversion of free fatty acids into alkanes in cyanobacteria using FAP.** (A) Graphic
553 representative of the plasmids used to transform *Synechocystis* sp. PCC 6803. (B) Total ion
554 chromatogram from Δaas -Pcoa-*TesA* (left) and $\Delta aas-1010$ -Pcoa-*TesA*-FAP (100 μmol
555 $\text{photons s}^{-1} \text{m}^{-2}$ (μE), middle; 300 $\mu\text{mol photons s}^{-1} \text{m}^{-2}$, right). The free fatty acid (C) and
556 alkane (D) yield in all tested strains. Data are mean \pm SD of three biological replicates.
557 Samples were extracted on day 10. Peak: (1) heptadecane, (2) octadecane (internal standard),
558 (3) pentadecane, (4) undecane, (5) tridecane, (6) hexadecanoic acid.

559

560

561

562 **REFERENCES**

- 563 Ajjawi, I., Verruto, J., Aqui, M., Soriaga, L. B., Coppersmith, J., Kwok, K., Peach, L., Orchard, E.,
564 Kalb, R., Xu, W., Carlson, T. J., Francis, K., Konigsfeld, K., Bartalis, J., Schultz, A., Lambert,
565 W., Schwartz, A. S., Brown, R., Moellering, E. R., 2017. Lipid production in
566 *Nannochloropsis gaditana* is doubled by decreasing expression of a single
567 transcriptional regulator. *Nat Biotechnol.* 35, 647-652.
- 568 Akhtar, M. K., Dandapani, H., Thiel, K., Jones, P. R., 2015. Microbial production of 1-octanol - a
569 naturally excreted biofuel with diesel-like properties. *Metabolic Engineering*
570 *Communications.* 2, 1-5.
- 571 Akhtar, M. K., Turner, N. J., Jones, P. R., 2013. Carboxylic acid reductase is a versatile enzyme
572 for the conversion of fatty acids into fuels and chemical commodities. *Proc Natl Acad*
573 *Sci U S A.* 110, 87-92.
- 574 Angermayr, S. A., van der Woude, A. D., Correddu, D., Vreugdenhil, A., Verrone, V., Hellingwerf,
575 K. J., 2014. Exploring metabolic engineering design principles for the photosynthetic
576 production of lactic acid by *Synechocystis* sp. PCC6803. *Biotechnol Biofuels.* 7, 99.
- 577 Baier, T., Wichmann, J., Kruse, O., Lauersen, K. J., 2018. Intron-containing algal transgenes
578 mediate efficient recombinant gene expression in the green microalga *Chlamydomonas*
579 *reinhardtii*. *Nucleic Acids Research.* gky532-gky532.
- 580 Bernard, A., Domergue, F., Pascal, S., Jetter, R., Renne, C., Faure, J. D., Haslam, R. P., Napier, J. A.,
581 Lessire, R., Joubès, J., 2012. Reconstitution of Plant Alkane Biosynthesis in Yeast
582 Demonstrates That *Arabidopsis* ECERIFERUM1 and ECERIFERUM3 Are Core
583 Components of a Very-Long-Chain Alkane Synthesis Complex. *Plant Cell.* 24, 3106-18.
- 584 Carneiro, M. L. N. M., Pradelle, F., Braga, S. L., Gomes, M. S. P., Martins, A. R. F. A., Turkovics, F.,
585 Pradelle, R. N. C., 2017. Potential of biofuels from algae: Comparison with fossil fuels,
586 ethanol and biodiesel in Europe and Brazil through life cycle assessment (LCA).
587 *Renewable and Sustainable Energy Reviews.* 73, 632-653.
- 588 Cho, H., Cronan, J. E., 1995. Defective export of a periplasmic enzyme disrupts regulation of
589 fatty acid synthesis. *J Biol Chem.* 270, 4216-9.
- 590 Cook, C., Dayananda, C., Tennant Richard, K., Love, J., 2017. Third-Generation Biofuels from the
591 Microalga, *Botryococcus braunii*. *Biofuels and Bioenergy.*
- 592 Delrue, F., Li-Beisson, Y., Setier, P. A., Sahut, C., Roubaud, A., Froment, A. K., Peltier, G., 2013.
593 Comparison of various microalgae liquid biofuel production pathways based on
594 energetic, economic and environmental criteria. *Bioresour Technol.* 136C, 205-212.

595 Elhai, J., Wolk, C. P., 1988. Conjugal transfer of DNA to cyanobacteria. *Methods Enzymol.* 167,
596 747-54.

597 Eroglu, E., Melis, A., 2010. Extracellular terpenoid hydrocarbon extraction and quantitation
598 from the green microalgae *Botryococcus braunii* var. *Showa*. *Bioresource Technology.*
599 101, 2359-2366.

600 Eser, B. E., Das, D., Han, J., Jones, P. R., Marsh, E. N., 2011. Oxygen-independent alkane
601 formation by non-heme iron-dependent cyanobacterial aldehyde decarbonylase:
602 investigation of kinetics and requirement for an external electron donor. *Biochemistry.*
603 50, 10743-50.

604 Gorman, D. S., Levine, R. P., 1965. Cytochrome f and plastocyanin: their sequence in the
605 photosynthetic electron transport chain of *Chlamydomonas reinhardtii*. *Proc Natl Acad*
606 *Sci U S A.* 54, 1665-9.

607 Hu, P., Borglin, S., Kamennaya, N. A., Chen, L., Park, H., Mahoney, L., Kijac, A., Shan, G.,
608 Chavarría, K. L., Zhang, C., Quinn, N. W. T., Wemmer, D., Holman, H.-Y., Jansson, C., 2013.
609 Metabolic phenotyping of the cyanobacterium *Synechocystis* 6803 engineered for
610 production of alkanes and free fatty acids. *Applied Energy.* 102, 850-859.

611 Jing, F., Cantu, D. C., Tvaruzkova, J., Chipman, J. P., Nikolau, B. J., Yandeu-Nelson, M. D., Reilly,
612 P. J., 2011. Phylogenetic and experimental characterization of an acyl-ACP thioesterase
613 family reveals significant diversity in enzymatic specificity and activity. *BMC Biochem.*
614 12, 44.

615 Kaczmarzyk, D., Cengic, I., Yao, L., Hudson, E.P., 2018. Diversion of the long-chain acyl- ACP
616 pool in *Synechocystis* to fatty alcohols through CRISPRi repression of the es- sential
617 phosphate acyltransferase *PlsX*. *Metab. Eng.* 45, 59-66.

618 Kageyama, H., Waditee-Sirisattha, R., Sirisattha, S., Tanaka, Y., Mahakhant, A., Takabe, T., 2015.
619 Improved Alkane Production in Nitrogen-Fixing and Halotolerant Cyanobacteria via
620 Abiotic Stresses and Genetic Manipulation of Alkane Synthetic Genes. *Curr Microbiol.*
621 71, 115-20.

622 Kallio, P., Pasztor, A., Thiel, K., Akhtar, M. K., Jones, P. R., 2014. An engineered pathway for the
623 biosynthesis of renewable propane. *Nature Communications.* 5:4731.

624 Kato, A., Takatani, N., Ikeda, K., Maeda, S.I., Omata, T., 2017. Removal of the product from the
625 culture medium strongly enhances free fatty acid production by genetically
626 engineered. *Biotechnol. Biofuels* 10, 141.

627 Khara, B., et al., 2013. Production of propane and other short-chain alkanes by structure-
628 based engineering of ligand specificity in aldehyde-deformylating oxygenase.
629 ChemBioChem 14, 1204–1208.

630 Kindle, K. L., 1990. High-frequency nuclear transformation of *Chlamydomonas reinhardtii*.
631 Proc Natl Acad Sci U S A. 87, 1228-32.

632 Lauersen, K. J., Baier, T., Wichmann, J., Wördenweber, R., Mussgnug, J. H., Hübner, W., Huser,
633 T., Kruse, O., 2016. Efficient phototrophic production of a high-value sesquiterpenoid
634 from the eukaryotic microalga *Chlamydomonas reinhardtii*. Metab Eng. 38, 331-343.

635 Lauersen, K. J., Kruse, O., Mussgnug, J. H., 2015. Targeted expression of nuclear transgenes in
636 *Chlamydomonas reinhardtii* with a versatile, modular vector toolkit. Appl Microbiol
637 Biotechnol. 99, 3491-503.

638 Lauersen, K. J., Wichmann, J., Baier, T., Kampranis, S. C., Pateraki, I., Møller, B. L., Kruse, O.,
639 2018. Phototrophic production of heterologous diterpenoids and a hydroxy-
640 functionalized derivative from *Chlamydomonas reinhardtii*. Metabolic Engineering.

641 Lea-Smith, D. J., Biller, S. J., Davey, M. P., Cotton, C. A., Perez Sepulveda, B. M., Turchyn, A. V.,
642 Scanlan, D. J., Smith, A. G., Chisholm, S. W., Howe, C. J., 2015. Contribution of
643 cyanobacterial alkane production to the ocean hydrocarbon cycle. Proc Natl Acad Sci U
644 S A. 112, 13591-6.

645 Lea-Smith, D. J., Ortiz-Suarez, M. L., Lenn, T., Nürnberg, D. J., Baers, L. L., Davey, M. P., Parolini,
646 L., Huber, R. G., Cotton, C. A., Mastroianni, G., Bombelli, P., Ungerer, P., Stevens, T. J.,
647 Smith, A. G., Bond, P. J., Mullineaux, C. W., Howe, C. J., 2016. Hydrocarbons Are Essential
648 for Optimal Cell Size, Division, and Growth of Cyanobacteria. Plant Physiol. 172, 1928-
649 1940.

650 Lin, F., Das, D., Lin, X. N., Marsh, E. N., 2013. Aldehyde-forming fatty acyl-CoA reductase from
651 cyanobacteria: expression, purification and characterization of the recombinant
652 enzyme. FEBS J. 280, 4773-81.

653 Liu, X., Sheng, J., Curtiss, R., 2011. Fatty acid production in genetically modified cya-
654 nobacteria. Proc. Natl. Acad. Sci. USA 108, 6899–6904.

655 Liu, Y., Wang, C., Yan, J., Zhang, W., Guan, W., Lu, X., Li, S., 2014. Hydrogen peroxide-
656 independent production of α -alkenes by OleTJE P450 fatty acid decarboxylase.
657 Biotechnol Biofuels. 7, 28.

658 Markley, A.L., Begemann, M.B., Clarke, R.E., Gordon, G.C., Pflieger, B.F, 2015. . A syn-
659 thetic biology toolbox for controlling gene expression in the cyanobacterium *Synechococcus*
660 sp. PCC 7002. ACS Synth. Biol. 4, 595–603.

661 Metzger, P., Largeau, C., 2005. *Botryococcus braunii*: a rich source for hydrocarbons and
662 related ether lipids. *Appl Microbiol Biotechnol.* 66, 486-96.

663 Neupert, J., Karcher, D., Bock, R., 2009. Generation of *Chlamydomonas* strains that efficiently
664 express nuclear transgenes. *Plant J.* 57, 1140-50.

665 Peca, L., Kós, P. B., Máté, Z., Farsang, A., Vass, I., 2008. Construction of bioluminescent
666 cyanobacterial reporter strains for detection of nickel, cobalt and zinc. *FEMS Microbiol*
667 *Lett.* 289, 258-64.

668 Peramuna, A., Morton, R., Summers, M. L., 2015. Enhancing alkane production in
669 cyanobacterial lipid droplets: a model platform for industrially relevant compound
670 production. *Life (Basel).* 5, 1111-26.

671 Qiu, Y., Tittiger, C., Wicker-Thomas, C., Le Goff, G., Young, S., Wajnberg, E., Fricaux, T., Taquet,
672 N., Blomquist, G. J., Feyereisen, R., 2012. An insect-specific P450 oxidative
673 decarboxylase for cuticular hydrocarbon biosynthesis. *Proc Natl Acad Sci U S A.*

674 Quinn, J. C., Davis, R., 2015. The potentials and challenges of algae based biofuels: a review of
675 the techno-economic, life cycle, and resource assessment modeling. *Bioresour Technol.*
676 184, 444-452.

677 Rasala, B. A., Barrera, D. J., Ng, J., Plucinak, T. M., Rosenberg, J. N., Weeks, D. P., Oyler, G. A.,
678 Peterson, T. C., Haerizadeh, F., Mayfield, S. P., 2013. Expanding the spectral palette of
679 fluorescent proteins for the green microalga *Chlamydomonas reinhardtii*. *Plant J.* 74,
680 545-56.

681 Rude, M. A., Baron, T. S., Brubaker, S., Alibhai, M., Del Cardayre, S. B., Schirmer, A., 2011.
682 Terminal olefin (1-alkene) biosynthesis by a novel p450 fatty acid decarboxylase from
683 *Jeotgalicoccus* species. *Appl Environ Microbiol.* 77, 1718-27.

684 Ruffing, A.M., 2014. Improved free fatty acid production in cyanobacteria with *Synechococcus*
685 sp. PCC 7002 as host. *Front. Bioeng. Biotechnol.* 2, 17.

686 Rui, Z., Harris, N. C., Zhu, X., Huang, W., Zhang, W., 2015. Discovery of a Family of Desaturase-
687 Like Enzymes for 1-Alkene Biosynthesis. *ACS Catalysis.* 5, 7091-7094.

688 Rui, Z., Li, X., Zhu, X., Liu, J., Domigan, B., Barr, I., Cate, J. H., Zhang, W., 2014. Microbial
689 biosynthesis of medium-chain 1-alkenes by a nonheme iron oxidase. *Proc Natl Acad Sci*
690 *U S A.* 111, 18237-42.

691 Schirmer, A., Rude, M., Li, X., Popova, E., del Cardayre, S., 2010. Microbial biosynthesis of
692 alkanes. *Science.* 329, 559-62.

693 Sheppard, M. J., Kunjapur, A. M., Prather, K. L. J., 2016. Modular and selective biosynthesis of
694 gasoline-range alkanes. *Metab Eng.* 33, 28-40.

695 Sorigué, D., Légeret, B., Cuiné, S., Blangy, S., Moulin, S., Billon, E., Richaud, P., Brugière, S.,
696 Couté, Y., Nurizzo, D., Müller, P., Brettel, K., Pignol, D., Arnoux, P., Li-Beisson, Y., Peltier,
697 G., Beisson, F., 2017. An algal photoenzyme converts fatty acids to hydrocarbons.
698 Science. 357, 903-907.

699 Storch, M., Casini, A., Mackrow, B., Fleming, T., Trewitt, H., Ellis, T., Baldwin, G. S., 2015.
700 BASIC: A New Biopart Assembly Standard for Idempotent Cloning Provides Accurate,
701 Single-Tier DNA Assembly for Synthetic Biology. ACS Synth Biol. 4, 781-7.

702 Wang, W., Liu, X., Lu, X., 2013. Engineering cyanobacteria to improve photosynthetic
703 production of alka(e)nes. Biotechnol Biofuels. 6, 69.

704 Warui, D. M., Pandelia, M. E., Rajakovich, L. J., Krebs, C., Bollinger, J. M., Booker, S. J., 2015.
705 Efficient delivery of long-chain fatty aldehydes from the Nostoc punctiforme acyl-acyl
706 carrier protein reductase to its cognate aldehyde-deformylating oxygenase.
707 Biochemistry. 54, 1006-15.

708 Wichmann, J., Baier, T., Wentnagel, E., Lauersen, K. J., Kruse, O., 2018. Tailored carbon
709 partitioning for phototrophic production of (E)- α -bisabolene from the green microalga
710 Chlamydomonas reinhardtii. Metab Eng. 45, 211-222.

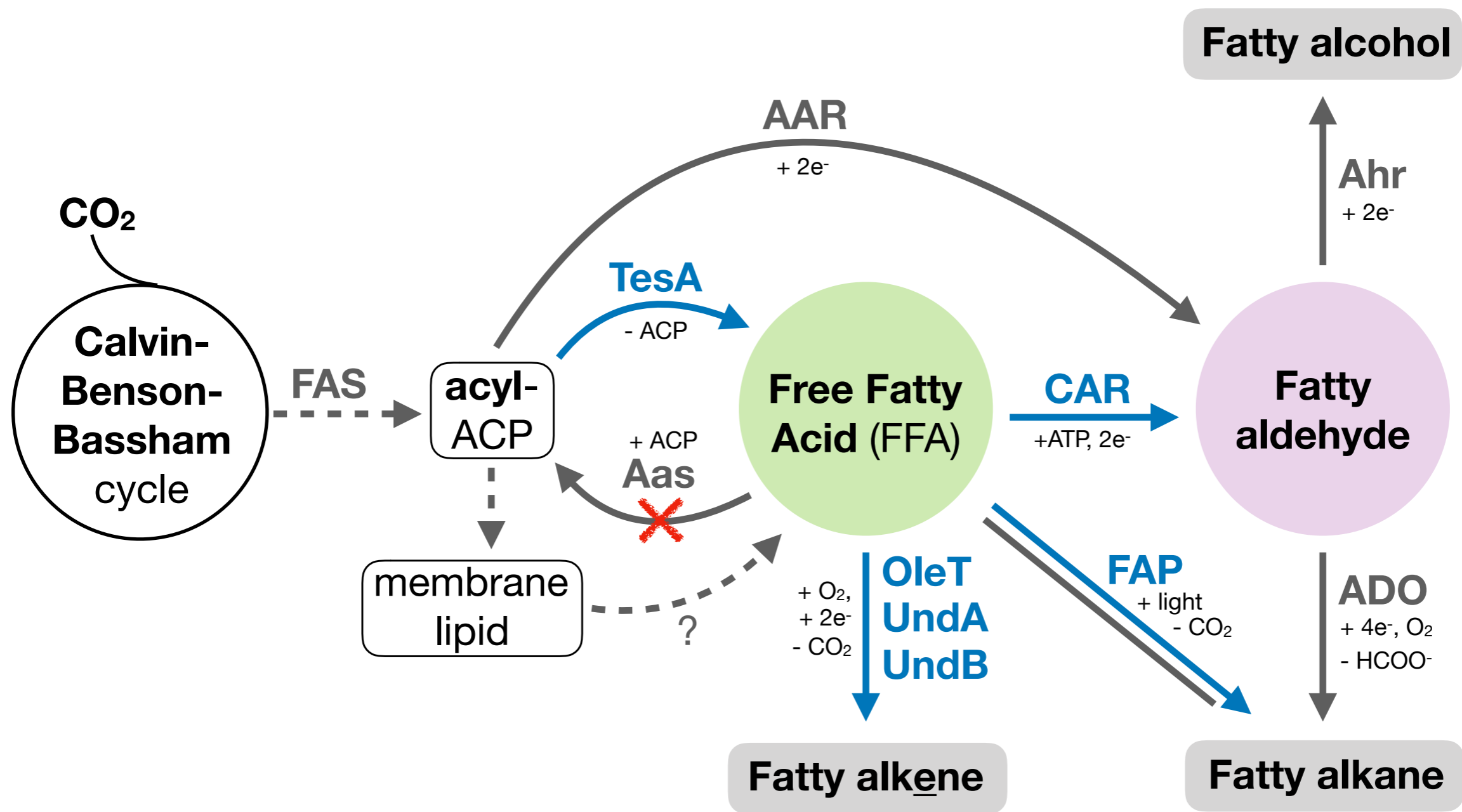
711 Work, V.H., Melnicki, M.R., Hill, E.A., Davies, F.K., Kucek, L.A., Beliaev, A.S., et al., 2015. Lauric
712 acid production in a glycogen-less strain of Synechococcus sp. PCC 7002. Front Bioeng.
713 Biotechnol. 3.

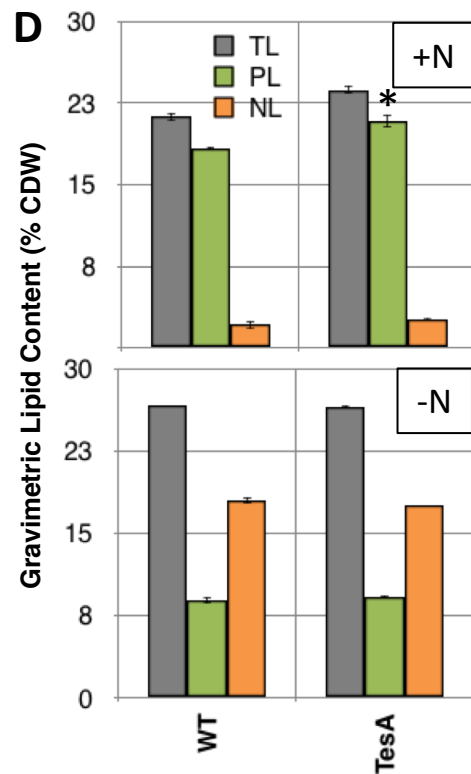
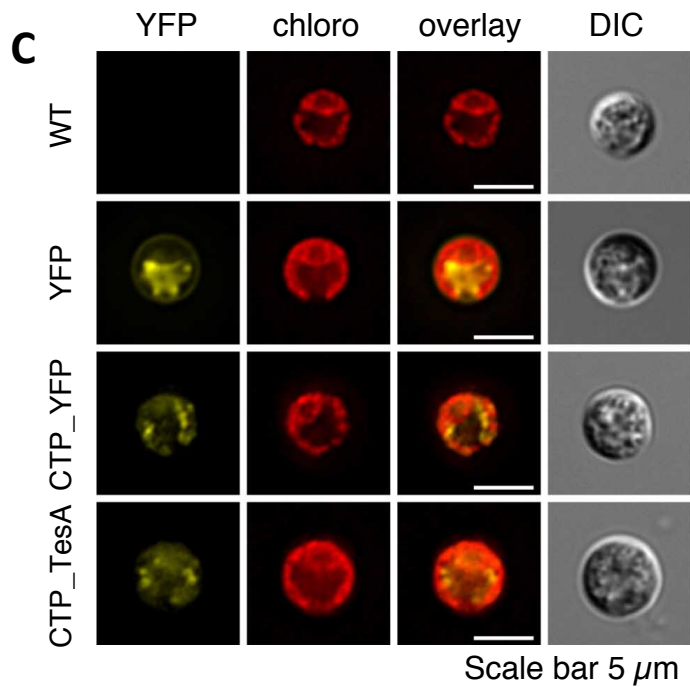
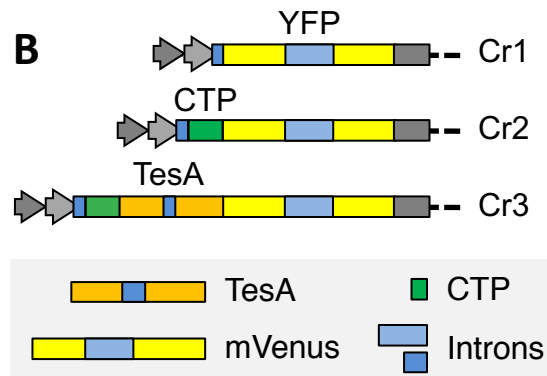
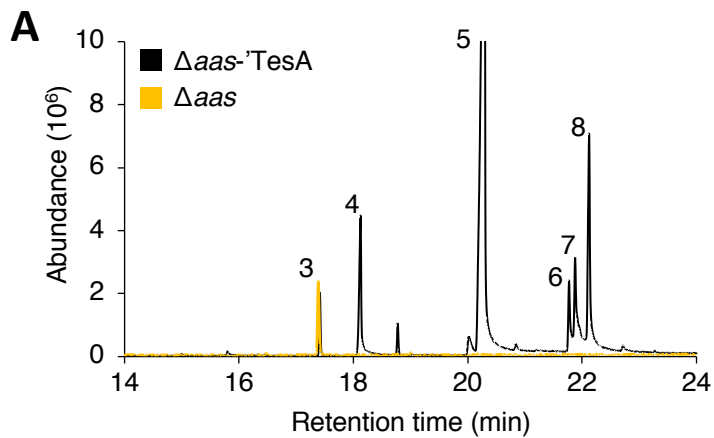
714 Yunus, I.Y., Jones, P.R., 2018. Photosynthesis-dependent biosynthesis of medium chain-length
715 fatty acids and alcohols. Metab Eng. 49, 59-68.

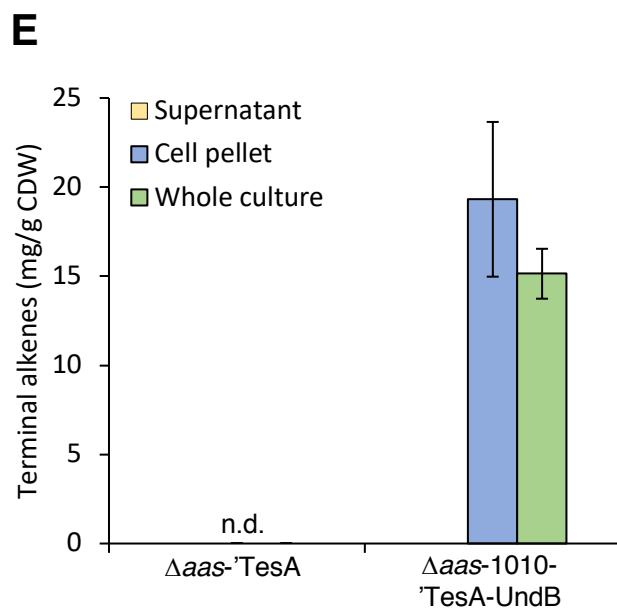
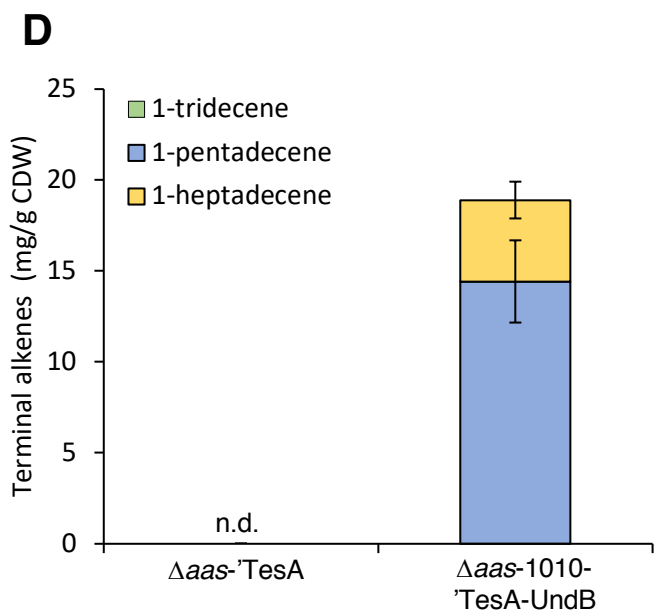
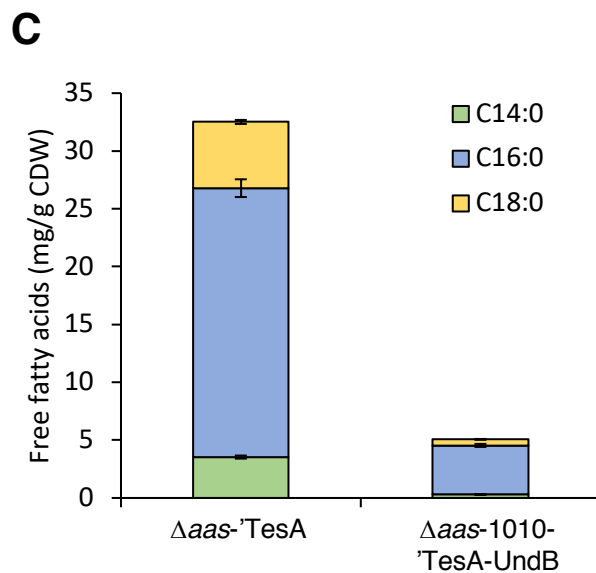
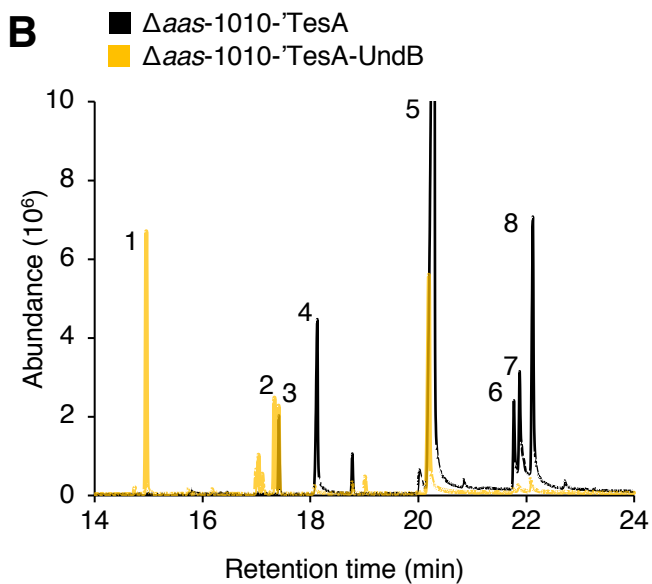
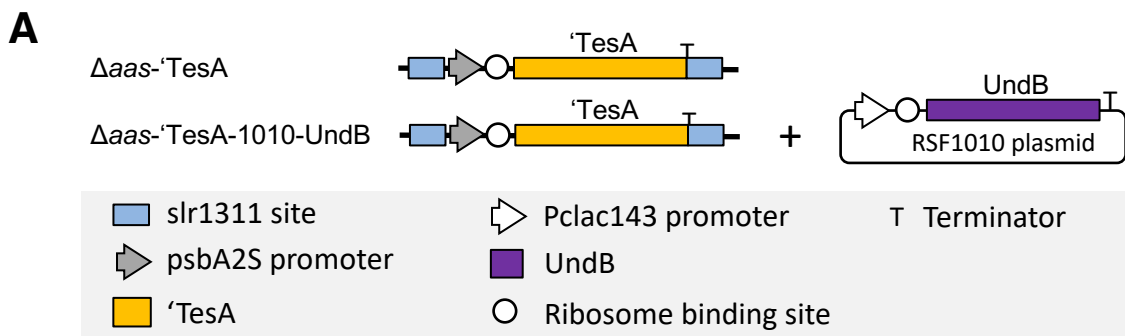
716 Zhou, Y. J., Hu, Y., Zhu, Z., Siewers, V., Nielsen, J., 2018. Engineering 1-Alkene Biosynthesis and
717 Secretion by Dynamic Regulation in Yeast. ACS Synth Biol. 7, 584-590.

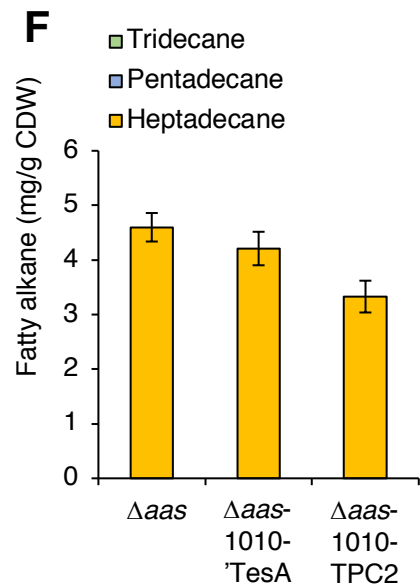
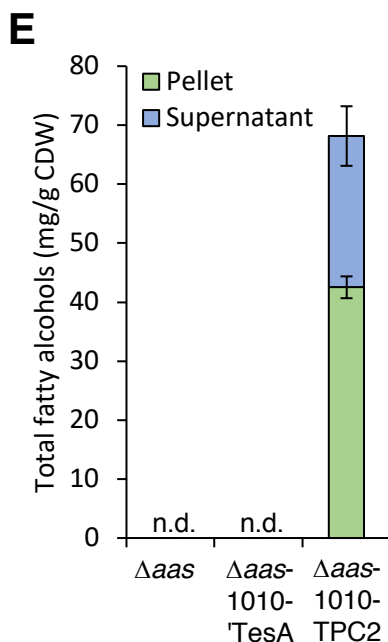
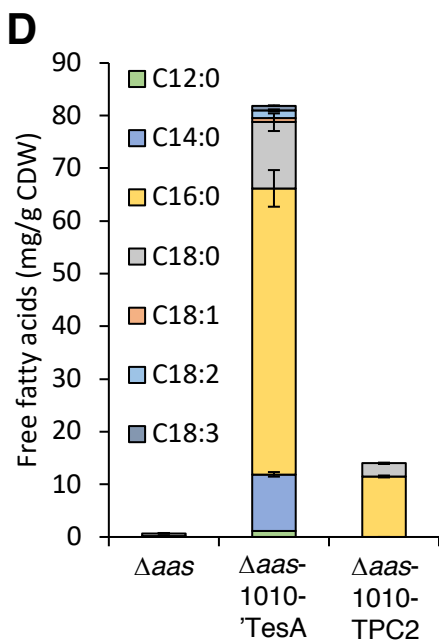
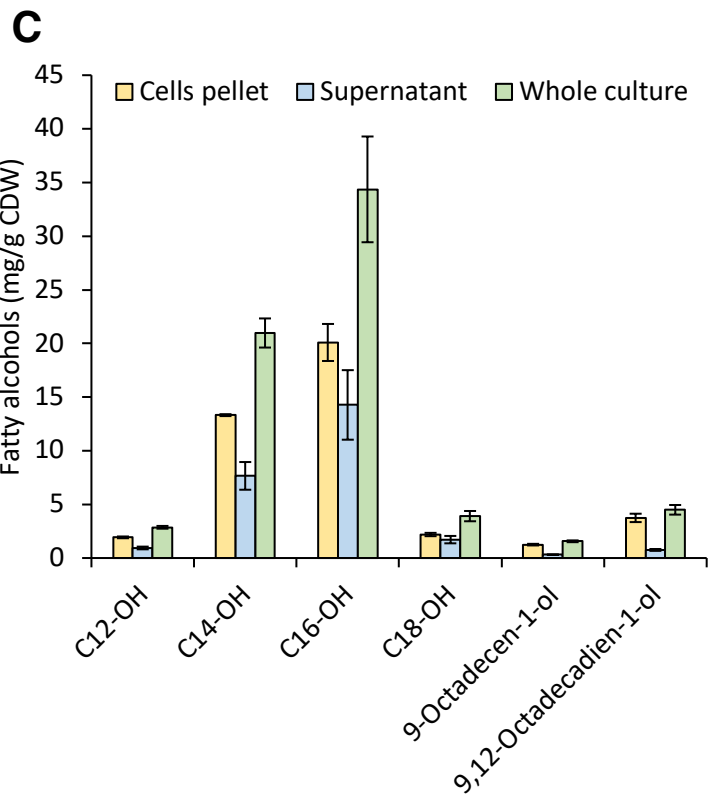
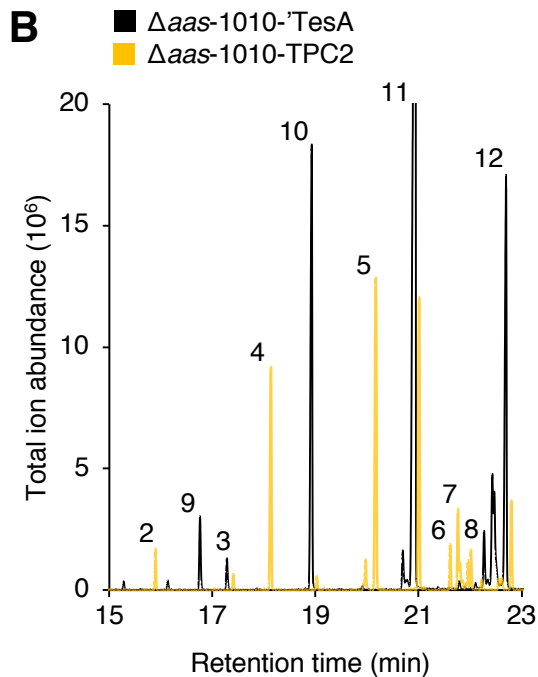
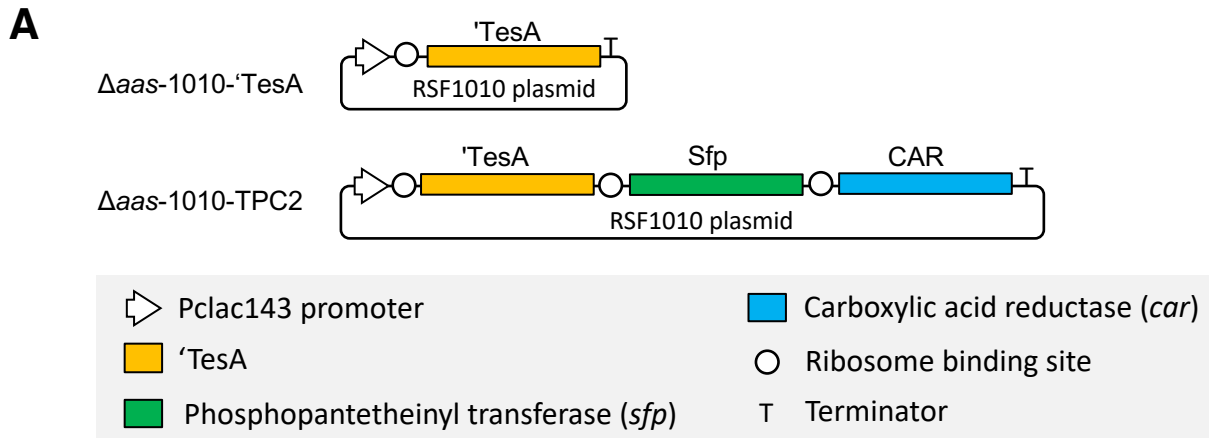
718 Zhu, Z., Zhou, Y. J., Kang, M. K., Krivoruchko, A., Buijs, N. A., Nielsen, J., 2017. Enabling the
719 synthesis of medium chain alkanes and 1-alkenes in yeast. Metab Eng. 44, 81-88.

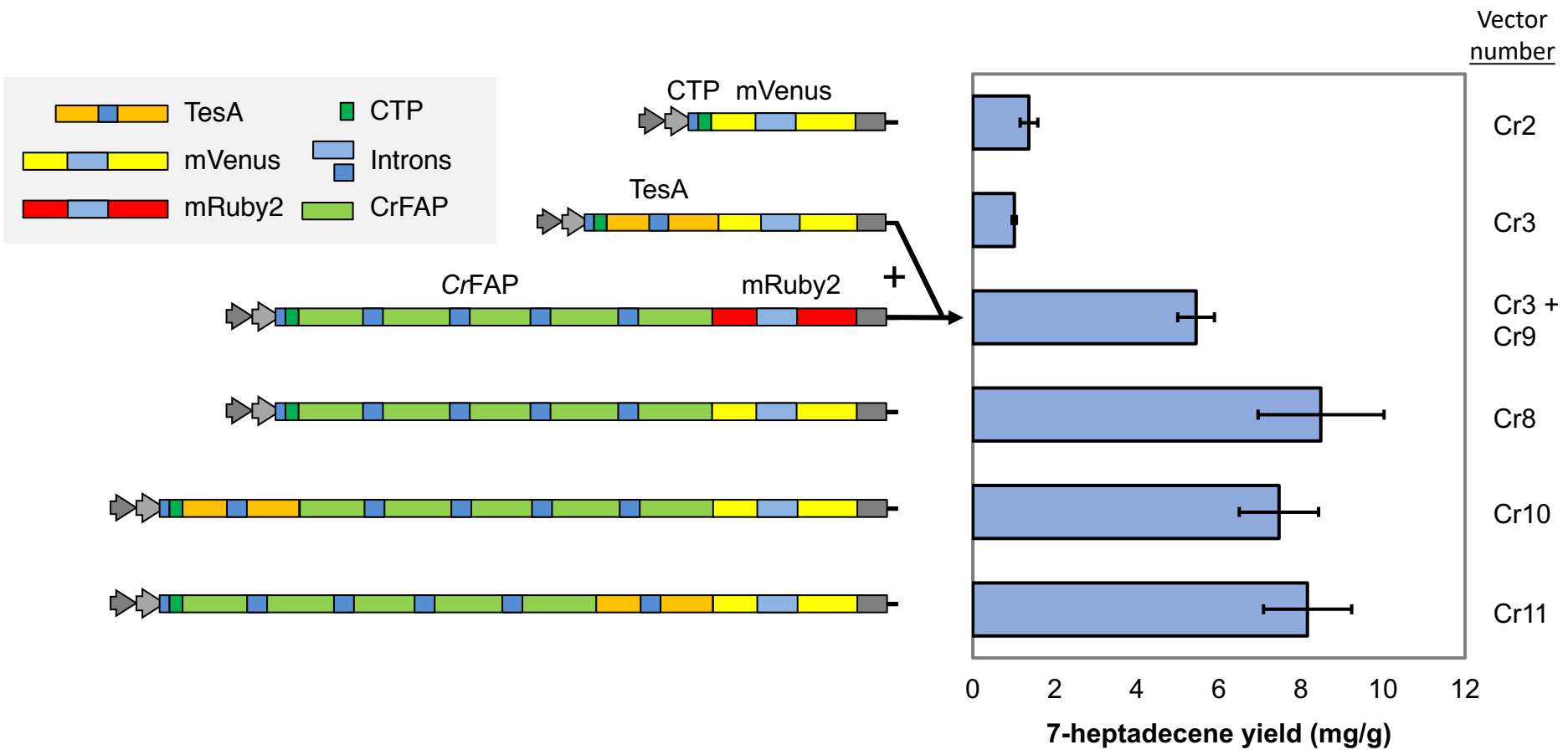
720

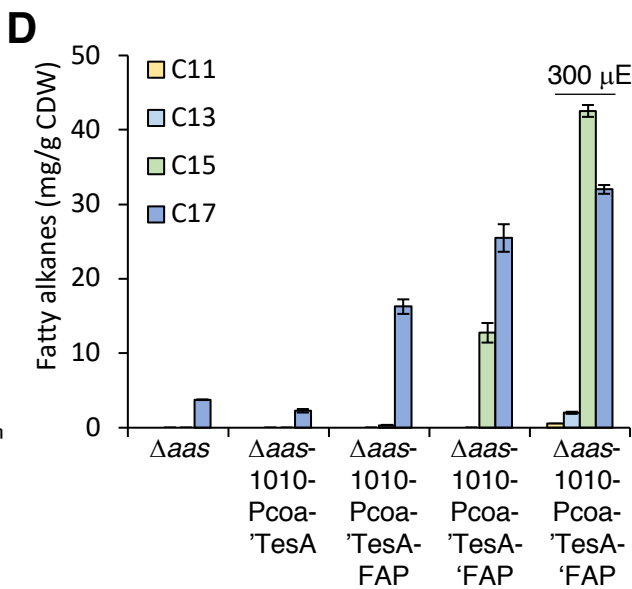
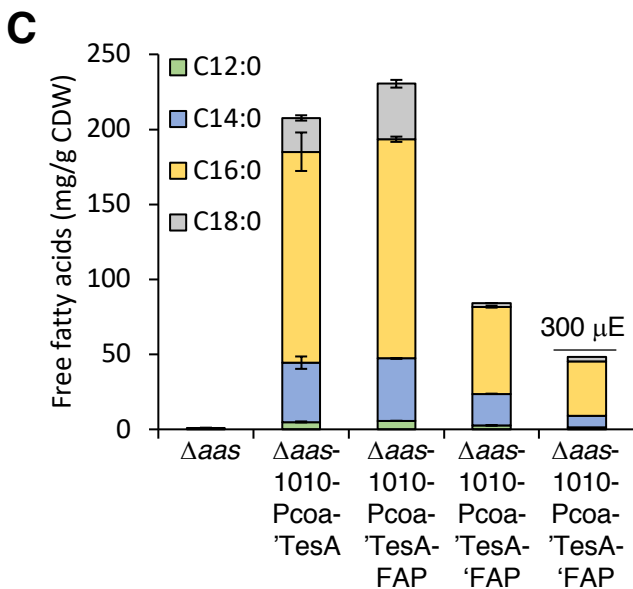
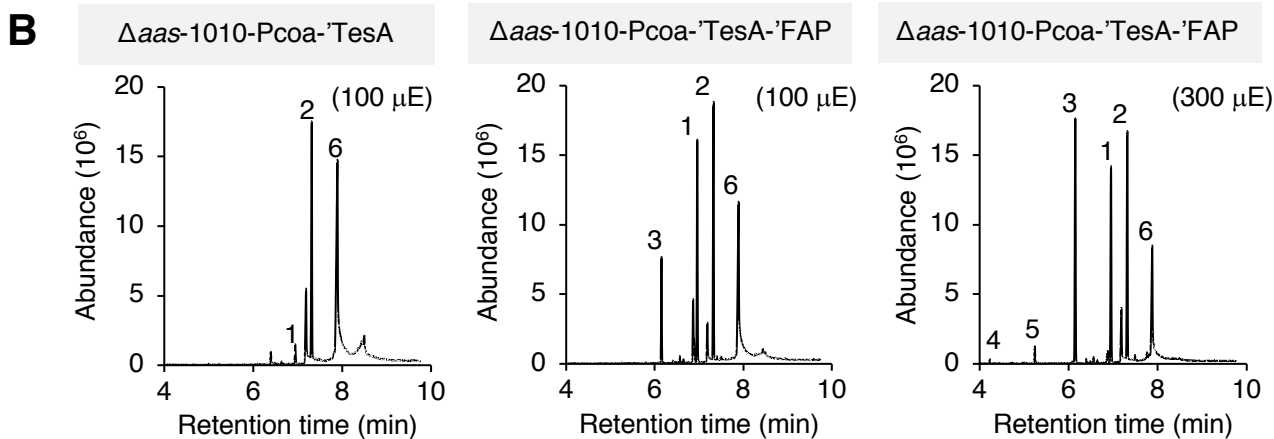
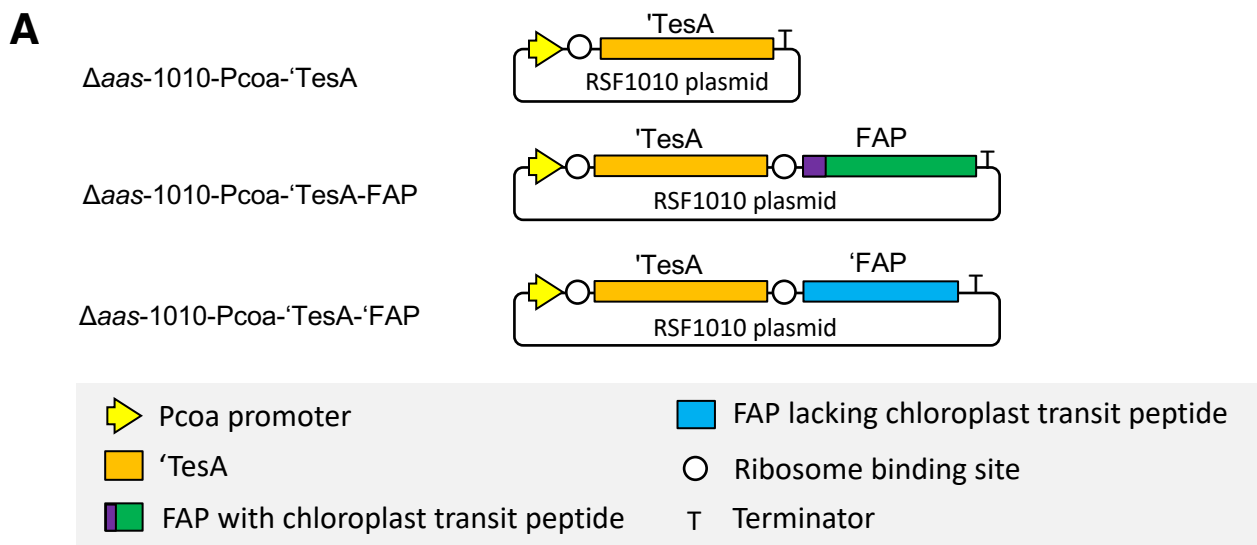












Supplementary Information

Synthetic metabolic pathways for photobiological conversion of CO₂ into hydrocarbon fuel

Ian Sofian Yunus^a, Julian Wichmann^b, Robin Wördenweber^b, Kyle J. Lauersen^b, Olaf Kruse^b
and Patrik R. Jones^{a*}

^aDepartment of Life Sciences, Imperial College London, SW7 2AZ London, UK

^bBielefeld University, Faculty of Biology, Center for Biotechnology (CeBiTec),
Universitätsstrasse 27, 33615, Bielefeld, Germany.

*Corresponding author: p.jones@imperial.ac.uk

Index

Supplementary Table 1. The inventory of materials ((A) plasmids, (B) linkers, (C) primers, (D) DNA parts) used to prepare DNA constructs for the creation of *Synechocystis* strains.

Supplementary Table 2. All *Synechocystis* sp. PCC 6803 strains used in the study.

Supplementary Table 3. All DNA constructs used for engineering *Chlamydomonas* (optimized transgenes, vector backbone, reporters, selection markers, NCBI accession numbers)

Supplementary Figure 1. Growth properties of engineered cyanobacteria strains. (A) The final OD₇₃₀ and biomass accumulation of the engineered strains on day 10 when samples were extracted. (B) Representative growth profile for the first three strains shown in (A).

Supplementary Figure 2. Graphic illustration of all (key) *Chlamydomonas* DNA constructs used in the study

Supplementary Figure 3. The inactivation of *aas* (acyl-ACP synthase).

Supplementary Figure 4. GC-MS chromatogram for 7-heptadecene in native *Chlamydomonas*.

Supplementary Figure 5. Western blot with proteins extracted from engineered *Chlamydomonas* strains. (A) OleTJE strains, (B) CrFAP strains.

Supplementary Figure 6. Fluorescence microscopy with *Chlamydomonas* OleTJE and CrFAP strains.

Supplementary Figure 7. Polar and neutral lipid profiles in *TesA*-overexpressing *Chlamydomonas* strains.

Supplementary Figure 8. GC-MS chromatograms of suspected alkenes in 6803-FAP strains.

Note that all of the supplementary information is presented in the order of mention in the main text.

Supplementary Table 1. The inventory of materials ((A) plasmids, (B) linkers, (C) primers, (D) DNA parts) used to prepare DNA constructs for the creation of *Synechocystis* strains.

(A) Plasmid DNA used for transformation of cyanobacteria

Assembly	Prefix Linker	Plasmid	Suffix Linker	Plasmid generated	Relevant Information
1	1MP	pIY67	1S	pIY370	pIY370 is a plasmid storage containing rrnB1 T1 terminator and T7Te terminator, gentamicin selection marker, and downstream region of slr1311 site.
	1P	pIY127	2S		
	2P	pIY353	2MS		
	2MP	pIY21	1MS		
2	1MP	pIY370	1S	pIY380	pIY380 is a plasmid used for chromosomal integration targeting the slr1311 site with PpsbA2S as a promoter. This plasmid contains a GFP dropout gene.
	1P	pIY23	2S		
	2P	pIY352	2MS		
	2MP	pIY24	1MS		
3	LRBS1-5P	pIY72	1S	pIY397	pIY397 is used to integrate 'tesA in slr1311 site under PpsbA2S promoter.
	1P	pIY380	LRBS1-5S		
4	1MP	pIY128	1S	pIY140	pIY140 is an RSF1010 overexpression plasmid with Pclac143 promoter and erythromycin as a selection marker. This plasmid contains a GFP dropout gene.
	1P	pIY51	2S		
	2P	pIY102	2MS		
	2MP	pIY24	1MS		
5	1MP	pIY128	1S	pIY417	pIY417 is an RSF1010 overexpression plasmid with Pcoa promoter and erythromycin as a selection marker. This plasmid contains a GFP dropout gene.
	1P	pIY51	2S		
	2P	pPB345	2MS		
	2MP	pIY24	1MS		
6	LRBS1-5P	pIY72	1S	pIY397	pIY397 is used to integrate 'TesA in slr1311 site under PpsbA2S promoter.
	1P	pIY380	LRBS1-5S		
7	LRBS1-5P	pIY72	1S	pIY196	pIY196 is a 'TesA overexpression plasmid with Pclac143 promoter and erythromycin selection marker.
	1P	pIY140	LRBS1-5S		
8	LRBS1-3P	pIY395	1S	pIY402	pIY402 is an UndB overexpression plasmid with Pclac143 promoter and erythromycin selection marker.
	1P	pIY140	LRBS1-3S		
9	1P	pIY67	2S	pIY608	pIY608 is an empty RSF1010 plasmid with Pclac143 promoter and erythromycin selection marker.
	2P	pIY140	1S		
10	1P	pIY67	2S	pIY606	pIY606 is an empty RSF1010 plasmid with Pcoa promoter and erythromycin selection marker.
	2P	pIY417	1S		
11	LRBS1-4P	pIY619	LRBS2-4S	pIY625	pIY602 is used to overexpress 'TesA and FAP under Pcoa promoter.
	LRBS2-4P	pIY499	1S		
	1P	pIY417	LRBS1-4S		
12	LRBS1-4P	pIY619	LRBS2-4S	pIY630	pIY630 is used to overexpress 'TesA and truncated FAP under Pcoa promoter.
	LRBS2-4P	pIY505	1S		
	1P	pIY417	LRBS1-4S		
13	LRBS1-5P	pIY354	1S	pIY440	pIY440 is used to overexpress 'TesA, Sfp, and CAR under Pclac143 promoter.
	1P	pIY140	LRBS1-5S		
14	LRBS1-4P	pIY619	1S	pIY679	pIY679 is used to overexpress 'TesA under Pcoa promoter.
	1P	pIY417	LRBS1-4S		

(B) DNA linkers used for preparation of constructs used to engineer cyanobacteria

Adapter		Linker		Mixed Prefix Linker (P linker)
Name	Sequence (5' to 3')	Name	Sequence (5' to 3')	
1P-A	TTTATTGAACTA	1P-L	GGACTAGTTCAATAAATACCCTCTGACTGTCTCGGAG	1P
2P-A	TTCTTATTACCT	2P-L	GGACAGGTAATAAGAAGTACACGACTGGATACTGACT	2P
3P-A	TGTTATTACAGA	3P-L	GGACTCTGTAATAACAATACCGATAAAGCAACGAGTG	3P
5P-A	TTGATTTATCCT	5P-L	GGACAGGATAAATCAACTCGTAAGCAATACTGTCTGT	5P
LRBS1-5P-A	ATTAGTGGAGGTTA	LRBS1-5P-L	GGACTAACCTCCACTAATTTACAACGATACTTACCTGA	LRBS1-5P
LRBS1-4P-A	ATCACAAGGAGGTA	LRBS1-4P-L	GGACTACCTCCTTGATTTACAACGATACTTACCTGA	LRBS1-4P
LRBS1-3P-A	AAAGAGGAGAAATA	LRBS1-3P-L	GGACTATTTCTCCTCTTTTTACAACGATACTTACCTGA	LRBS1-3P
LRBS2-4P-A	ATCACAAGGAGGTA	LRBS2-4P-L	GGACTACCTCCTTGATTTCTGCTACCCTTATCTCAG	LRBS2-4P
1MP-A	TCTGGTGGGT/iMe-dC/TCT	1MP-L	GGACAGAGACCCACCAGATAATAGTGTTCACGAAGTG	1MP
2MP-A	AACTTCGGAATC	2MP-L	GGACGATTCCGAAGTTACACCAGATTGGACTGTTATTAC	2MP

Adapter		Linker		Mixed Suffix Linker (S linker)
Name	Sequence (5' to 3')	Name	Sequence (5' to 3')	
1S-A	TGTCGTAAGTAA	1S-L	CTCGTTACTTACGACACTCCGAGACAGTCAGAGGGTA	1S
2S-A	TTTCACACCGAT	2S-L	CTCGATCGGTGTGAAAAGTCAGTATCCAGTCGTGTAG	2S
3S-A	TAGTGCCGTGAT	3S-L	CTCGATCACGGCACTACACTCGTTGCTTTATCGGTAT	3S
5S-A	GGCACTACTTCT	5S-L	CTCGAGAAGTAGTGCCACAGACAGTATTGCTTACGAG	5S
LRBS1-5S-A	GACGGTGTTCAA	LRBS1-5S-L	CTCGTTGAACACCGTCTCAGGTAAGTATCAGTTGTAA	LRBS1-5S
LRBS1-4S-A	GACGGTGTTCAA	LRBS1-4S-L	CTCGTTGAACACCGTCTCAGGTAAGTATCAGTTGTAA	LRBS1-4S
LRBS1-3S-A	GACGGTGTTCAA	LRBS1-3S-L	CTCGTTGAACACCGTCTCAGGTAAGTATCAGTTGTAA	LRBS1-3S
LRBS2-4S-A	CCAATAGTAACA	LRBS2-4S-L	CTCGTGTTACTATTGGCTGAGATAAGGGTAGCAGAAA	LRBS2-4S
1MS-A	CGAGTTCTTACC	1MS-L	CTCGGGTAAGAAGTTCGACTTCGTGGAAACACTATTA	1MS
2MS-A	CGATAGGT/iMe-dC/TCC	2MS-L	nTATCGGTAATAACAGTCCAATCTGGTGT	2MS

(C) DNA primers used for preparation of constructs used to engineer cyanobacteria

Primer	Sequence (5' to 3')
IY107	TCTGGTGGGTCTCTGTCCTTTACAGCTAGCTCAGTCCTAG
IY108	CGATAGGTCTCCCGAGCCTGTGTGAAATTGTTATCCGCTCAC
IY113	GCACCAAGTACGGGAATTGGATTCCGGTG
IY114	CCGAGGTAATGGAGAGGACTAAGCACCAAG
IY145	TCTGGTGGGTCTCTGTCCCCAGGCATCAAATAAAACGAAAGGCTC
IY146	CGATAGGTCTCCCGAGCCCGCCGGCAGGAGCAGAAGAGCATAAC
IY155	CGATAGGTCTCCCGAGCCGTGGCAGCAGCCTAGGGAATTCTTACAGC
IY211	TCTGGTGGGTCTCTGTCCGGCTTGATAGAACCTTACTTGATGCC
IY212	CGATAGGTCTCCCGAGCCAAGTACTAACTTAGTCTAAAGGATTAATGAG
IY213	TCTGGTGGGTCTCTGTCCTTCTTGGTGAATGCCAACTGAATAATCTG
IY214	CGATAGGTCTCCCGAGCCGCAATCGAGACAATTATTTCTCTAGACG
IY238	TCTGGTGGGTCTCTGTCCATGGCCGACACGTTATTGATTCTGG
IY258	TCTGGTGGGTCTCTGTCCATGGCGTCTGCTGTAGAAGATATTCGCAAAG
IY259	CGATAGGTCTCCCGAGCCTTACG
PB208	TCTGGTGGGTCTCTGTCCCTGCACTAAAGACAAGTGAG
PB209	CGATAGGTCTCCCGAGCCGCTTTTAACTTGGATTTTACC
PB78	TCTGGTGGGTCTCTGTCCAAGAGGAGAAAGGTACCATGGCCGACACGTTATTGATTCTGG
PB79	CGATAGGTCTCCCGAGCCTTATGAGTCATGATTACTAAAGGCTGCAACTGC

(D) DNA parts used for preparation of constructs used to engineer cyanobacteria. All DNA parts were amplified from DNA templates using primers listed above (C) and stored in pJET1.2 blunt (Thermo Fischer).

Template	Primer		Plasmid Generated	Plasmid Contained	Relevant information
	F	R			
pDF-lac ^a	IY145	IY146	pIY128	pJET-RSF1010	A plasmid storage containing a broad-host-range vector RSF1010 backbone
-	-	-	pIY127	pJET-Gm	A plasmid storage containing gentamicin cassette. A gift from Dr. Geoff Baldwin (Imperial College)
pPB223	IY107	IY108	pIY102	pJET-lacI-Pclac143	A plasmid storage containing a lac repressor and Pclac143 promoter
-	-	-	pIY24	pJET-GFP	A plasmid storage containing a superfold green fluorescence protein. GFP was ordered as a gBlock.
pET-TPC2 ^b	PB78	PB79	pIY72	pJET-'TesA	A plasmid storage containing 'TesA
pET-TPC2 ^b	PB78	IY155	pIY354	pJET-TPC2	A plasmid storage containing 'TesA, Sfp, and CAR.
-	-	-	pIY51	pJET-Ery	A plasmid storage containing erythromycin cassette. Erythromycin cassette was ordered as a gBlock.
6803-WT genomic DNA	IY211	IY212	pIY352	pJET-slr1311_up	A plasmid storage containing the upstream region of slr1311.
6803-WT genomic DNA	IY213	IY214	pIY353	pJET-slr1311_down	A plasmid storage containing the downstream region of slr1311.
6803-WT genomic DNA	PB208	PB209	pPB345	pJET-Pcoa	A plasmid storage containing CoaR and Pcoa promoter.
-	-	-	pIY395	pJET-UndB	A plasmid storage containing UndB. UndB was ordered as a gBlock from IDT DNA.
-	-	-	pIY499	pJET-FAP	A plasmid storage containing FAP. FAP was ordered as a gBlock from IDT DNA.
pIY499	IY258	IY259	pIY505	pJET-'FAP	A plasmid storage containing truncated FAP.
-	-	-	pIY21	pMB1-Kan	A plasmid backbone harbouring ColE1 ori and a kanamycin selection marker.
-	-	-	pIY23	pMB1-Amp	A plasmid backbone harbouring ColE1 ori and a ampicillin selection marker.
-	-	-	pIY67	pJET-termB15	A plasmid storage containing rrnB T1 terminator and T7Te terminator.
pIY72	IY238	PB79	pIY619	pJET-'TesA	A plasmid storage containing 'TesA.

^aGuerrero et al., *Plos ONE*, 2012

^bAkhtar et al., *PNAS*, 2013

Supplementary Table 2. All *Synechocystis sp.* PCC 6803 strains used in the study.

Strain	Relevant information
WT	<i>Synechocystis sp.</i> PCC 6803 wild-type strain obtained from Prof. Klaas Hellingwerf (Univ of Amsterdam)
Δaas	<i>Synechocystis sp.</i> PCC 6803 acyl-ACP synthetase deletion strain.
Δaas - ['] TesA	Δaas harbouring chromosomal integration of ['] tesA under PpsbA2S promoter. This strain was obtained by transforming plasmid pLY397.
Δaas - ['] TesA-1010-UndB	Δaas - ['] TesA carrying UndB overexpression RSF1010 plasmid pLY402.
Δaas -1010- ['] TesA	Δaas carrying ['] TesA overexpression RSF1010 plasmid pLY196 using a Pclac143 promoter
Δaas -1010-TPC2	Δaas carrying ['] TesA, Sfp, and CAR overexpression RSF1010 plasmid pLY440 using a Pclac143 promoter
Δaas -1010-Pcoa- ['] TesA	Δaas carrying ['] TesA overexpression RSF1010 plasmid pLY679 using a Pcoa promoter
Δaas -1010-Pcoa- ['] TesA-FAP	Δaas carrying ['] TesA and FAP overexpression RSF1010 plasmid pLY625 using a Pcoa promoter
Δaas -1010-Pcoa- ['] TesA- ['] FAP	Δaas carrying ['] TesA and truncated FAP overexpression RSF1010 plasmid pLY630 using a Pcoa promoter

Supplementary Table 3. All constructs used for engineering *Chlamydomonas*.

Vector number in manuscript	Overexpression plasmids	Resistance in Cr	Proteins produced	StrepII tag y/n?	Gene length with introns	CDS	RBCS2 intron 1 copies in complete cassette	Protein size (aa)	Predicted molecular mass	Reference
Cr1	pOpt2_mVenus_Paro	paromomycin	mVenus (YFP)	y	1287	813	1	270	30.6	Wichmann et al. 2018
Cr2	pOpt2_PsaD_mVenus_Paro	paromomycin	PsaD_YFP	y	1395	921	1	306	34.3	Lauersen et al. 2016
Cr3	pOpt2_PsaD_TesA_mVenus_Paro	paromomycin	PsaD_TesA_YFP	y	2107	1448	2	495	55.3	This work
Cr4	pOpt2_PsaD_OleTJE_mVenus_Paro	paromomycin	PsaD_OleTJE_YFP	y	3090	2181	4	726	82.2	This work
Cr5	pOpt2_PsaD_OleTJE_RhFRED_mVenus_Paro	paromomycin	PsaD_OleTJE_RhFRED_YFP	y	4527	3183	7	1060	118.3	This work
Cr6	pOpt2_PsaD_RhFRED_OleTJE_mVenus_Paro	paromomycin	PsaD_RhFRED_OleTJE_YFP	y	4527	3183	7	1060	118.3	This work
Cr7	pOpt2_*CrFAP_mVenus_Paro	paromomycin	CrFAP_YFP	y	3694	2640	5	879	94.8	This work
Cr8	pOpt2_PsaD_CrFAP_mVenus_Paro	paromomycin	PsaD_CrFAP_YFP	y	3709	2655	5	884	95.3	This work
Cr9	pOpt2_PsaD_CrFAP_mRuby2_Ble	zeocin	PsaD_CrFAP_RFP	y	3703	2649	5	882	94.9	This work
Cr10	pOpt2_PsaD_TesA_CrFAP_mVenus_Paro	paromomycin	PsaD_TesA_CrFAP_YFP	y	4427	3228	6	1075	116.6	This work
Cr11	pOpt2_PsaD_CrFAP_TesA_mVenus_Paro	paromomycin	PsaD_CrFAP_TesA_YFP	y	4427	3228	6	1075	116.6	This work
Genes synthesized for Cr expression in this work			NCBI accession number for Cr optimized transgene							
CrcoTesA	-	-	TesA	MH004289	712	573	1	193	21.4	Cho and Cronan, 1995
CrcoOleTJE	-	-	OleTJE	MH248837	1707	1272	3	428	48.4	Rude et al. 2011
CrcoRhFRED	-	-	RhFRED	MH248838	1431	996	3	336	36.2	Liu et al. 2014
CrcoCrFAP	-	-	CrFAP	MH248839	2416	1836	4	612	64.5	Soriqué et al. 2017

Notes

*Native CrFAP secretion signal

Synthesized gene sizes include any linkers designed into the genes without restriction sites

Predicted molecular weights contain targeting peptides and the StrepII tag, actual sizes of mature proteins may be variable in the algal chloroplast

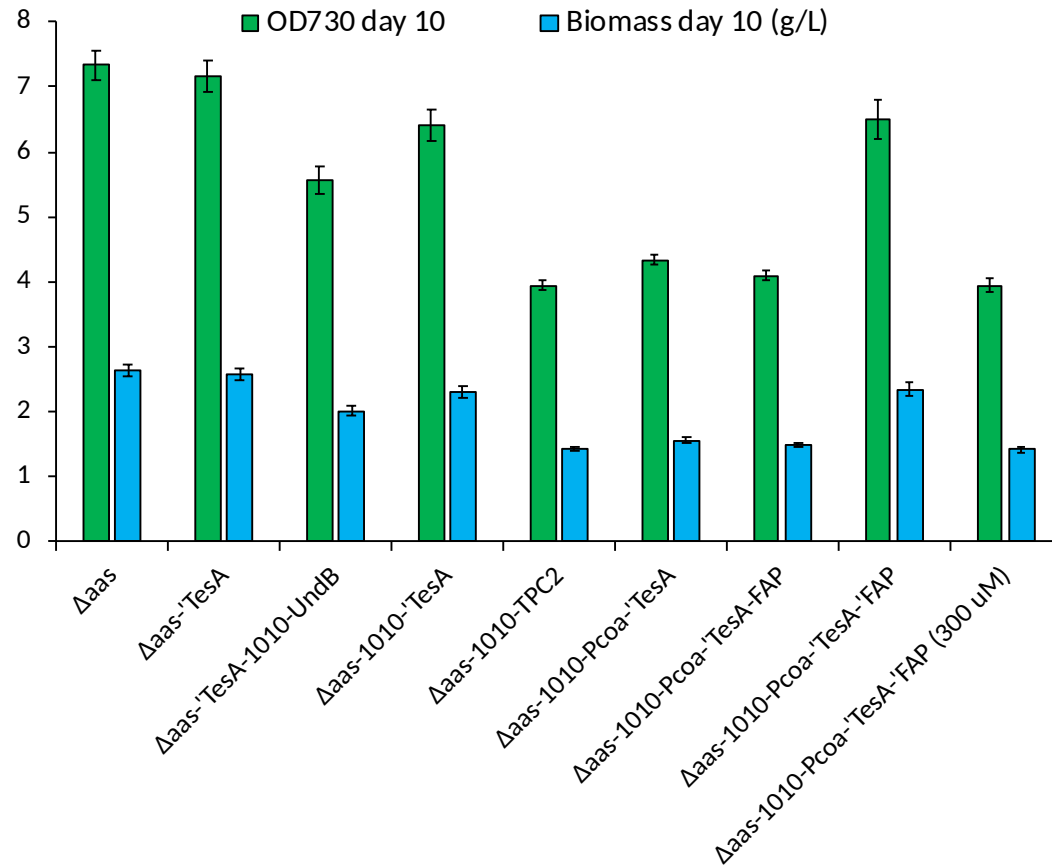
The HSP70-RBCS2-i1 promoter contains an additional copy of the 145 bp rbc2 intron 1 sequence which is added to the intron 1 copy number column for plasmids

Wichmann J., Baier T., Wentmagel E., Lauersen K. J., Kruse O. 2018. Tailored carbon partitioning for phototrophic production of (E)- α -bisabolene from the green microalga *Chlamydomonas reinhardtii*. *Metabolic Engineering* 45: 211-222.

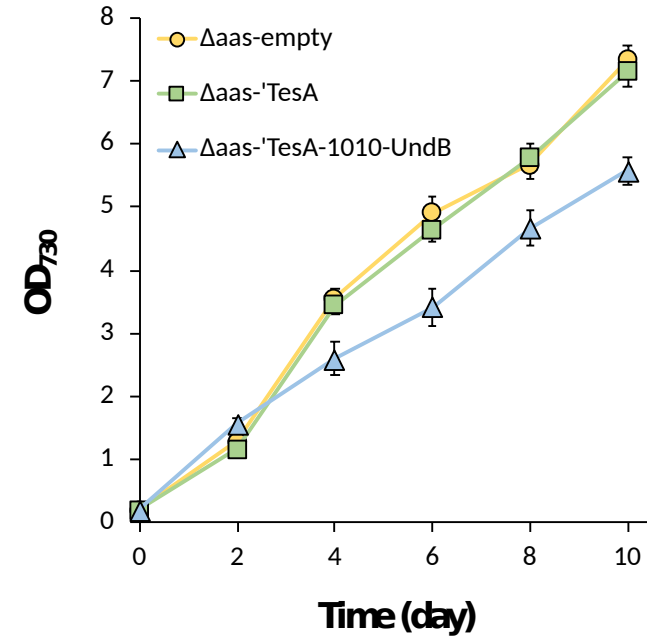
Lauersen K. J., Baier T., Wichmann J., Wördenweber R., Hübner W., Huser T., Kruse O. 2016. Efficient phototrophic production of a high-value sesquiterpenoid from the eukaryotic microalga *Chlamydomonas reinhardtii*. *Metabolic Engineering* 38: 331-343.

Supplementary Figure 1. Growth properties of engineered cyanobacteria strains. (A) The final OD₇₃₀ and biomass accumulation of the engineered strains on day 10 when samples were extracted. (B) Representative growth profile for the first three strains shown in (A).

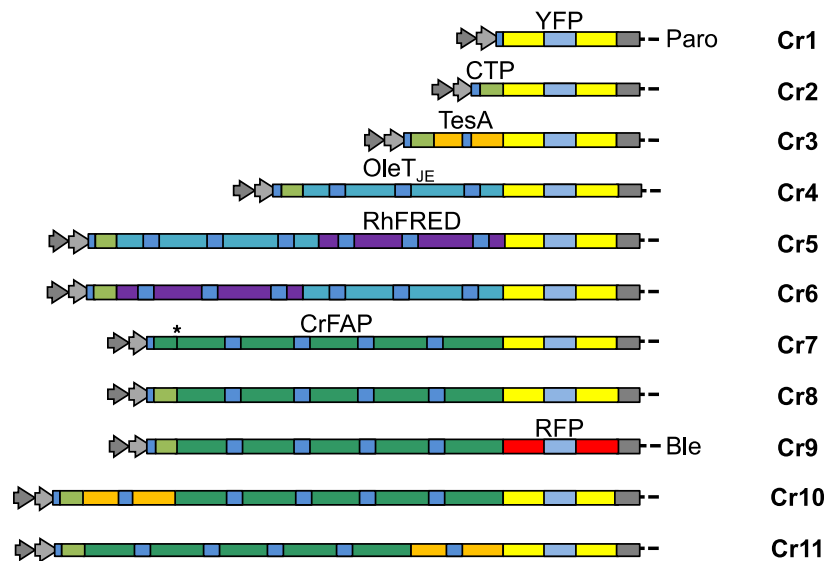
A



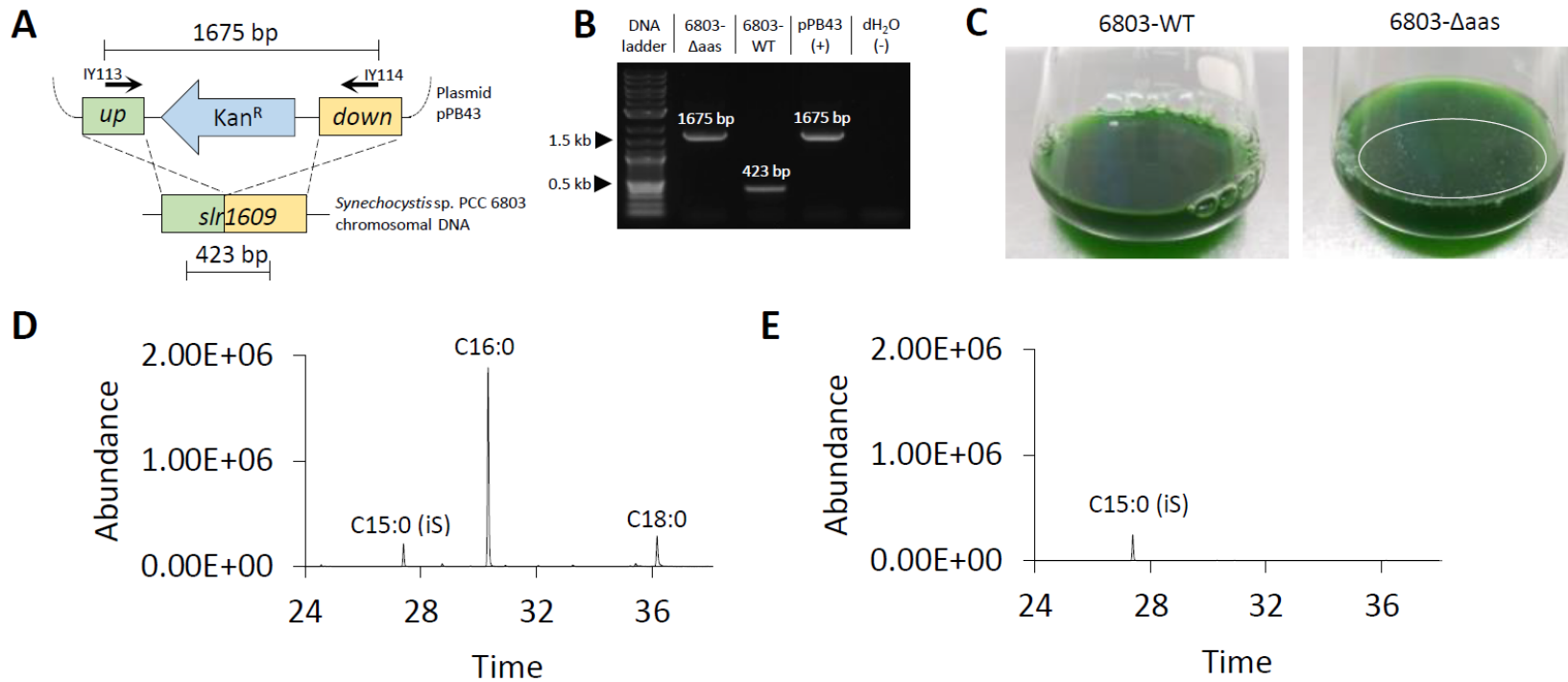
B



Supplementary Figure 2. Graphic illustration of all (key) *Chlamydomonas* DNA constructs used in the study. Vector constructs for nuclear transgene expression from *C. reinhardtii*. The base pOpt2_YFP_Paro vector (Wichmann et al 2018) was used to construct chloroplast targeted protein products using the photosystem I reaction center subunit II (PsaD) chloroplast targeting peptide (CTP). All other constructs were fused to create protein products with C-terminal mVenus (YFP) or mRuby2 (RFP) reporters. Nuclear expression constructs all contain the *rbcS2* i1 intron in copies spread throughout their sequence (blue boxes). The fluorescent reporters contain *rbcS2* i2 as previously described (Lauersen et al 2015). *E. coli* thioesterase A' (TesA), *Jeotgalicoccus* sp. terminal olefin-forming fatty acid decarboxylase (OleT_{JE}) and its fusion to *Rhodococcus* sp. P450 reductase RhFRED. *C. reinhardtii* native fatty acid photodecarboxylase (CrFAP) was synthesized with its own native CTP (*), but was also cloned with the PsaD CTP instead and expressed as YFP or RFP fusions, as well as in fusion with the TesA construct mediated by the modular nature of the pOpt2 vectors. All vectors use the common HSP70-RBCS2-i1 fusion promoter and corresponding 3' UTR and either paromomycin (Paro) or zeocin/bleomycin (Ble) resistance cassettes from the pOpt2 vectors (Wichmann et al. 2018). * indicates site of additional glycine to add *Bam*HI site and allow cloning removal of the native chloroplast targeting peptide and replacement with the PsaD CTP. Paro – all vectors confer paromomycin resistance except the single zeocin (Ble) resistance vector. The vector numbers are shown to the right.

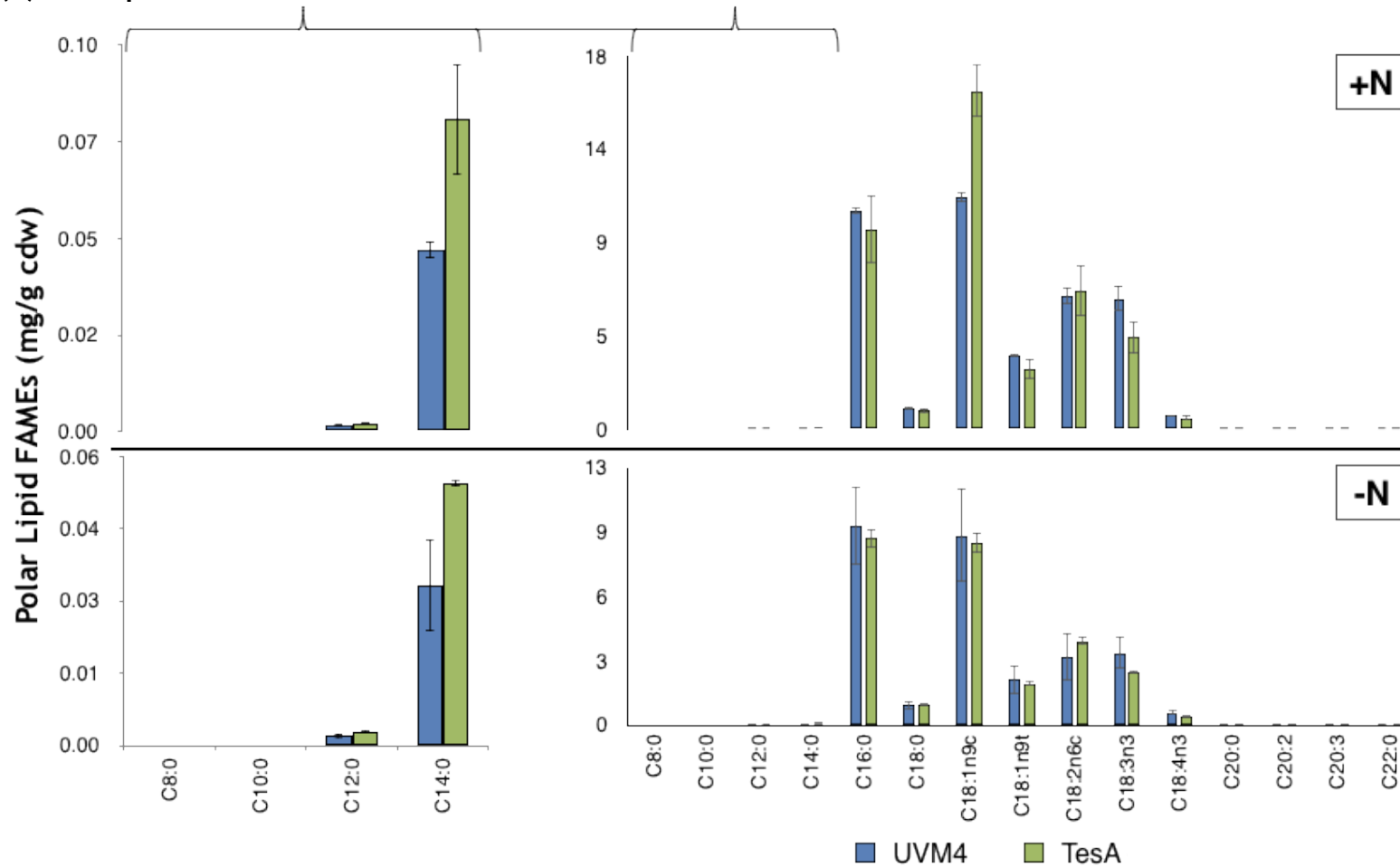


Supplementary Figure 3. Inactivation of *aas*. (A) Schematic diagram of acyl-ACP synthetase (encoded by *slr1609*) knockout. (B) Colony PCR analysis of Δaas and the wild-type strain with positive and negative controls using primers IY113 and IY114. (C) Image of the wild-type (left) and Δaas (right) strains after 10 days of cultivation. Circle highlight visible precipitates forming in the Δaas culture. Representative chromatograms from extracted (D) Δaas and (E) wild-type cultures. C15:0 pentadecanoic acid was used as internal standard.

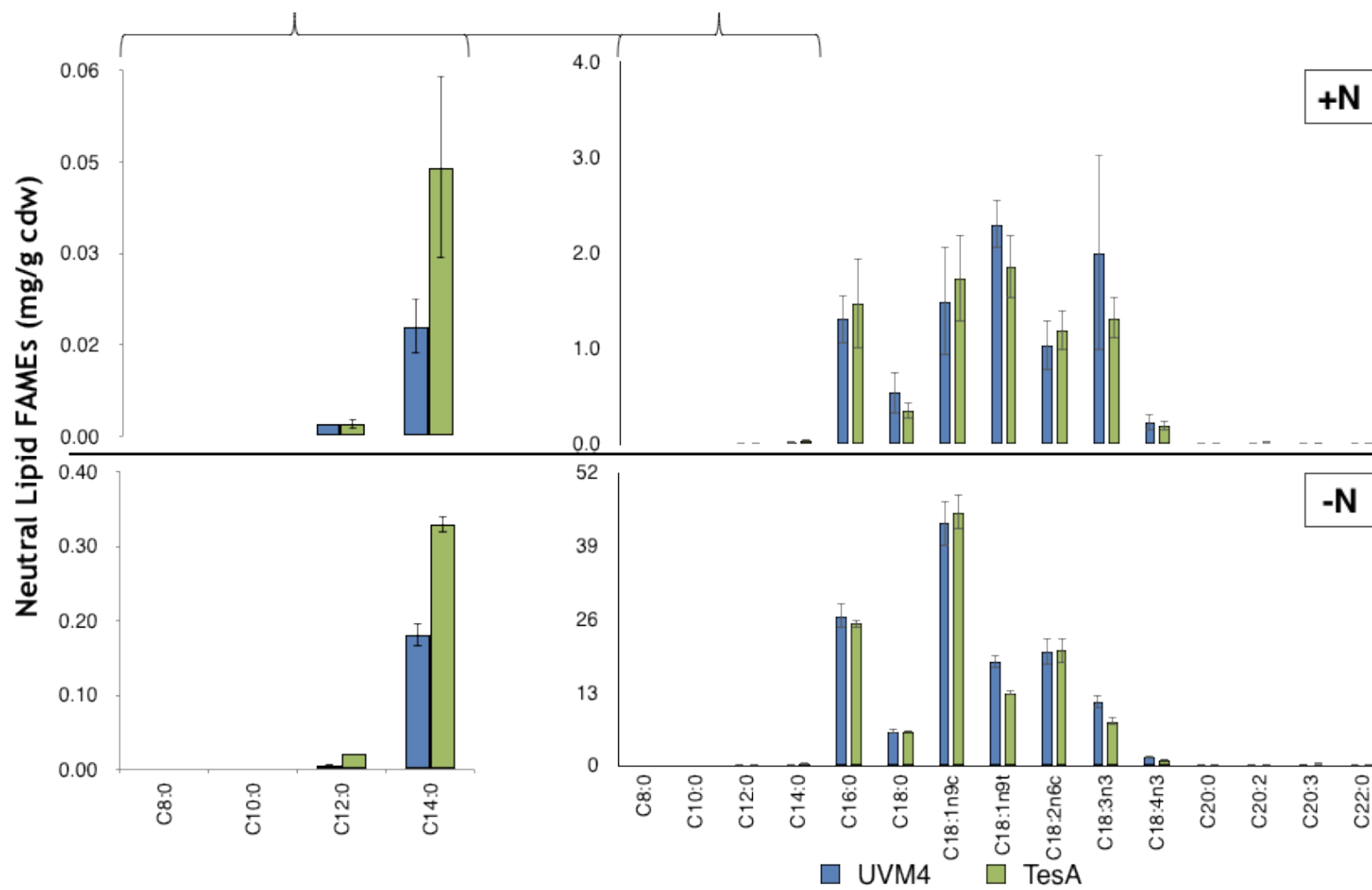


Supplementary Figure 4. Polar and neutral lipid profiles in the wild-type control (UVM4) and *TesA*-overexpressing *Chlamydomonas* strains under nitrogen replete (+N) and deficient (-N) conditions. Extraction of total lipids, separation into neutral and polar lipids, transesterification and GC-MS analysis were performed to determine relative lipid profiles for each strain under each condition. The left section of the graph displays quantities for C8-C12 FAMES only, using a different axis.

(A) Polar lipids.

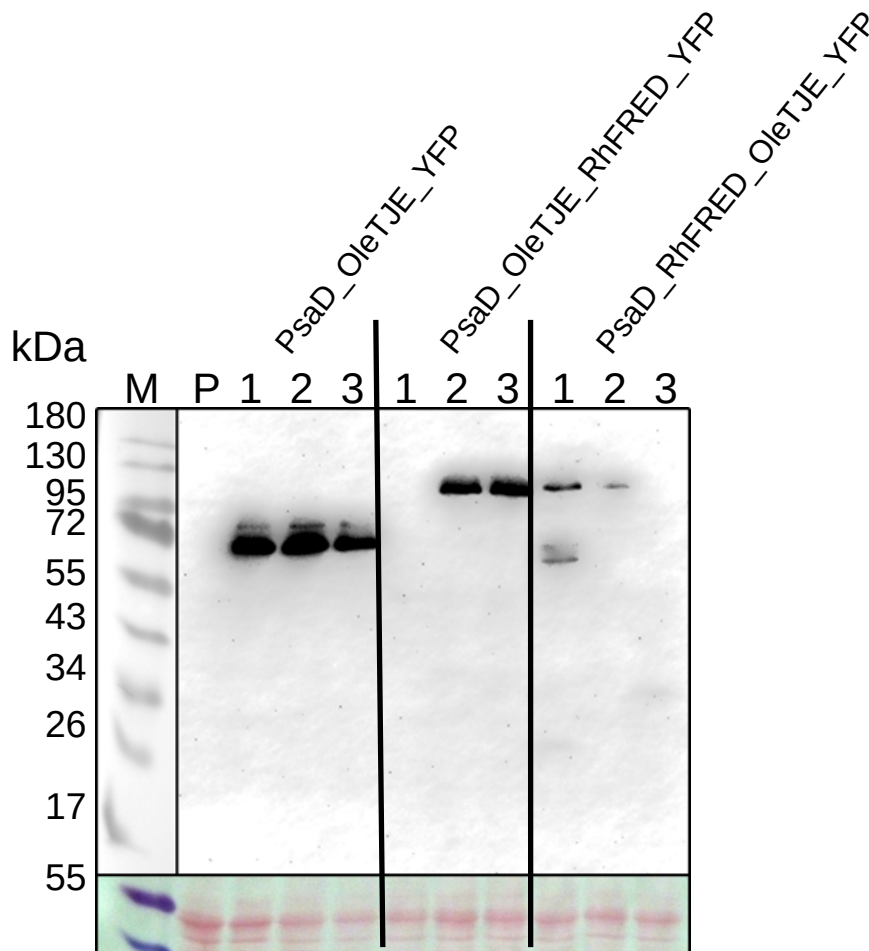


(B) Neutral lipids.



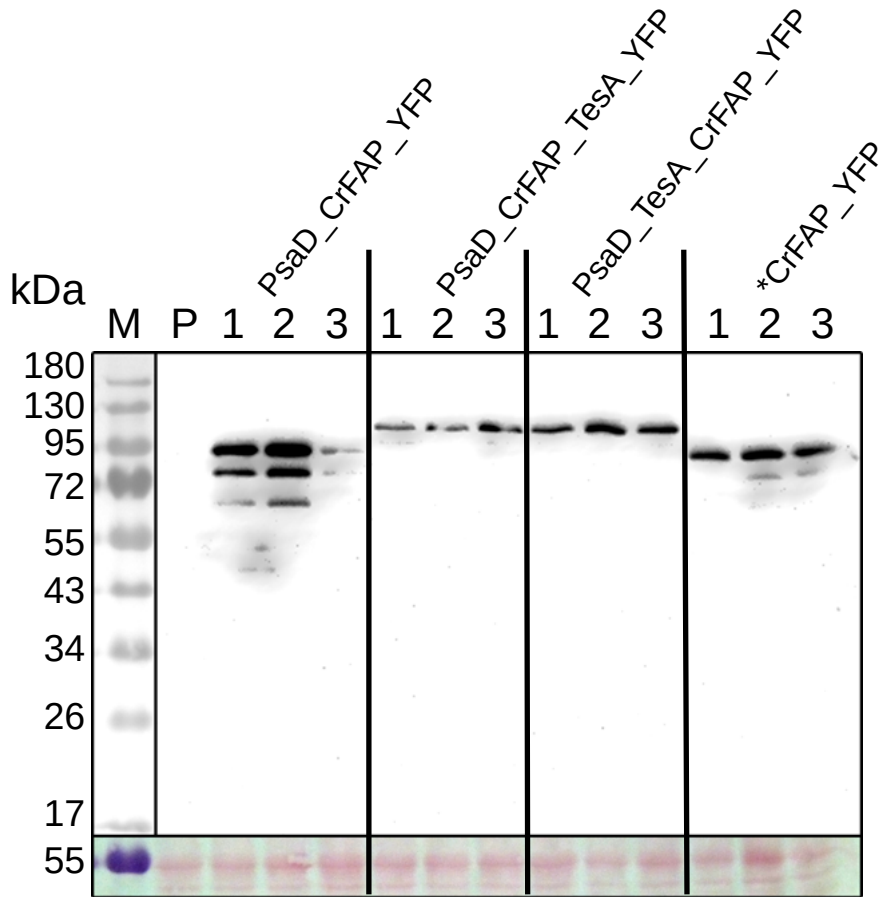
Supplementary Figure 5. Western blot to determine full-length fusion protein expression from the nuclear genome of *C. reinhardtii*.

(A) OleTJE strains. Proteins were extracted from 2 day old cultures in logarithmic phase. An anti-GFP HRP linked polyclonal antibody (Thermo Fisher Scientific) was used for detection of YFP-fused proteins on nitrocellulose membranes. Ponceau S staining of the membrane is shown as a protein loading control. M – PageRuler Prestained protein ladder (Thermo). P – UVM4 parental strain.

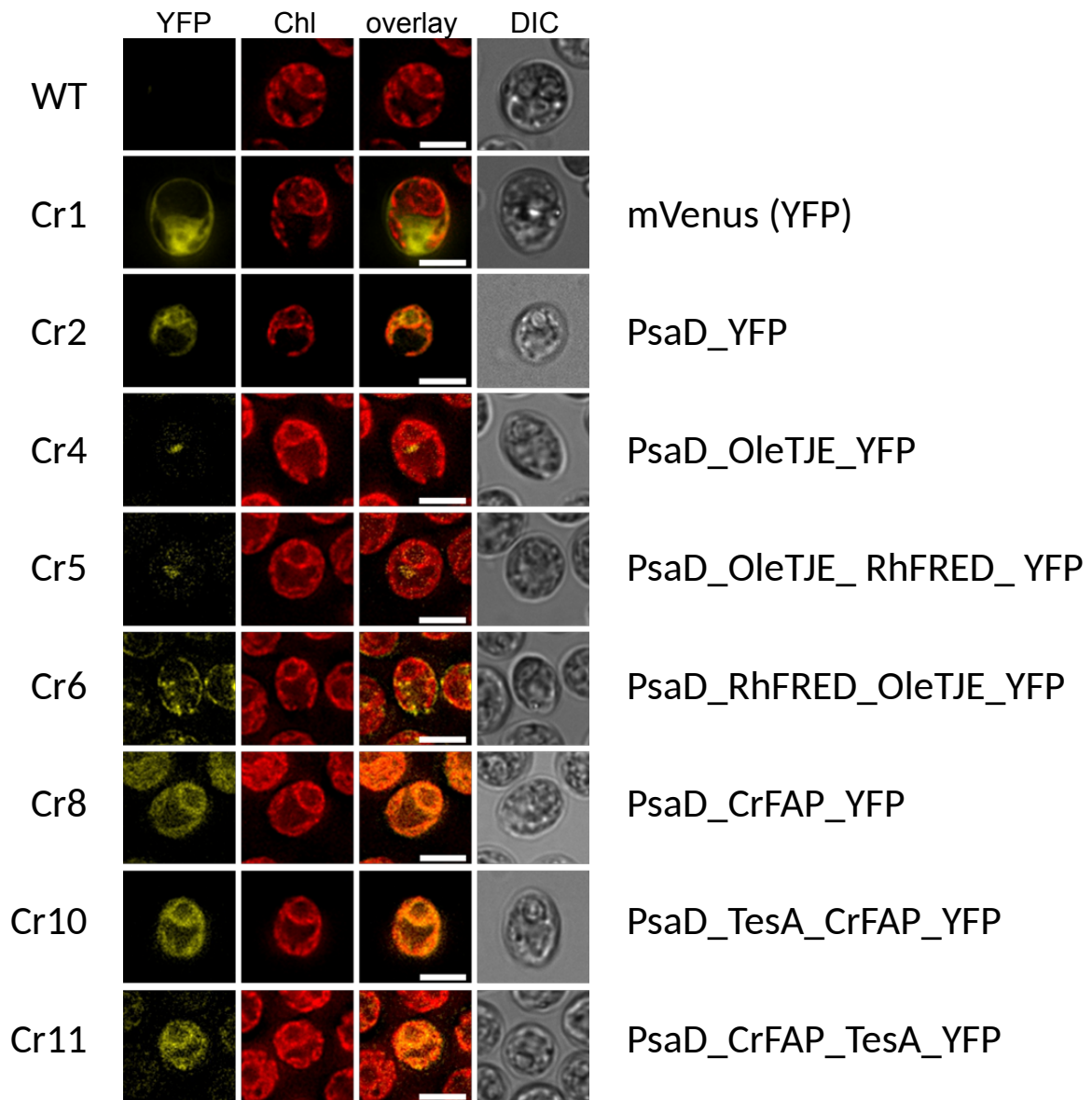


a-GFP antibody whole cell lysates
*native CrFAP CTP

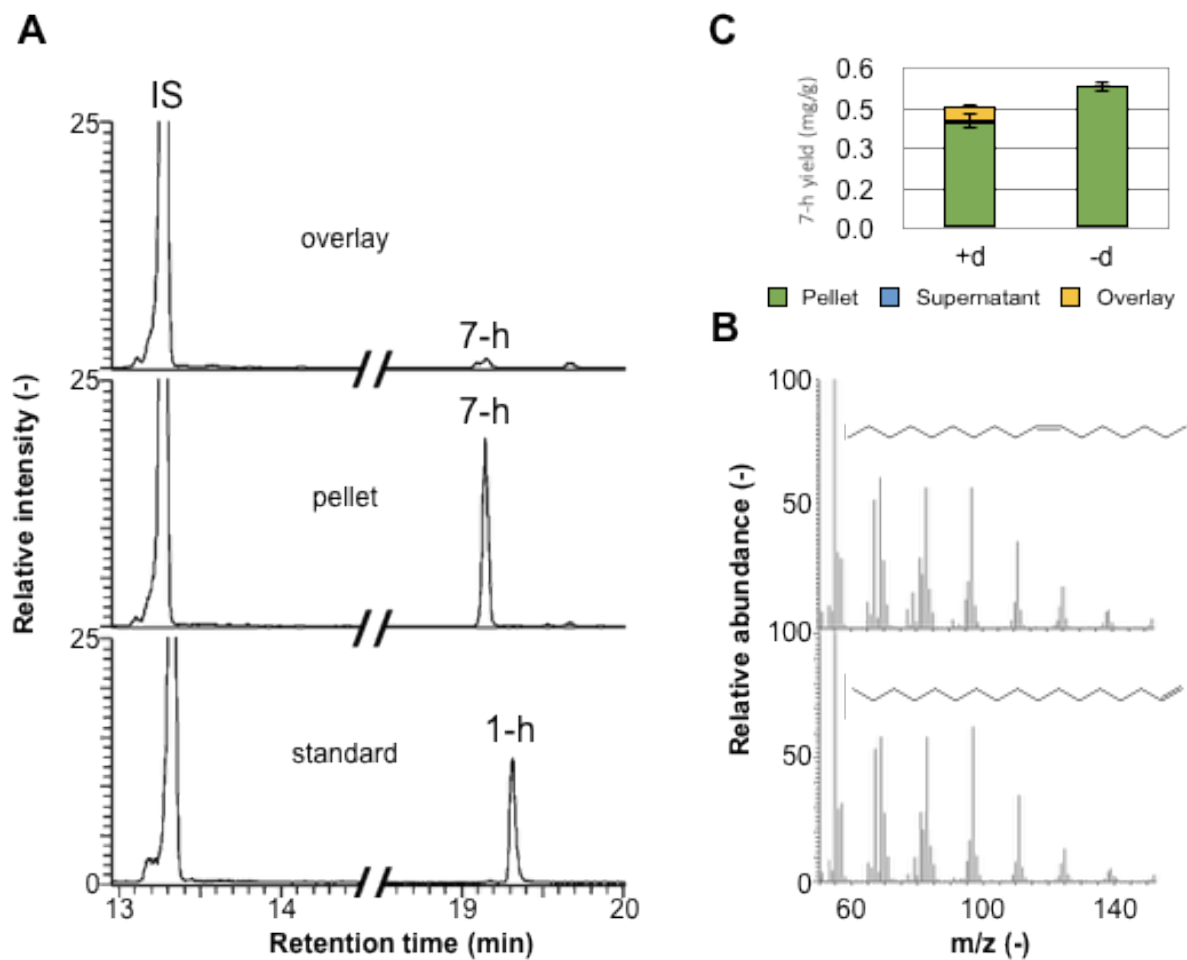
(B) CrFAP and CrFAP-TesA fusion expressing strains. Same methods as above. * indicates native CrFAP chloroplast targeting peptide construct (vector Cr7).



Supplementary Figure 6. Fluorescence microscopy with *Chlamydomonas* strains expressing various OleT and CrFAP constructs. Wide-field fluorescence microscopy was used to confirm chloroplast localization of YFP-linked constructs as previously described (Lauersen et al 2016). The over-expressed proteins, from vectors listed in Supp. Table 3 (above), in each strain is listed on the right, and the vector numbers are shown on the left.



Supplementary Figure 7. GC-MS chromatogram for 7-heptadecene in wild-type *Chlamydomonas*. Identification of 7-heptadecene (7-h) and product partitioning between cells, culture medium (supernatant), and a dodecane overlay. **A** *Chlamydomonas reinhardtii* strain UVM4 was cultivated in TAP medium for 5 d in constant light with and without an overlay of 5% dodecane. (A) Only traces of the product were detectable in the overlay, and the major fraction was found in the cell pellet (middle panel and C). α -humulene served as internal standard (IS). 7-heptadecene was detected at earlier retention times than the commercial 1-heptadecene (1-h) standard (lower panel), however, it showed (B) similar mass fractionation pattern. (C) Presence (+d) or absence (-d) of the dodecane overlay did not affect total product yields. Error bars represent 95% confidence intervals of strains cultivated in biological triplicate.



Supplementary Figure 8. Unidentified alkenes accumulating in the 6803- Δ as-'TesA-FAP strain. Two unique (relative to wild-type) products that accumulated in the 6803- Δ as-'TesA-'FAP strain are most likely also alkenes based on NIST mass spectrometry (2.2) analysis of individual peaks eluting at 6.86 ((A) 6,9-heptadecadiene) and 6.88 minutes ((B) 8-heptadecene), respectively (indicated by the arrow).

